Sustainable Alternative Materials in Unbound Granular Layers of Pavement Structures

by

Adam C. Schneider

A thesis
presented to the University of Waterloo
in fulfillment of the
thesis requirement for the degree of
Master of Applied Science
in
Civil Engineering

Waterloo, Ontario, Canada, 2017

© Adam C. Schneider 2017

AUTHOR'S DECLARATION

I hereby declare that I am the sole author of this thesis. This is a true copy of the thesis, including any required final revisions, as accepted by my examiners.

I understand that my thesis may be made electronically available to the public.

ABSTRACT

In Part 1 of this thesis, reclaimed cement concrete (commonly referred to as recycled concrete aggregate or RCA) and reclaimed asphalt pavement (RAP) are investigated as potential alternative construction materials for Granular B Type II subbase fill. Ontario Provincial Standard Specification (OPSS) 1010 currently allows the common use of processed reclaimed construction materials in a variety of road base, subbase and asphaltic concrete layers, with the notable exception of Granular B Type II, which at present may only include 100% crushed bedrock, talus, iron blast furnace slag or nickel slag. As more restrictions are placed on zoning and approvals for new natural aggregate extraction sites in Ontario, there is a need to better understand the performance of materials such as RCA and RAP as economically beneficial potential aggregate sources for granular base and subbase fill layers.

An experimental program was created to assess and analyze the performance characteristics of a series of different subbase test mixtures incorporating RCA and/or RAP, either pure or blended with crushed bedrock, and the impact of the inclusion of these materials when compared to a conventional 100% crushed bedrock test mix meeting OPSS 1010 requirements for Granular B Type II. The performance characteristics to be assessed were field compactibility, gradations before and after field compaction, physical properties, standard and modified Proctor tests, California Bearing Ratio (CBR), permeability, resilient moduli and lightweight deflectometer (LWD) resilient moduli.

Field testing programs conducted at Quarry 1 in Ottawa, Ontario and Quarry 2 in Burlington, Ontario indicate that the subbase test mixtures meeting OPSS Granular B Type II gradation requirements and incorporating different proportions of crushed rock, RCA and/or RAP exhibit similar field rolling compactibility relative to 100% crushed rock. Grain size analysis testing showed some aggregate breakdown in multiple test mixes, with only minimal increases in material passing the 75 μm sieve, which is crucial to preserving permeability and drainage characteristics. Tests using a lightweight deflectometer (LWD) were subject to substantial variability but indicated that mixes using elevated levels of RCA (50% and 100%) can potentially have lower in-situ moduli compared to the other blends tested.

Laboratory tests indicate that high replacement levels of RCA can be used in subbase materials as a substitute for 100% crushed rock while maintaining good water permeability characteristics and similar or higher resilient moduli in blends incorporating RCA and/or RAP. CBR testing results were similar across all test blends incorporating crushed rock and RCA, but also indicated that the inclusion of 30% RAP can potentially reduce the bearing capacity of the granular material by approximately 30-40% in comparison to all other blends which do not contain RAP. Based on the overall results of this study, RCA and RAP appear to be capable of successfully substituting for natural aggregates in Granular B Type II in a range of compositional proportions. It is recommended that test sections should be completed on highway contracts with subbase mixture blends incorporating RCA and/or RAP in order to verify their performance in pavement structures in the field.

In Part 2 of this thesis, foam glass lightweight aggregates (LWA) are investigated as a potential pavement engineering design alternative in order to mitigate roadway loading impacts upon underlying subgrade soils while promoting the sustainable and economical use of recycled waste glass. Foamyna Canada Inc. supplied the Centre for Pavement and Transportation Technology (CPATT) with two foam glass lightweight aggregate materials, designated in this thesis as LWA-A and LWA-B. Physical properties testing was carried out by CPATT, including grain size analysis, crushed particle content, flat and elongated particle content, Micro-Deval abrasion resistance, cyclic freezing-and-thawing resistance and resilient modulus testing procedures. These procedures were conducted in order to evaluate the LWA materials against locally applicable standards, namely Ontario Provincial Standard Specification document OPSS 1010 as currently used by the Ministry of Transportation of Ontario (MTO).

The laboratory testing detailed in Part 2 indicates that both LWA-A and LWA-B have a very consistent and repeatable gradation with a high percentage of coarse aggregates. Both foam glass materials have very high crushed particle contents and very low flat and elongated particle contents. Micro-Deval abrasion resistance, freeze-and-thaw resistance and resilient moduli were also excellent for both materials, while relative density testing indicated LWA material specific gravity values which were substantially lower than that of water. However, it was found that the gradations of these two tested materials do not satisfy the existing requirements of OPSS 1010, which were developed for natural aggregates and, as currently constituted, may not be appropriately adapted to artificial lightweight aggregates. The coarse nature of the LWA materials would be highly beneficial to ensure the stability of the granular layers and prevent upward capillary water movement into other layers of the pavement structure.

Pavement design calculations were carried out using the AASHTO 1993 empirical design procedure and found that utilizing foam glass LWA as a lightweight subgrade replacement fill material can result in substantially leaner pavement structures as compared to the use of conventional expanded polystyrene (EPS) geofoam blocks as an artificial subgrade. A life-cycle cost analysis (LCCA) procedure carried out on these pavement designs showed that the use of foam glass LWA as a lightweight fill material underlying pavement can result in overall cost savings of over 30 percent relative to pavement structures which are underlain by EPS geofoam. Overall, the two tested LWA materials showed excellent physical and mechanical characteristics, and would be suitable for use in pavement structures as innovative lightweight and environmentally friendly alternatives to natural aggregate materials.

ACKNOWLEDGEMENTS

I would first like to sincerely thank my supervisor, Professor Hassan Baaj, for giving me the opportunity to pursue graduate studies at the Centre for Pavement and Transportation Technology (CPATT) and for his invaluable support, guidance, instruction and patience over the course of my MASc program. My appreciation is also extended to Professor Susan L. Tighe and Professor Eric Soulis for serving as members of the review committee for my thesis.

For the project on reclaimed materials in Granular B Type 2, I would first like to thank the Ontario Ministry of Transportation (MTO), and in particular Mr. Stephen Senior and Mr. John Blair, for their crucial support. I would also like to thank Mr. Paul Lum, formerly of Lafarge Canada Inc. (LafargeHolcim), for his instrumental guidance and leadership throughout the testing, analysis and reporting program. My sincere appreciation goes out to Mr. Ahmed el-Baghdadi, Mr. Abdurahman Lotfy, Mr. Anto Sucic and their colleagues at the Lafarge Canada Inc. Innovation and Training Centre (ITC) in Toronto, Ontario for donating their assistance and the use of their equipment in the laboratory testing phase of this project. Many thanks are also extended to the many partners and supporters of this research project, including Mr. Brian Messerschmidt and Aggregate Recycling Ontario (ARO), Mr. Jim Karageorgos and Steed & Evans Ltd., R.W. Tomlinson Ltd., Nelson Aggregate Co., Golder Associates Ltd. and other associated stakeholders.

For the project on foam glass lightweight aggregate (LWA), my thanks goes out first and foremost to Ms. Yassaman Yousefi, the Yousefi family, and their firm Foamyna Canada Inc. for initiating this project, for donating their innovative materials for testing, and for supporting this study every step of the way. I would also like to recognize the Ontario Centres of Excellence (OCE) for their generous financial support of this project. Additionally, I would like to thank Professor Guy Doré, research associate Dr. Jean-Pascal Bilodeau, undergraduate research assistant Ms. Marielle Fauteux and their colleagues at the Department of Civil Engineering at Université Laval in Québec for their expert assistance with conducting resilient modulus testing on the foam glass LWA materials.

There are a number of individuals I would like to recognize for their support and assistance throughout my research and academic endeavours. In particular, many thanks go to several of the outstanding technical staff members at the Department of Civil and Environmental Engineering, Mr. Terry Ridgway, Ms. Anne Allen, Mr. Richard Morrison, Mr. Mark Sobon, Mr. Douglas Hirst and their manager Mr. Christopher Peace, for their assistance and instruction on many of the testing procedures detailed in this thesis. Much appreciation goes to Ms. Laura Anderton and Ms. Jessica Rossi for their enthusiastic and dedicated administrative support at CPATT, and to Ms. Victoria Tolton and Ms. Eleanor Clarke for their assistance and coordination at the Department of Civil and Environmental Engineering.

CPATT would not be the leading research centre that it is without the community of students who have come to call it their second home and who pull together to help each other succeed on a daily and weekly basis. With this in mind, I would like to personally thank many current and former CPATT graduate students for their unwavering support and encouragement, in particular Dr. Sina Varamini, Mr. Taher Baghaee Moghaddam, Mr. Eskedil Melese, Ms. Sonia Rahman, Mr. Zaid Alyami, Ms. Hanaa al-Bayati, Mr. Daniel Pickel, Mr. Shenglin Wang, Mr. Andy (Zhong) Jian, Ms. Donghui Lu, Mr. Yashar Azimi Alamdary, Dr. Magdy Shaheen, Dr. Gulfam Jannat, Ms. Haya Almutairi, Mr. Frank (Yang) Liu, Ms. Rahanuma Wafa, Mr. Drew Dutton, Ms. Julia (Ju) Huyan, Mr. Seyedata Nahidi, Mr. Taha Younes and past and present research associates Dr. Mohab el-Hakim, Dr. Prabir Das, Dr. Peter Mikhailenko, Dr. Cristina Torres Machi, Dr. Kamal Hossain and Dr. Qingfan Liu. Appreciation is also extended to visiting scholars Dr. Wei Li and Dr. Thunder (Ting) Cao, fellow Waterloo graduate students Mr. Hamed Shahrokhi Shahraki, Mr. Mohammadamin Jahanpour, Ms. Diana Gomez Rodriguez and Mr. William Sellier, and many other friends and colleagues who are not named here. I would also like to thank CPATT undergraduate co-op students Cynthia Lane, Hannah Yu, Andrew Girgis, Junaid Farooq, Daniel Deacon, Spencer Townsend, Ninweh Jeorje, Kenechi Chidolue, Guillermo Pekny, Lucas Menezes, Thiago Haddad, Aditi Sharma and Mitchell Uku for their capable assistance at many points over the course of my research projects, and I wish them all the best as they continue in their studies.

Dedication

This thesis is dedicated to my family – my parents, Georg and Ann, and my sister Laurel – without whose love and support this would never have been possible.

TABLE OF CONTENTS

LIST OF FIGURES

LIST OF TABLES

CHAPTER 1
OVERVIEW

Reclaimed or recycled construction materials are substances that originate from pre-existing anthropogenic sources and are processed for reuse in new construction or infrastructure applications. In civil engineering, this can commonly take the form of rigid concrete sourced from demolished structures such as buildings, bridges, sidewalks, curbs and culverts, or asphalt material sourced from pavement which has been broken up and removed in the process of replacement or rehabilitation. Reclaimed construction materials can also originate from other sources, such as glasses or plastics that are collected and sorted by municipal or regional waste disposal systems.

These reclaimed materials can serve as sustainable design solutions in engineered infrastructure systems. Within a pavement engineering context, materials that have been reclaimed and reprocessed into artificial aggregates can be selected to replace newly extracted (or "virgin") natural aggregates within unbound granular fills, or to augment bound substances such as flexible asphalt concrete mixes or rigid cement concrete mixes. This can impart benefits from a sustainability perspective, such as reducing environmental harm by diverting waste from disposal facilities, reducing pollution emissions from production and from shipping, and decelerating the degradation of land that is designated and used for the extraction of natural aggregates. Expanding the use of reclaimed materials also can bring economic benefits by reducing the financial costs to companies in the construction industry, which could then utilize substantial stockpiles of reclaimed or recycled materials available in urbanized areas instead of sourcing newly extracted natural aggregates from more distant rural areas.

Consequently, if reclaimed or recycled construction materials are to be permitted to replace conventional aggregates in elements of pavement structures, it is crucial to confirm that they perform at an acceptable level and do not pose additional risks or hazards to the users of transportation infrastructure or to others who may be affected, whether directly or indirectly. This necessitates the completion of accurate and sufficiently comprehensive testing and analysis work to characterize the properties and performance of reclaimed materials before enabling their use in infrastructure applications.

1.1 Thesis Structure and Organization

This thesis incorporates information on two research projects which shared a common theme and which were carried out independently at the Centre for Pavement and Transportation Technology (CPATT) at the University of Waterloo. Both projects are closely related to one another as they focus on the testing and evaluation of recycled and reclaimed materials used in unbound granular fill applications. These two projects differ in the materials being examined as well as the scope of the research being carried out, including necessary testing procedures, analysis and design, and the number and identity of the supporting research partners.

Part 1 of this thesis details a research program centering on the use of reclaimed and recycled materials in Ontario Provincial Standard Specification (OPSS) Granular B Type II. Part 1 begins with an introduction in Chapter 2, followed by a literature review in Chapter 3. The field and laboratory test procedures included in this study are detailed in Chapters 4 and 5 respectively, while the results of these tests are presented in Chapter 6. The conclusions of this study are presented in Chapter 7, and further data tables can be found in Appendices A, B and C.

Part 2 of this thesis presents a research program investigating foam glass lightweight aggregate (LWA). An introduction is given in Chapter 8, followed by a literature review in Chapter 9. Experimental procedures and results are presented in Chapter 10, with a pavement design and life-cycle cost analysis (LCCA) in Chapter 11. The conclusions of this study are presented in Chapter 12, and further data tables can be found in Appendix D.

Overall conclusions of this thesis are presented in Chapter 13, followed by a list of works cited and by the aforementioned appendices.

PART 1:

RECLAIMED MATERIALS IN OPSS GRANULAR B TYPE II

CHAPTER 2
INTRODUCTION

Ontario Provincial Standard Specification (OPSS) 1010, Material Specification for Aggregates – Base, Subbase, Select Subgrade, and Backfill Material, contains requirements for a wide variety of aggregate products utilized in the construction of road base and subbase layers. Among these requirements, OPSS 1010 permits the use of several types of recycled or reclaimed materials, including recycled concrete aggregate (RCA) and recycled asphalt pavement (RAP), in a number of designated classes of aggregate subbase products including Granular B Type I and Granular B Type III. However, at present, RCA and RAP materials are prohibited from use in Granular B Type II mixes, as this specification only permits the inclusion of 100% crushed bedrock, talus, iron blast furnace slag or nickel slag.

As aggregate production pits and quarries progress through and complete their operational lifespans, and as the zoning and application process for new aggregate extraction sites in Ontario grows more restrictive over time, there is a need to continue to characterize and develop sources of reclaimed materials as a sustainable alternative to natural aggregates. Materials such as RCA and RAP are readily available in urbanized regions of Ontario in large quantities as a potential alternative material in road structure layers. Consequently, there is a need to examine, assess and validate the performance of RCA and RAP in a variety of potential alternative applications, including as potential replacements for crushed rock in Granular B Type II unbound subbase materials.

2.1 Objective and Scope

The objective of this project and of the testing described in the following sections of this report is to evaluate the performance of reclaimed materials meeting the particle size and physical quality requirements of OPSS 1010 for Granular B Type II unbound dense graded subbase materials as an alternative to the use of crushed rock (either in whole or in part). The study has included the evaluation of five subbase test mixtures of differing volumetric proportions of crushed rock, crushed RCA and processed RAP in the following combinations from two different source locations:

- 100% crushed rock (used as a control mix);
- 25% crushed RCA blended with 75% crushed rock;
- 50% crushed RCA blended with 50% crushed rock;
- 100% crushed RCA; and
- 70% crushed RCA blended with 30% crushed RAP.

The field testing program consisted of the construction and compaction of a set of five test pads at two separate test sites, with each pad containing both a lower prepared subgrade layer consisting either a 26.5mm crushed dense graded unbound material or existing compacted granular fill, and a top layer consisting of one of the five proposed subbase test mixtures under examination (differing for each test pad). Density testing and lightweight deflectometer (LWD) testing was carried out on each layer of each test pad, and samples of each of the test mixtures were taken for gradation both before and after compaction.

The laboratory testing program consisted of the following tests:

- Gradation (or Sieve Analysis);
- Physical Properties;
- Standard and Modified Proctor;
- Permeability;
- California Bearing Ratio (CBR); and
- Resilient Modulus.

These tests were carried out a specified number of times on each test mixture from each of the two test sites. The above laboratory test procedures were conducted in accordance with the applicable current Ontario Ministry of Transportation (MTO) Laboratory Testing Manual (LS) test methods, American Society for Testing and Materials (ASTM) test methods, and American Association of State Highway and Transportation Officials (AASHTO) test methods.

CHAPTER 3
LITERATURE REVIEW

A number of previous studies conducted in Ontario and elsewhere in North America and around the world have examined the impact and viability of RCA and/or RAP as constituent materials of unbound granular layers in the pavement structure.

The use of crushed, reclaimed materials such as asphaltic concrete and hydraulic cement concrete as acceptable substitutes for natural mineral aggregates is well established in Ontario. OPSS 1010 allows the use of 100% RCA and up to 30% RAP in a number of unbound granular base and subbase pavement layers for infrastructure projects. However, the specification does not allow RCA or RAP to be used in Granular B Type II unbound subbase materials.

As a recent example of the successful use of recycled materials in Ontario municipal infrastructure projects, a recent paper by Moore, Jagdat, Kazmierowski and Ng (2014) presented to the Transportation Association of Canada (TAC) examined a case study of a six-kilometre-long section of Ontario Highway 7 running between the Town of Richmond Hill and the City of Markham in the Regional Municipality of York. This stretch of Highway 7 was being reconstructed to include an at-grade centerline bus rapid transit right-of-way incorporating RCA into its granular base and subbase layers. The authors analyzed the results of a number of standard granular laboratory tests and concluded that, with proper quality control practices during crushing and manufacturing, RCA is a viable and economical solution for conserving high-quality natural aggregates and can be used successfully as replacement material in granular subbase layers.

In a 1989 MTO report, Hanks and Magni completed a field and laboratory study investigating the use of recovered bituminous material (RBM, another term for RAP) in crushed rock granular base material, both pulverized in-situ as well as processed and blended at the aggregate source. Laboratory data indicated that the strength of the blended product will be of the same order as that of a standard naturally-sourced granular material, and may increase with time. The permeability of the blended granular materials was found to be of the same order as compacted natural granular materials and, in some cases, higher. The authors recommended that contracts to be constructed in the near future should use a maximum of 30 percent RBM (RAP) content based on the California Bearing Ratio (CBR) performance values in the study. By contrast, granular materials blended with greater than 30 percent RAP were found to have much lower CBR results.

A later MTO report by Senior, Szoke and Rogers (1994) to the International Road Federation and TAC addresses the use of RAP in Ontario along with other reclaimed materials including steel slag, glass, ceramic whiteware (porcelain), brick and crumb rubber. The report notes that RAP has been in use in Ontario since 1971 and has been successful at a variety of percent content levels and in a number of paving applications including direct recycling into new asphalt and unbound applications such as the construction of highway shoulders. This report also notes that the presence of RAP tends to lower the maximum compacted density of granular fill, increases the optimum moisture content for compaction, lowers the material's California Bearing Ratio (CBR) and, depending on the amount of fine material in the RAP gradation, can negatively impact permeability of the granular material, necessitating tight control over the consistency of the RAP utilized in any given project.

Outside Ontario's borders, a synthesis of current practices by the Transportation Research Board's National Cooperative Highway Research Program (2013) includes sections on the use of reclaimed materials in the pavement structure. The report states that RAP performance is comparable to that of a crushed stone base, though concerns remain about lower bearing capacities and the potential for the aggregate to expand during aging and oxidation similar to metal slag. The report also notes the feasibility of the use of RCA as a substitute aggregate, while mentioning a number of areas where processed reclaimed concrete materials typically differ from conventional natural aggregates, such as increased absorption capacity, lower specific gravity and high angularity. The authors go on to stress the need for strong quality control practices during the production of RCA as well as testing to confirm its performance when used in construction projects.

Two similar documents by the United States Department of Transportation's Federal Highway Administration (2010) and the Recycled Materials Resource Center at the University of New Hampshire (2008) both note that the use of RCA as a cost-effective aggregate substitute in pavement construction is well-established for a variety of potential applications. Both organizations note a number of areas in which the physical properties of RCA differ from natural aggregates, including RCA generally having a rougher surface texture, lower specific gravity and higher water absorption than similarly-sized natural aggregate particles, with a corresponding increase in water absorption for RCA relative to natural materials in finer sizes of crushed aggregates. Both guidelines state that although variations in RCA can readily occur due to differences between the types of concrete being processed, RCA overall has favourable mechanical properties including good abrasion resistance, soundness characteristics and bearing strength.

An earlier report by Kuo, Mahgoub, Ortega, Chini and Monteiro (2001) to the Florida Department of Transportation included examination of RCA through a variety of field and laboratory tests, and concluded that RCA can be used effectively as a base course material as long as strong quality control techniques are applied during its manufacture, mixing and placement. The authors went on to specify a number of recommended guidelines for the use of RCA in roads within the state of Florida.

In a more global context, two papers by Aurstad, Asknes, Dahlhaug, Berntsen and Uthus (date at least 2004) and Aurstad, Berntsen and Petkovic (date at least 2006) examine the use of RCA in a field trial of a segment of the major Highway E6 south of Trondheim, Norway. These reports analyzed a range of field and laboratory tests on the granular materials incorporating RCA in the project and found good mechanical strength properties including bearing capacity, shear strength, elastic stiffness (modulus) and resistance to in-situ deformation. Both papers noted the high absorption and optimum water content of RCA and stressed the need for abundant water addition during construction to improve workability and compaction and to guard against crushing and disintegration during the construction process. It was also noted that field bearing capacity measurements taken later after construction of the highway segment yielded increased stiffness values for the test sections constructed using RCA.

An earlier report by Yeo and Sharp (1997) to the State Road Authority of Victoria (VicRoads) in Australia examined the existing standard specifications in force at the time for RCA as well as a laboratory-based study which investigated the properties of RCA stabilized using cementitious binders. The report noted that RCA had been used successfully in Australia for some time as of the date of writing, and also recommended the use of blends of ground blast furnace slag with either lime or Portland cement as effective binders in mixes incorporating RCA.

CHAPTER 4
FIELD TESTING PROGRAM

4.1 Field Test Sites

Two test sites were selected for the field tests detailed in this report and are designated as follows:

- Quarry 1: Moodie Drive Quarry, R.W. Tomlinson Ltd., Ottawa, ON; and
- Quarry 2: Nelson Quarry, Nelson Aggregate Co., Burlington, ON.

Both quarries produce aggregates from Paleozoic carbonate bedrock and sell OPSS granular base products along with recycled granular base materials incorporating RCA and RAP.

At each test site, five different subbase test mixtures (listed and described in Section 2.1) were blended and stockpiled adjacent to the locations where the test pads were to be built. Approximately 300 tonnes of each test mixture was produced and each aggregate supplier performed gradation and physical property tests on each produced material to compare to the OPSS 1010 Granular B Type II specifications, as shown in Tables A-11 to A-22 in Appendix A.

4.2 Test Section Construction

At Quarry 1, the test mixtures utilized crushed rock sourced from the quarry itself, RAP sourced from local parking lots, municipal roads and highways (excluding premium "FC2" friction course material) and concrete rubble from a variety of sources (excluding concrete wash-out material), where each material was crushed to 75mm and below to meet OPSS 1010 Granular B Type II gradation requirements. The mixing process took place after the materials were crushed separately and was completed using a front-end loader keeping to the test mix proportions specified in Section 2.1 by counting filled buckets from each material and blending until visually consistent. During construction of the test pads at Quarry 1, 26.5mm dense-graded crushed rock was placed and compacted as a subgrade layer 150mm in thickness underneath the subbase test mixtures. The purpose for placing a 26.5mm dense-graded crushed rock material was to provide consistent subgrade conditions at the test pad sections, as well as a cushion on top of the exposed bedrock upon which the subbase test mixtures were being constructed so as to minimize the potential for prematurely shattering stone aggregate in the test mixtures due to the rigid underlying bedrock.

At Quarry 2, the test mixtures were pre-blended on site utilizing crushed rock sourced from the quarry itself, RAP sourced from local parking lots, municipal roads and highways (excluding premium “FC2” friction course material) and RCA sourced from demolished bridge, curb and sidewalk concrete material. The pre-blending process was completed using a front-end loader keeping to the test mixture proportions specified in Section 2.1 by counting filled buckets from each material and blending until visually consistent. The pre-blended test mixtures were then introduced into the crushing process and reduced to 75mm and below to meet OPSS 1010 Granular B Type II gradation requirements. Prior to the construction of the test pads, a granular layer of indeterminate thickness existed at the test site, necessitating localized fine grading and compaction to prepare the site for the test pads. This granular layer consisted of an existing compacted haul road and surrounding compacted fill forming the floor of the aggregate pit. As local bedrock was not in proximity to the working surface, additional placement of a 26.5mm dense-graded crushed rock material was considered unnecessary, except where needed to level out irregularities in the immediate test area.

In total, five (5) test pads were constructed at each test site, each using one of the five individual subbase test mixtures listed previously. Each test pad measured approximately 40 metres in length and 3 metres in width, comprising a compacted 150mm thick dense-graded crushed rock subgrade layer on top of the quarry bedrock floor (at Quarry 1) or an existing in-situ dense-graded crushed granular subgrade material (at Quarry 2) underlying a compacted 300mm thick subbase test mixture layer. An example of a finished test pad is shown in Figure 4-1.

Figure 4-1. Example of a test pad constructed at Quarry 1

4.3 Compaction

At Quarry 1, a Bomag BW 211D-40 12-tonne single drum vibratory roller set on vibration mode (shown in Figure 4-2) was utilized to compact the different subgrade and subbase layers, while at Quarry 2, a Volvo SD 115 12-tonne single drum vibratory roller set on vibration mode was utilized to compact the different subgrade and subbase layers.

Figure 4-2. Test pad at Quarry 1 undergoing vibratory compaction

Dry density measurements were completed using a calibrated nuclear densometer. The prepared 26.5mm dense graded crushed rock subgrade layer was measured to ensure that it was properly compacted in comparison to its maximum dry density and optimum moisture content before the placement of the different subbase test mixtures. The densometer probe was set to depths of 100mm and 250mm, respectively, for the prepared subgrade and subbase test mix layers. The density measurements were obtained at points spaced five (5) metres apart along the centerline of each pad as shown in Figures 4-3 and 4-4, corresponding to locations where deflectometer measurements were also taken as described in Section 4.6.

Density measurements were taken after each roller pass, and both the compaction process and the densometer testing were discontinued when it was determined that there was no further significant increase in dry density measurements. Water was added before and after each pass of the vibratory roller when it was deemed necessary based on the material’s dryness appearance, or when the moisture content readings from the nuclear densometer indicated that it was lower than expected for the given material (Figure 4-5). Density testing results are discussed in Section 6.1 and full data tables may be found in Appendix A, specifically Tables A-1 to A-5 for Quarry 1 and Tables A-6 to A-10 for Quarry 2.

Figure 4-3. Densometer and deflectometer testing locations on a test pad at Quarry 1

Figure 4-4. Nuclear densometer testing in progress at Quarry 2

Figure 4-5. Addition of water to a test pad under compaction at Quarry 1

4.4 Sampling

A front end loader was utilized in obtaining all samples, either by means of digging into the stockpile and building a sampling pad, or by scraping off the 300mm granular subbase layer at four separate locations on the test pad for sampling purposes, as shown below in Figures 4-6, 4-7 and 4-8. Generally, at least one sample was taken from each test mixture stockpile for gradation and quality testing. Four samples were taken from each test mixture pad layer after compaction was completed for gradation determinations.

Figure 4-6. Test pad sampling at Quarry 2 using a front-end loader

Figure 4-7. Prepared sampling locations on a test pad at Quarry 2

Figure 4-8. Sampling at a test pad at Quarry 2

4.5 Gradation and Physical Properties Testing

For both quarries, gradation and physical property testing was performed on each test mixture. In Appendix A, the results of this testing can be found in Tables A-11 to A-16 for Quarry 1 and in Tables A-17 to A-22 for Quarry 2. The physical property tests performed were:

- Micro-Deval Abrasion in Coarse Aggregate;
- Micro-Deval Abrasion in Fine Aggregate;
- Asphalt-Coated Particle Content;
- Amount of Contamination; and
- Plasticity Index.

Gradation tests conducted before and after compaction of each test mixture at each test site were completed by the quarry owner or contractor completing the test sections. Grain size testing and analysis was completed in accordance with MTO LS-602, Method of Test for Sieve Analysis of Aggregates. The average gradation before compaction was compared to the average gradation of samples after compaction for each test mixture at each test site; results discussion can be found in Section 6.2 and full data tables are in Appendix A as listed above.

Micro-Deval abrasion testing of coarse aggregate was completed in accordance with LS-618, Method of Test for the Resistance of Coarse Aggregate to Degradation by Abrasion in the Micro-Deval Apparatus. Micro-Deval abrasion testing of fine aggregate was completed in accordance with LS-619, Method of Test for the Resistance of Fine Aggregate to Degradation by Abrasion in the Micro-Deval Apparatus. Asphalt-coated particle content testing was completed in accordance with LS-621, Method of Test for Determination of Amount of Asphalt-Coated Particles in Coarse Aggregate. Amount-of-contamination testing was completed in accordance with LS-630, Method of Test for Amount of Contamination of Coarse Aggregates. Plasticity Index testing was completed in accordance with LS-703/704, Method of Test for Liquid Limit, Plastic Limit and Plasticity Index of Soils.

4.6 Field Deflection Measurements

A Dynatest Keros Prima 100 portable falling weight deflectometer (FWD), commonly known as a lightweight deflectometer (LWD), was utilized to measure deflection after compaction at the surface of the subgrade layer and at the surface of the subbase layer in each test pad as seen in Figure 4-9. Seven test points were completed on each test pad, spaced five (5) metres apart along the pad centerline. At each test point, a number of measurements were taken in succession; typically, the first one to three measurements were discarded as anomalous due to the need to allow the LWD to seat itself properly on the compacted granular material. Once relatively consistent measurements were obtained, a minimum of five successful drops were conducted at each test point in order to obtain average deflection and loading values with which to determine the modulus of the compacted material in the field. LWD measurements and discussion of results may be found in Section 6.3, while full data tables are in Appendix B.

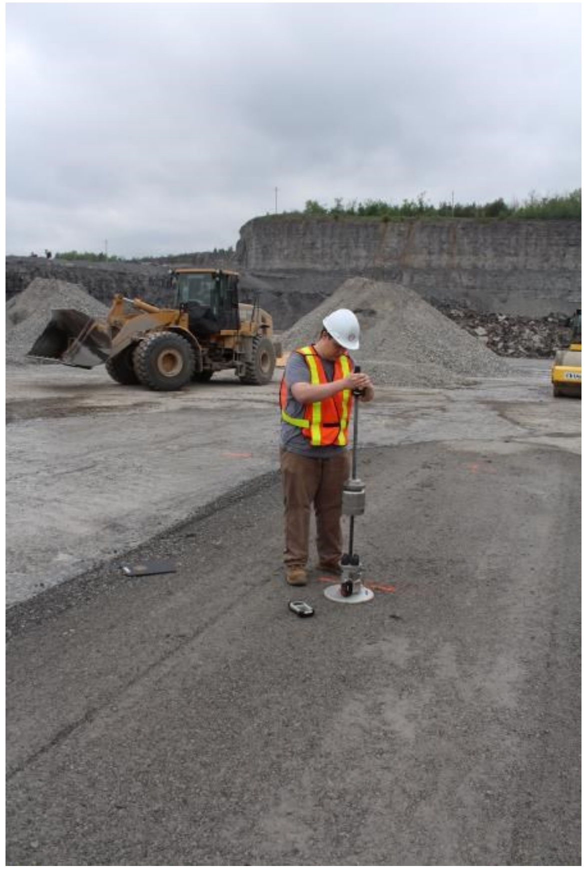

Figure 4-9. Lightweight deflectometer testing in progress at Quarry 1

CHAPTER 5
LABORATORY PERFORMANCE TESTS

The tests described in the following sections were completed on each subbase test mixture from each test site.

5.1 Standard and Modified Proctor

The standard and modified Proctor tests were used to determine the optimum moisture content and maximum compacted dry density for each test mixture. The difference between the two methods lies in the number of layers in which the material is compacted (three layers for the standard Proctor and five layers for the modified Proctor), the drop height for the Proctor hammer (305mm for the standard test and 457mm for the modified test) and the weight of the hammer (2.5kg for the standard test and 4.5kg for the modified test). All these factors typically contribute to lower optimum moisture contents and higher compacted densities under the modified Proctor test relative to the standard Proctor results. In Ontario, the standard Proctor test is typically conducted on pavements such as roads, highways and parking lots, whereas modified Proctor tests are typically conducted on pavements such as major airports and port facilities. The modified Proctor test was not specifically required to be conducted during the testing program, but was included in order to further characterize the test mixtures and their response to greater compactive effort.

The standard Proctor test was conducted in accordance with MTO specification LS-706, Method of Test for Moisture-Density Relationship of Soils Using 2.5 kg Rammer and 305 mm Drop, and the modified Proctor test was conducted in accordance with LS-707, Method of Test for Moisture-Density Relationship of Soils Using 4.5 kg Rammer and 457 mm Drop. For the purposes of these tests, a mechanical Proctor hammer apparatus, shown in Figure 5-1, was used to aid in ensuring consistent compaction of the test materials at 56 blows per layer under both the standard and modified conditions. Cylindrical metal moulds of 150mm diameter were used in the Proctor tests, and any oversized particles in the test samples 26.5mm in size or greater were removed and replaced with a blend of finer particles from the same test mix ranging from 26.5mm to 4.75mm, in accordance with the LS-706 and LS-707 test procedures.

The standard and modified Proctor test results are presented and discussed in Section 6.4.

Figure 5-1. Mechanical Proctor hammer apparatus at Lafarge Canada ITC

5.2 California Bearing Ratio

The California Bearing Ratio (CBR) test is used as a measurement of the bearing capacity of granular materials compared to a reference material. The test equipment is shown in Figure 5-2. The primary specification for the CBR test is ASTM D1883-14, Standard Test Method for California Bearing Ratio (CBR) of Laboratory-Compacted Soils. Each sample was compacted in 150mm diameter moulds using the mechanical Proctor hammer apparatus with compactive effort equal to the standard Proctor test (three layers each receiving 56 blows of a 2.5kg hammer with a 305mm drop) and with moisture content equal to the optimum moisture content determined by the standard Proctor test. During mixing, material retained on the 26.5mm sieve was removed and replaced with an equal mass of material from the same test mixture passing the 26.5mm sieve and retained on the 4.75mm sieve in accordance with the ASTM D1883 procedure. After compaction, each sample was subjected to a 4.5kg surcharge weight while being immersed in water for a period of 96 hours.

For this study, two CBR tests were conducted on each test mixture from each of the two test sites, and the results were combined to obtain an average CBR value for each test mixture. The results of this test are presented and discussed in Section 6.5.

Figure 5-2. California Bearing Ratio testing apparatus at Lafarge Canada ITC

5.3 Permeability

The permeability testing was completed in accordance with MTO test method LS-709, Method of Test for Determination of Permeability of Granular Soils. The testing apparatus is shown in Figure 5-3. For this study, two permeability tests were conducted on specimens of each test mixture from each of the two test sites, and the results were combined to obtain an average permeability value for each test mixture. The results of this test are presented and discussed in Section 6.6.

Figure 5-3. Permeability testing apparatus at Lafarge Canada ITC

5.4 Resilient Modulus

The samples for the resilient modulus were prepared in accordance with AASHTO T307, Standard Method of Test for Determining the Resilient Modulus of Soils and Aggregate Materials. The triaxial test apparatus used in the Lafarge Canada Inc. ITC laboratory was a Servo-Hydraulic Universal Testing Machine manufactured by Cooper Research Technology Ltd., shown in Figure 5-4.

Figure 5-4. Triaxial resilient modulus testing apparatus at Lafarge Canada ITC

For this study, three specimens were compacted and tested for each test mixture from each of the two test sites. Each specimen was compacted by adding the test mixture into a cylindrical mould 100mm in diameter and 200mm in height in a series of six equal layers, with any oversized particles (26.5mm or greater in diameter) removed and replaced with equal mass of material from the same test mixture passing the 26.5mm sieve and retained on the 4.75mm sieve. The total mass of material for each test mixture was calculated based on the maximum dry density, with the moisture content reduced by 1% from the standard optimum moisture content as permitted by AASHTO T307. This reduction from the optimum moisture content is a standard practice with the apparatus at the ITC laboratory in order to achieve a dry density at or near the maximum dry density determined by the standard Proctor test.

As the six equal layers were added, they were each compacted for a period of two to three seconds using a Bosch 11264EVS handheld combination hammer, with an additional slight downwards pressure applied to keep the vibratory hammer head in contact with the sample.

Once all six layers were compacted, the completed sample was removed from the mould, surrounded with an impermeable rubber membrane and placed into the loading cell as seen above in Figure 5-4. Each test yields a range of resilient modulus values as the apparatus cycles through a pre-programmed standard series of stages which vary the levels of applied axial stress and confining pressure on the compacted sample.

Results of the resilient modulus testing are presented and discussed in Section 6.7 and full data tables can be found in Appendix C.

CHAPTER 6
RESULTS AND DISCUSSION

6.1 Test Pad Density and Moisture Measurements

At Quarry 1, field dry density and moisture content measurements are shown in Tables A-1 to A-5 in Appendix A. The 100% crushed rock Granular B Type II material required between 5 and 7 roller passes to achieve maximum compaction (Figure 6-1), whereas the different blend ratios of crushed rock to RCA and RCA to RAP required anywhere from 4 to 8 roller passes to achieve maximum compaction (Figures 6-2, 6-3, 6-4 and 6-5). For all graphs pertaining to Quarry 1 test mixes, the maximum compacted density of the subgrade layer is shown for comparison. The test mixtures modified with RCA or RCA with RAP required an equal number of roller passes to achieve maximum density as compared to the 100% crushed rock control material.

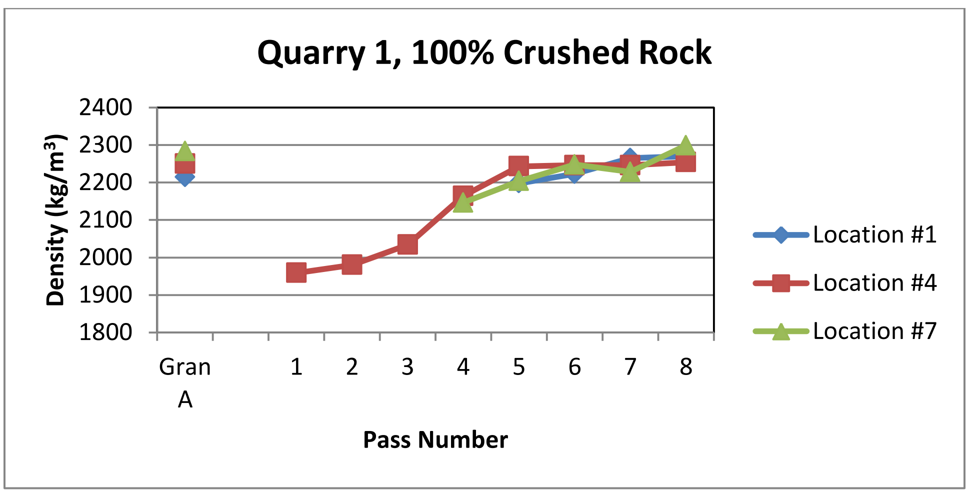

Figure 6-1. Compaction results for 100% crushed rock test mix at Quarry 1

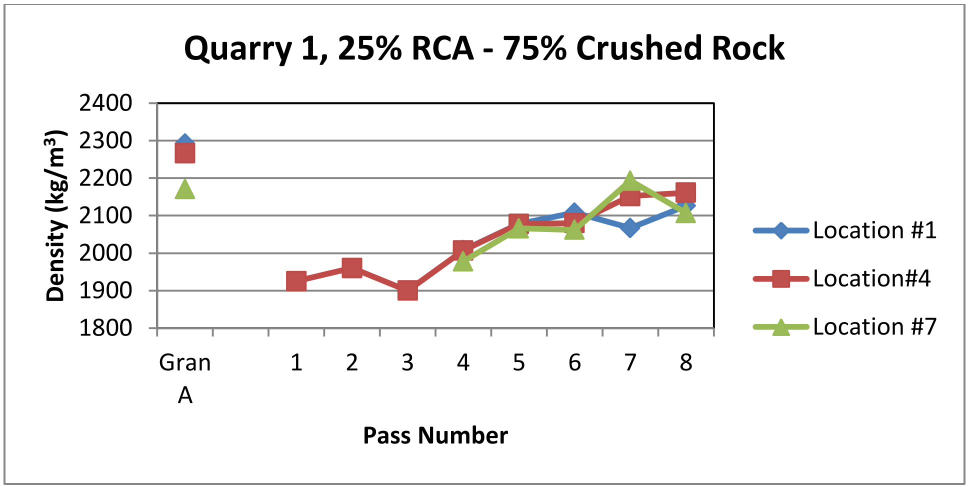

Figure 6-2. Compaction results for 25% RCA - 75% crushed rock test mix at Quarry 1

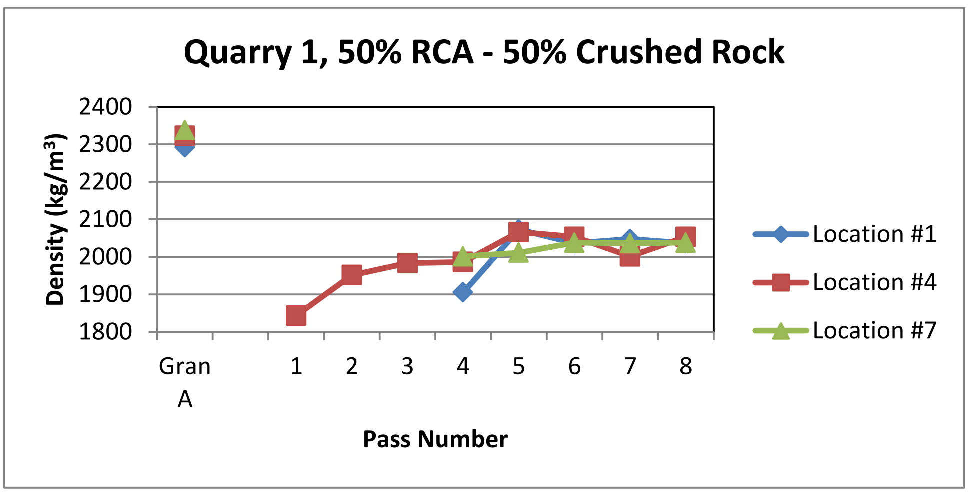

Figure 6-3. Compaction results for 50% RCA - 50% crushed rock test mix at Quarry 1

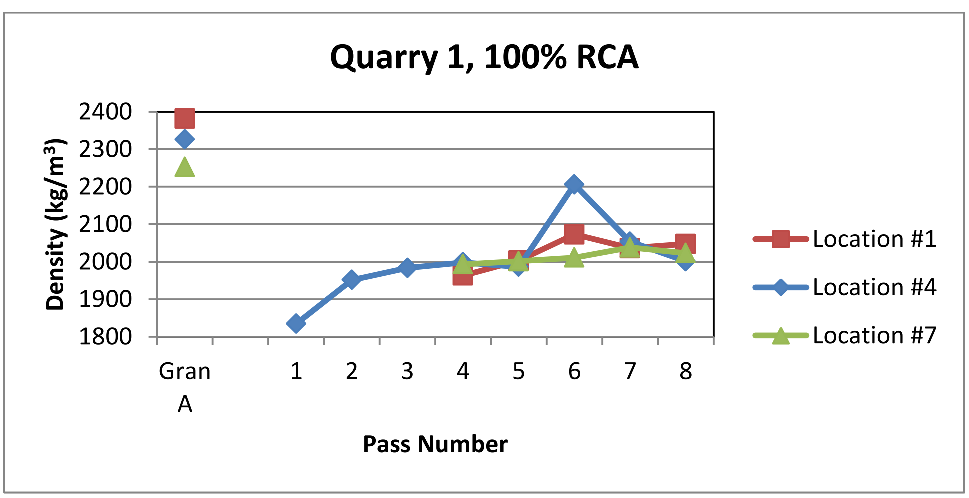

Figure 6-4. Compaction results for 100% RCA test mix at Quarry 1

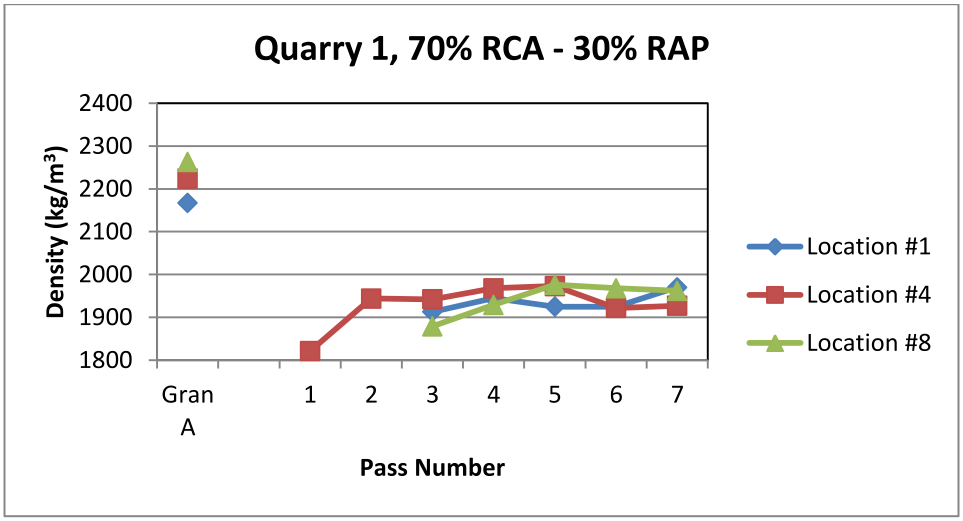

Figure 6-5. Compaction results for 70% RCA - 30% RAP test mix at Quarry 1

At Quarry 2, field dry density and moisture content measurements are shown in Tables A-6 to A-10 in Appendix A. The 100% crushed rock Granular B Type II material required between 5 and 7 roller passes to achieve maximum compaction (Figure 6-6), whereas the different blend ratios of crushed rock to RCA and RCA to RAP required anywhere from 3 to 8 roller passes to achieve maximum compaction (Figures 6-7, 6-8, 6-9 and 6-10). The test mixtures modified with RCA or RCA with RAP required a similar number of roller passes to achieve maximum density as compared to the 100% crushed rock control material.

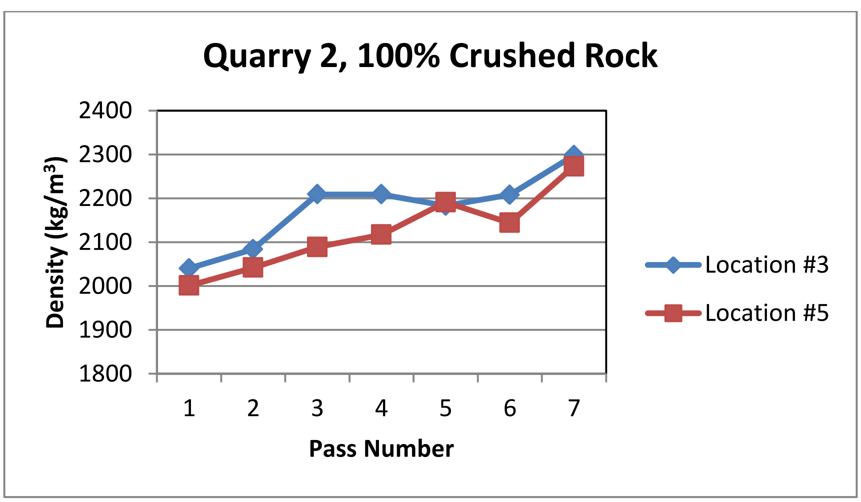

Figure 6-6. Compaction results for 100% crushed rock test mix at Quarry 2

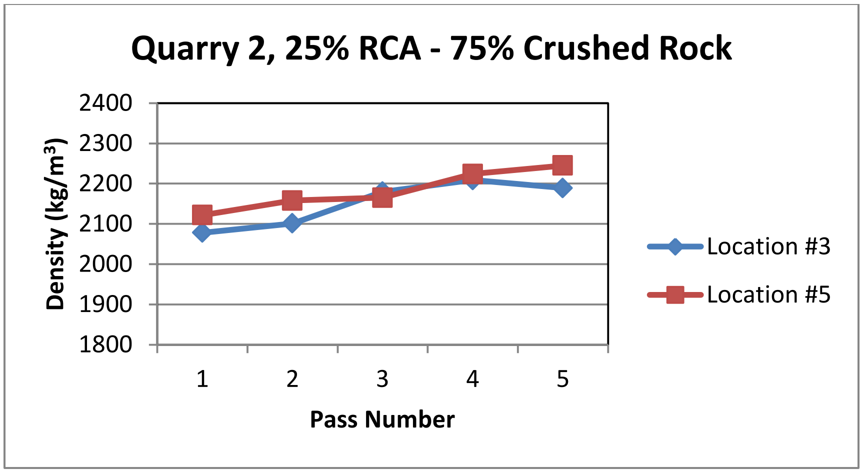

Figure 6-7. Compaction results for 25% RCA - 75% crushed rock test mix at Quarry 2

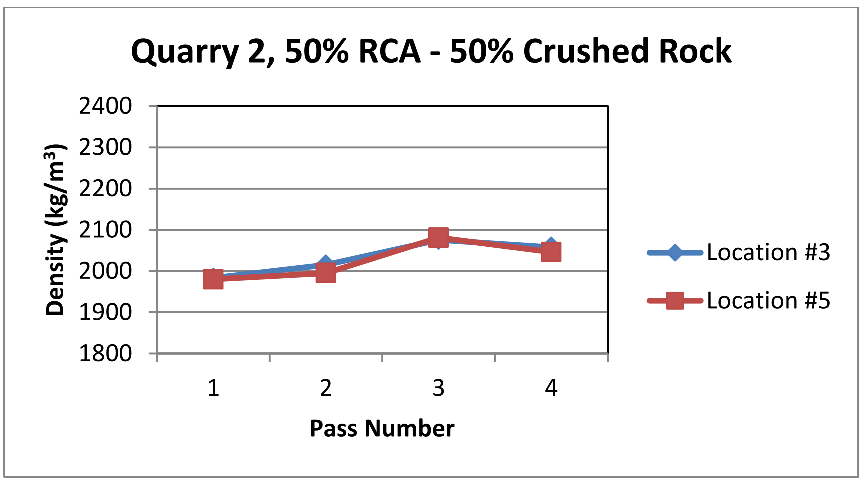

Figure 6-8. Compaction results for 50% rock / 50% RCA Granular B Type II at Quarry 2

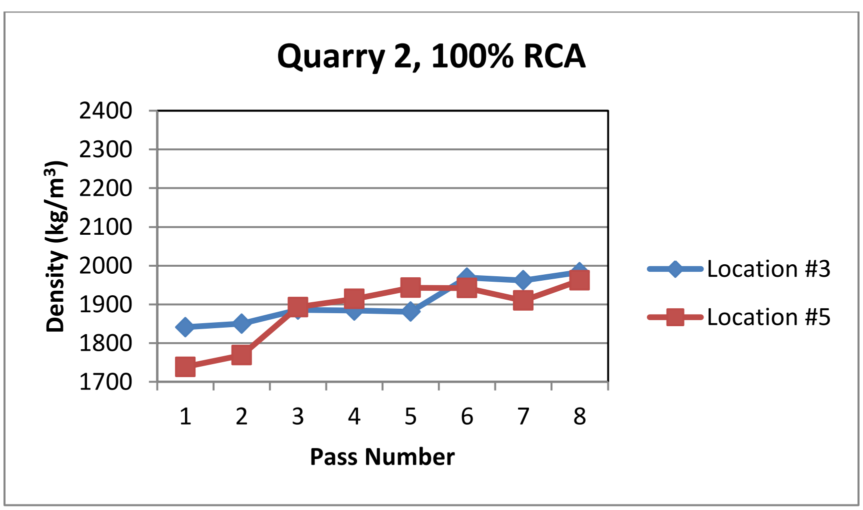

Figure 6-9. Compaction results for 100% RCA test mix at Quarry 2

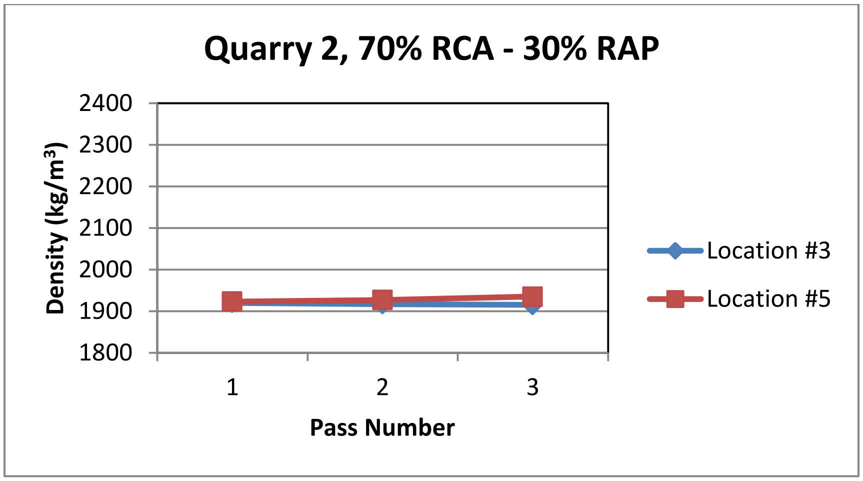

Figure 6-10. Compaction results for 70% RCA - 30% RAP test mix at Quarry 2

6.2 Gradation and Physical Properties

At Quarry 1, the 100% crushed rock and 100% RCA test mixture gradations indicate that there is a propensity to further break down during roller compaction (Tables A-11 and A-14). The 100% crushed rock test mix had an increase of 1.5 percent in the material passing the 75 µm sieve after compaction. However, the 100% RCA test mix and the blended materials using crushed rock with RCA and RCA with RAP show only a slight increase in the material passing the 75 µm sieve (Tables A-12, A-13 and A-15).

The test mixtures at Quarry 1 had coarse aggregate Micro-Deval abrasion losses ranging from 17.7 to 19.8 percent and the OPSS Granular B Type II maximum loss is 30 percent. The fine aggregate losses ranged from 11.2 to 24.1 percent and the OPSS Granular B Type II maximum loss is 35 percent. The asphalt-coated particle content for the 70% RCA - 30% RAP test mixture was 28.5 percent. The amount of contamination in the 100% crushed rock test mixture was 0 percent and the other mixtures were not tested. The plasticity index testing found both the 100% crushed rock and 100% RCA test mixtures to be non-plastic, while the remaining mixtures were not tested for plasticity (Table A-16).

At Quarry 2, the 100% crushed rock test mix shows a propensity to break down further during roller compaction (Table A-17). The 100% crushed rock had an increase of 1.9 percent in the material passing the 75 μm sieve after roller compaction. However, the 100% RCA test mix and blended materials using crushed rock with RCA and RCA with RAP show minimal degradation due to roller compaction (Tables A-18 to A-21).

The test mixtures at Quarry 2 had coarse aggregate Micro-Deval abrasion losses ranging from 12.8 to 15.8 percent and the OPSS Granular B Type II maximum loss is 30 percent. The fine aggregate losses ranged from 10.6 to 25.7 percent and the OPSS Granular B Type II maximum loss is 35 percent. The asphalt-coated particle content for test mixture 70% RCA and 30% RAP was 29.3 percent. The 100% RCA test mixture had 3.0 percent asphalt-coated particles resulting in the test mixtures of 25% RCA - 75% crushed rock and 50% RCA - 50% crushed rock having asphalt-coated particles of 0.5 and 0.8 percent respectively. The amount of contamination in the test mixture 100% crushed rock was 0 percent and the other test mixtures ranged from 0.1 to 2.7 percent. The plasticity index testing found all test mixtures to be non-plastic (Table A-22).

All of the tables referenced above in this section may be found in Appendix A.

6.3 Lightweight Deflectometer Measurements

As described in Section 4.6, a portable lightweight deflectometer (LWD) unit was used to obtain field values for the moduli of the compacted prepared subgrade and test mixture layers in the test pads at each field test site. The in-situ moduli were calculated using the following equation, from Boussinesq's theory for an elastic half-space assuming a rigid plate:

$$E = \frac{\pi\left(1-v^2\right)\mathrm{r}\sigma_0}{2\mathrm{d}_1} \quad (1)$$

Where:

- E = material modulus (MPa);
- v = Poisson's ratio (assumed to be 0.35);

- r = radius of the LWD loading plate (150 mm);
- σ_0 = maximum applied stress (kPa); and
- d_1 = maximum deflection under the plate center (μm).

Average, minimum and maximum in-situ moduli and standard deviations, were calculated for each test pad at Quarry 1 and Quarry 2 and are shown in Table 6-1. Full LWD measurement data tables can be found in Appendix B.

Table 6-1. Granular material moduli calculated from LWD measurements

Source	Test Pad	LWD Modulus Values (MPa)								Test Mixture
		Prepared Subgrade Layer				Subbase Test Mixture Layer				
		Avg.	Std. Dev.	Lowest	Highest	Avg.	Std. Dev.	Lowest	Highest	
Quarry 1	#1	97.5	13.8	66.8	124.1	85.3	8.0	64.7	99.4	100% Crushed Rock
Quarry 1	#4	103.2	15.0	67.2	131.6	79.6	11.0	57.7	96.4	25% RCA - 75% CR
Quarry 1	#3	91.5	26.3	50.4	143.7	60.4	12.6	38.0	78.8	50% RCA - 50% CR
Quarry 1	#2	91.2	8.8	74.0	104.9	59.9	6.1	47.7	73.6	100% RCA
Quarry 1	#5	98.3	15.0	63.2	123.3	75.9	9.7	52.2	93.7	70% RCA - 30% RAP
Quarry 2	#1	100.2	32.0	63.0	172.3	73.0	19.2	39.5	109.3	100% Crushed Rock
Quarry 2	#4	227.5	76.0	85.9	339.5	85.3	12.9	62.9	108.6	25% RCA - 75% CR
Quarry 2	#5	125.6	35.6	64.2	188.0	62.1	23.3	23.7	92.2	50% RCA - 50% CR
Quarry 2	#2	133.3	63.7	61.7	267.7	64.6	16.5	26.5	88.0	100% RCA
Quarry 2	#3	119.8	37.9	72.9	185.0	81.1	20.9	47.0	124.0	70% RCA - 30% RAP

At Quarry 1, the average compacted in-situ moduli for the compacted test materials appear to generally be lowest for the 100% RCA and 50% RCA - 50% crushed rock mixes relative to the 100% crushed rock, 25% RCA - 75% crushed rock, and 70% RCA - 30% RAP test mixes. Both of the test pads where the lowest average results occurred also had the lowest average in-situ moduli in the underlying 15 cm thick Granular A layer.

At Quarry 2, the 25% RCA - 75% crushed rock and 70% RCA - 30% RAP mixes were found to have higher in-situ moduli on average than the respective 100% crushed rock control material. Correspondingly, the 50% RCA - 50% crushed rock and 100% RCA test mixes showed lower average in-situ moduli compared to the control material test pad. It should, however, be noted that the elevated average modulus for the compacted 25% RCA - 75% crushed rock test mix at

Quarry 2 occurred in a test pad that also exhibited an unusually high average in-situ modulus for the underlying existing granular fill layer, which showed high variability at all Quarry 2 test pads.

All of the average in-situ moduli for the Granular B Type II test mixtures in Table 6-1 are substantially lower than the values obtained through the triaxial resilient modulus testing, which are presented in Section 6.7. Some level of difference should reasonably be expected to exist between these test results, as LWD measurements take place at the top surfaces of the compacted test pad layers, with the near-surface material experiencing a correspondingly low or near-zero level of confining bulk stress. This stress condition would not normally exist for a subbase layer in a typical pavement structure, as such a layer is normally subject to stresses from overlying granular base and bound surface layers. The maximum vertically applied stresses measured in the individual LWD tests were applied in separate single drops of the testing weight upon the unconfined surface of the test pad and generally varied from 235 to 245 kPa (see Appendix B). This significantly exceeded the axial stresses applied cyclically by the load cell in the lowest bulk stress stages of the resilient modulus testing procedure, where the lowest confining pressure applied to the sample in three dimensions was approximately 20 kPa (see Appendix C). In addition to these factors, the on-site LWD testing took place on test pads consisting of the in-situ test mixtures, whereas the laboratory resilient modulus tests involved the removal of oversized particles with no compensation applied for the removal of oversize particles.

A further comparison of the test mixture in-situ moduli mean values, with error bars representing single standard deviations, can be seen in Figure 6-11.

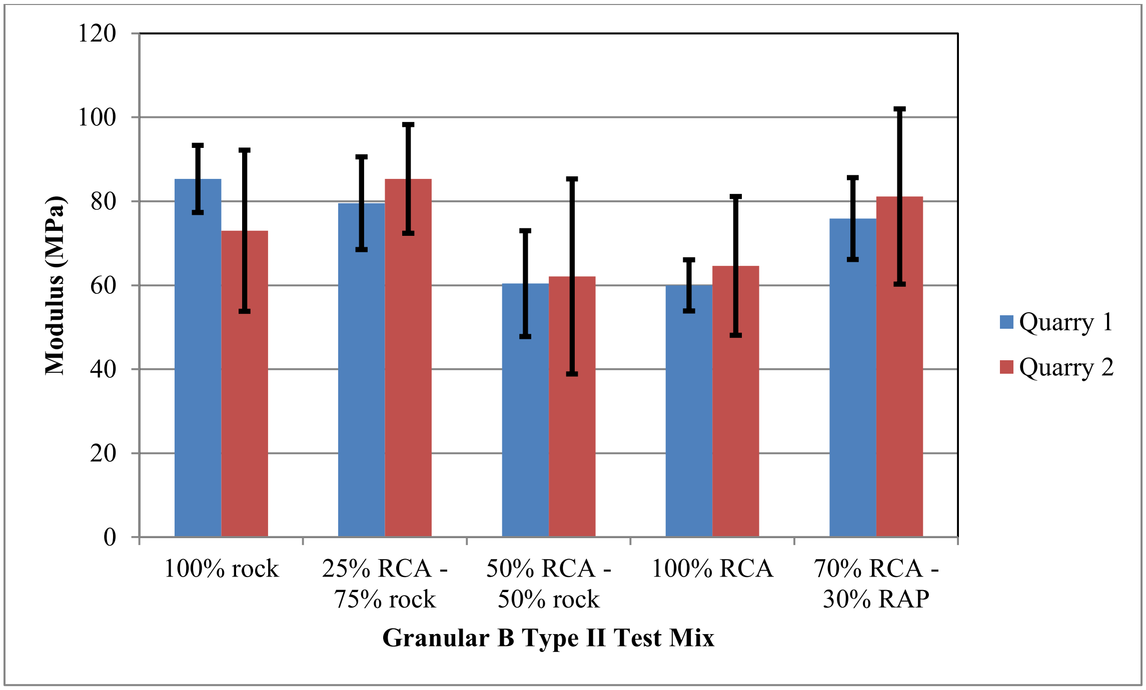

Figure 6-11. Granular B Type II test pad moduli mean values and standard deviations

As shown above in Figure 6-11, the subbase test mixture layer moduli generally exhibit greater variability at Quarry 2 relative to Quarry 1, possibly as a result in differences in the subgrade layer conditions between both quarries. The test pads at Quarry 1 were constructed with a prepared subgrade layer (26.5mm dense graded crushed rock) in each test pad placed and compacted directly on top of the bedrock prior to the addition and compaction of the subbase test mixtures. By contrast, Quarry 2 utilized an existing granular haul road as the working area for the construction of the test pads. As described in Section 4.2, localized grading and compacting was conducted to level the test pad locations at Quarry 2 prior to adding the subbase test mixtures. The existing haul road materials which formed the subgrade layer at Quarry 2 appeared inconsistent in both composition and gradation and would have been subject to highly variable compaction and intermittent disturbances over the entire operational lifespan of the local portion of Quarry 2. Additional variation in both the existing road granular material and the subbase test mixtures at Quarry 2 may have been introduced due to local rainfall which occurred on the days leading up to the test pad construction as well as on the morning of the field test.

If the single standard deviation bars in Figure 6-11 are extended to the 95% confidence interval (approximately 1.96 standard deviations), it can be noted that the wide variability of in-situ testing results causes most of the individual average material moduli to fall within the 95% confidence intervals of each other. Mixes produced at other quarries may also differ depending on the characteristics of the natural aggregates, RCA and RAP produced in different regions. The LWD apparatus itself may also be highly sensitive to seating conditions and to localized variations in the material upon which it sits.

Previous studies have also noted the high variability of in-situ modulus results using LWD testing and expressed the need for caution when using the LWD to examine the stiffness of pavement layers. Volovski, Arman and Labi (2014) noted that such a level of variability was observed across different LWD contact locations, even locations with the same material type, that it was not possible to guarantee that measurements obtained from a limited number of test sections could be transferred with confidence to another site of the same material type. In an earlier report, Hossain and Apeagyei (2010) investigated the suitability of the LWD in measuring in-situ pavement layer moduli and recommended that LWD testing should not be used for construction quality control until further research could be conducted to determine the underlying causes of the high spatial variability on moduli measured using an LWD and the effect of moisture content on the same results.

6.4 Standard and Modified Proctor Results

Standard and modified Proctor tests were conducted on each test mix from Quarry 1 and from Quarry 2 as outlined in Section 5.1. Full plots of the unmodified laboratory Proctor test results for the test mixes may be found below in Figures 6-12 to 6-21.

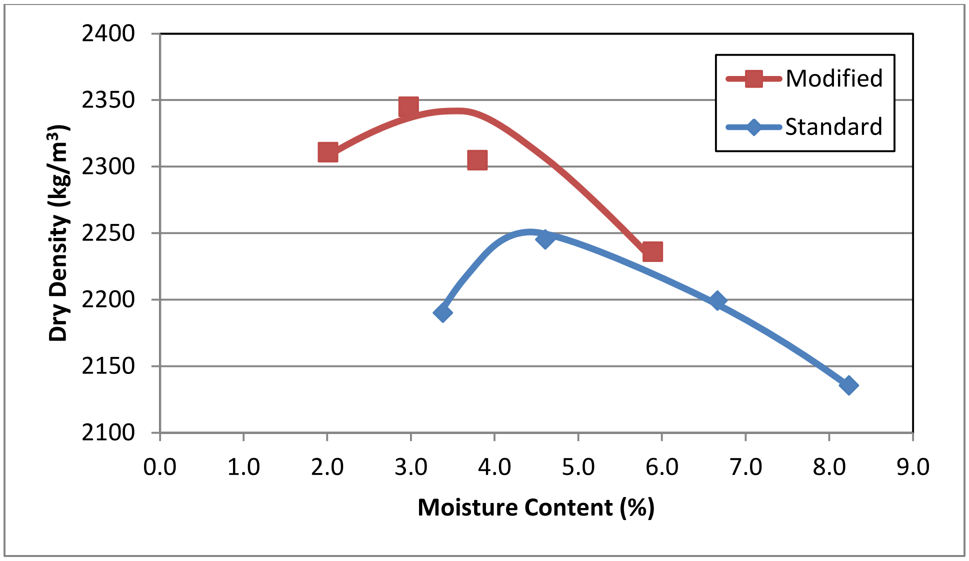

Figure 6-12. Proctor test results for 100% crushed rock test mix at Quarry 1

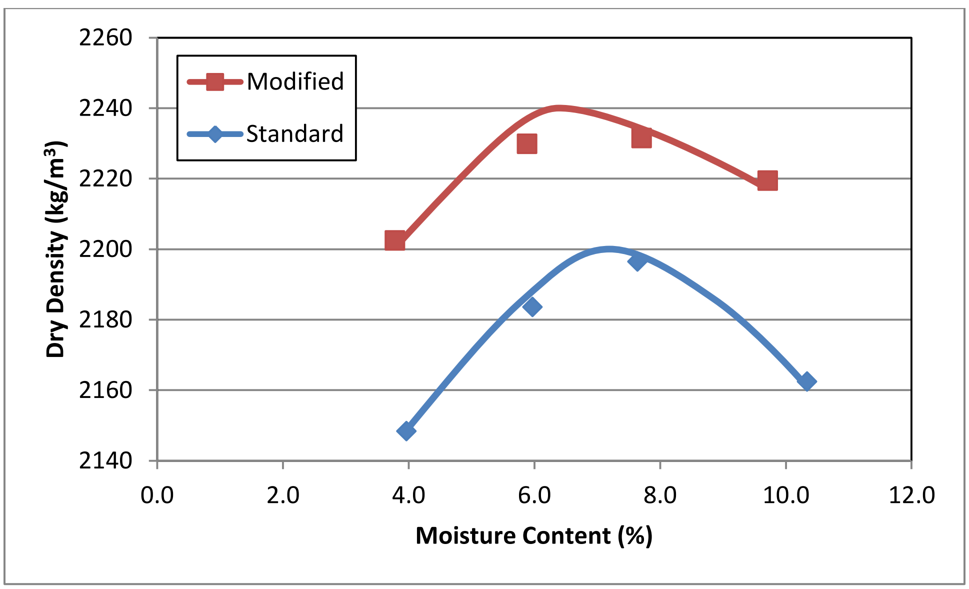

Figure 6-13. Proctor test results for 25% RCA - 75% crushed rock test mix at Quarry 1

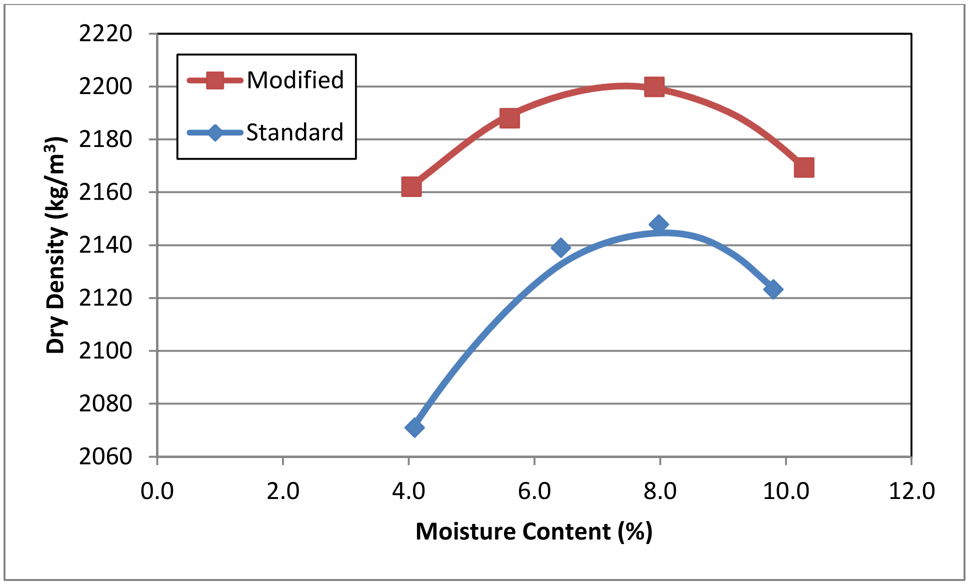

Figure 6-14. Proctor test results for 50% RCA - 50% crushed rock test mix at Quarry 1

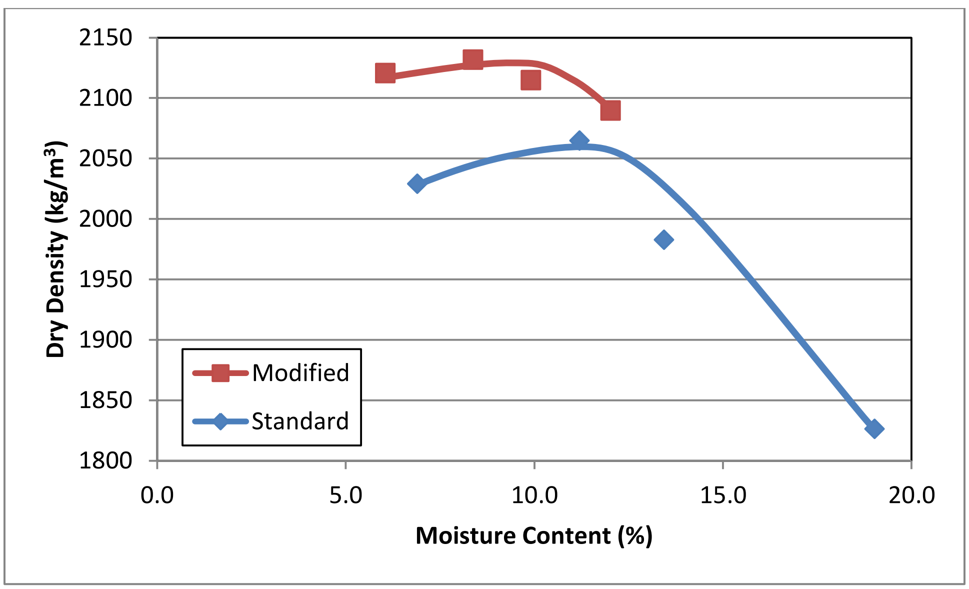

Figure 6-15. Proctor test results for 100% RCA test mix at Quarry 1

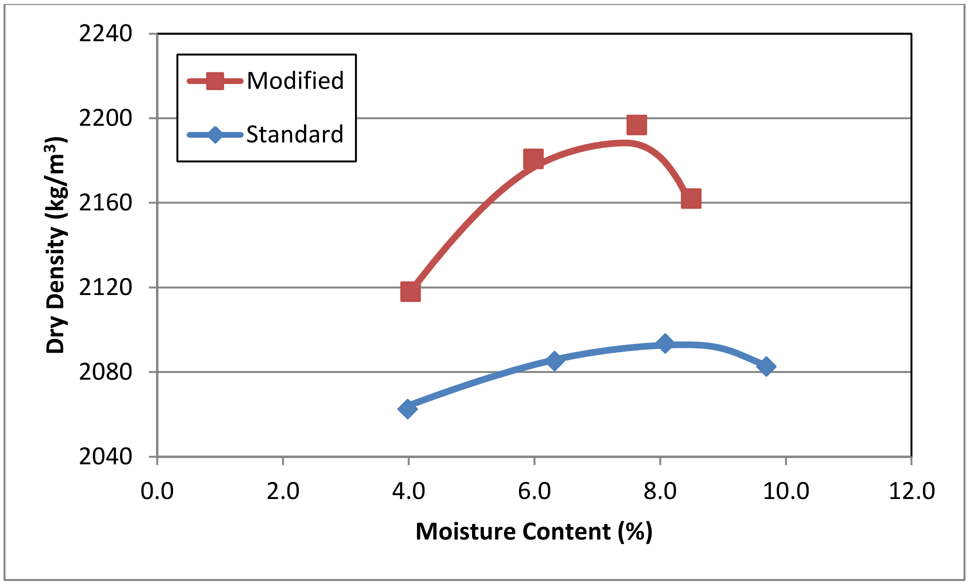

Figure 6-16. Proctor test results for 70% RCA - 30% RAP test mix at Quarry 1

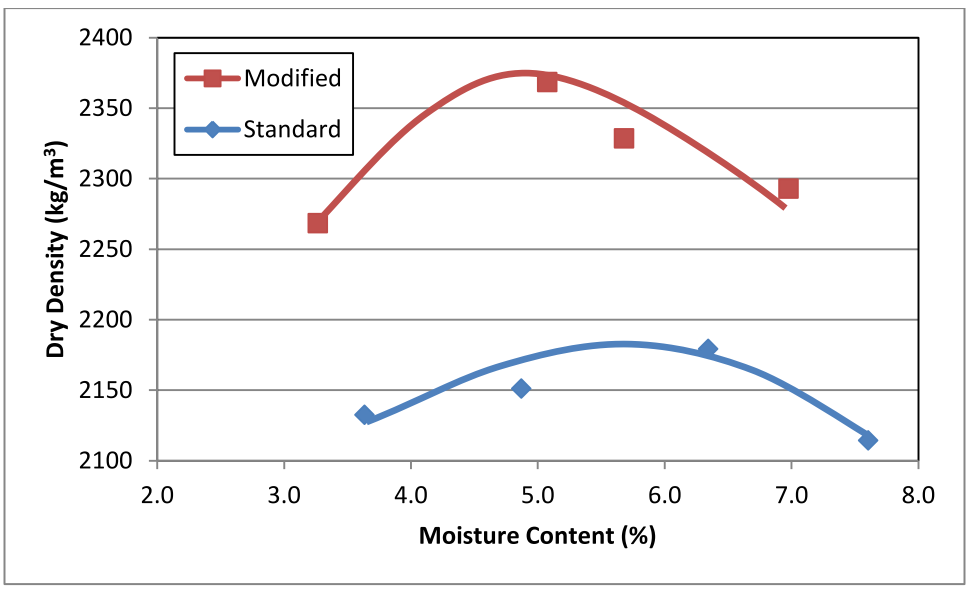

Figure 6-17. Proctor test results for 100% crushed rock test mix at Quarry 2

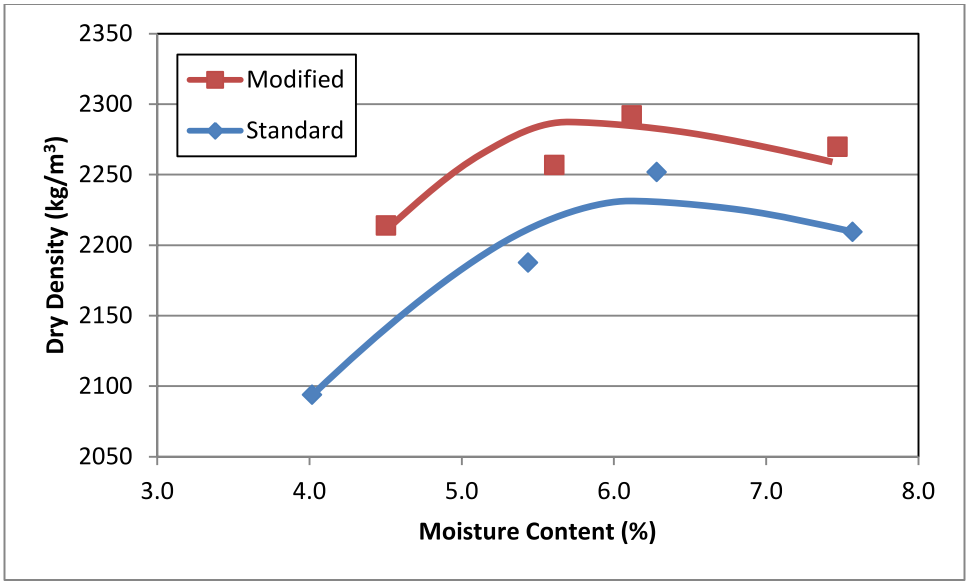

Figure 6-18. Proctor test results for 25% RCA - 75% crushed rock test mix at Quarry 2

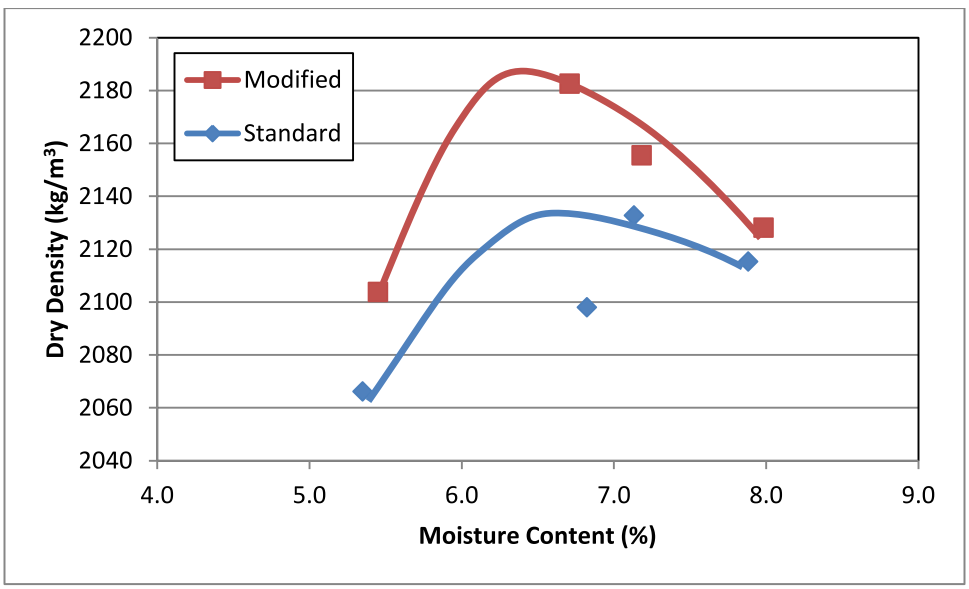

Figure 6-19. Proctor test results for 50% RCA - 50% crushed rock test mix at Quarry 2

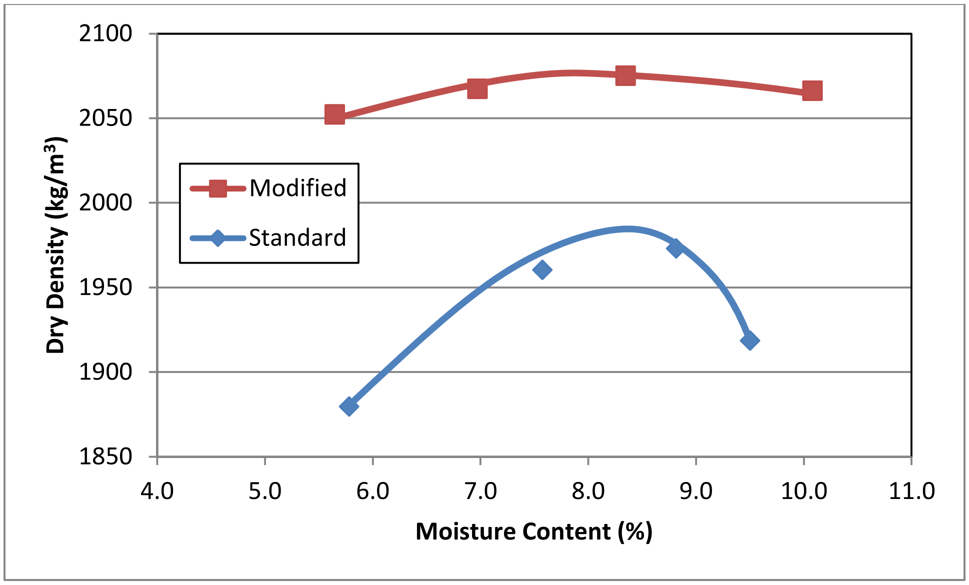

Figure 6-20. Proctor test results for 100% RCA test mix at Quarry 2

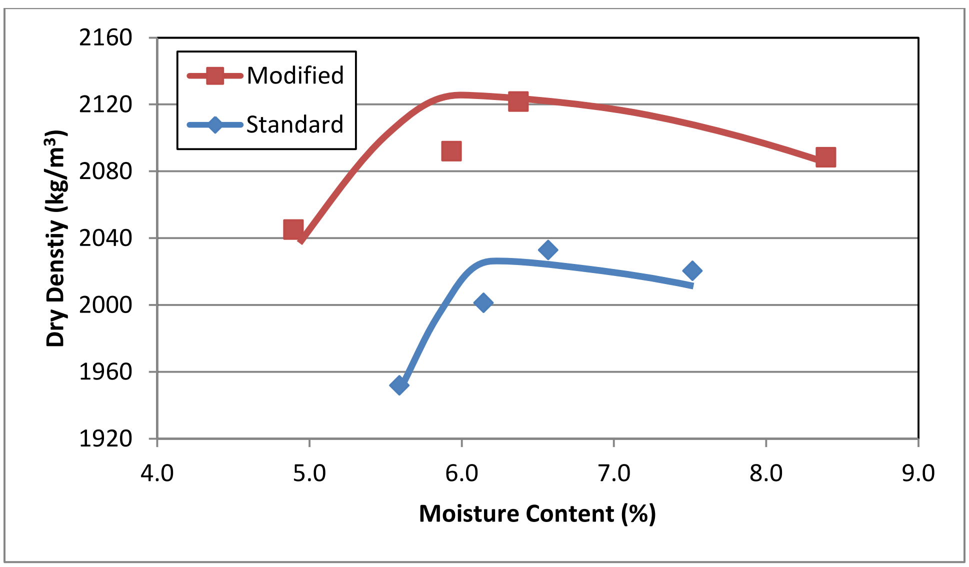

Figure 6-21. Proctor test results for 70% RCA - 30% RAP test mix at Quarry 2

The standard and modified Proctor test results are summarized below in Table 6-2. These results are also compared to the final field compaction dry density and moisture content averages for each test pad which are presented in Section 6.1 and included in Appendix A.

Table 6-2. Standard and Modified Proctor test results

Test Mix Blend	Standard Optimum Moisture Content	Standard Maximum Dry Density	Modified Optimum Moisture Content	Modified Maximum Dry Density	Average Final Field Moisture Content	Average Final Field Dry Density	Difference of FFDD Relative to SMDD
	(%)	(kg/m^3)	(%)	(kg/m^3)	(%)	(kg/m^3)	(%)
Quarry 1 - 100% Crushed Rock	4.4	2250	3.6	2344	2.6	2274	+ 1.1%
Quarry 1 - 25% RCA - 75% Crushed Rock	7.2	2201	6.4	2241	5.3	2131	- 3.2%
Quarry 1 - 50% RCA - 50% Crushed Rock	8.1	2144	7.5	2200	6.0	2042	- 4.8%
Quarry 1 - 100% RCA	11.5	2055	9.8	2130	5.4	2024	- 1.5%
Quarry 1 - 70% RCA - 30% RAP	8.5	2094	7.8	2184	10.6	1953	- 6.7%
Quarry 2 - 100% Crushed Rock	5.7	2183	4.9	2375	3.5	2286	+ 4.7%
Quarry 2 - 25% RCA - 75% Crushed Rock	6.1	2231	5.7	2285	5.9	2217	- 0.6%
Quarry 2 - 50% RCA - 50% Crushed Rock	6.6	2135	6.4	2188	6.6	2052	- 3.9%
Quarry 2 - 100% RCA	8.4	1983	7.9	2077	8.7	1973	- 0.5%
Quarry 2 - 70% RCA - 30% RAP	6.2	2025	6.0	2125	8.4	1925	- 4.9%

The laboratory test results seen in Table 6-2 reflect the general expectation that greater compaction efforts seen in the modified Proctor test yield lower optimum moisture contents and higher compacted dry densities relative to the standard Proctor test. Furthermore, as the percentage content of RCA increases, the standard and modified optimum moisture contents also increase and the respective optimum dry densities decrease, in accordance with the higher absorption characteristics and lower bulk density of crushed concrete aggregate relative to natural aggregate noted by a number of studies reviewed in Chapter 3. No absorption or petrographic testing was carried out on the test mixes from Quarry 1 and Quarry 2, although percent RAP content testing was completed and is included in Tables A-16 and A-22 in Appendix A.

For the Quarry 1 test mixtures, the field moisture contents to achieve maximum field dry density were generally lower than the optimum moisture contents determined by standard Proctor testing, with the exception of the 70% RCA - 30% RAP blend where the field moisture content was higher than the standard Proctor result for the same blend. The average compacted field dry densities were lower than the optimal dry densities determined by the standard Proctor test, except for the 100% crushed rock control mix, where the field dry density was slightly higher than the standard Proctor density. Furthermore, as the proportion of RCA increased, the resulting standard and modified maximum Proctor density values and final field densities decreased correspondingly.

For the Quarry 2 test mixtures, the field moisture contents to achieve maximum field dry density were lower than the optimum moisture contents determined by standard Proctor testing, with the exception of the 100% RCA and 70% RCA and 30% RAP test mixtures where the field moisture content were higher than the moisture content as determined by the standard Proctor test. The field dry density results were lower than the standard Proctor result for each blend, with the exception of the 100% crushed rock test mixture, where the field dry density was higher than the standard Proctor density result for the same material. Similar to Quarry 1, as the proportion of RCA increased, the resulting standard and modified maximum dry density values and final field densities decreased correspondingly.

When comparing the standard Proctor density and field dry density of the 100% crushed rock control mixes at Quarries 1 and 2 to gradations before and after field compaction (see Appendix A), there is a pattern indicating that as the gradation gets finer and there is an increase in material passing the 75 μm sieve, then there is also an increase in the dry density value. However, the field moisture contents decreased in both materials compared to the standard Proctor moisture content results. A comparison of the remaining test mixtures indicates the field dry densities are lower than the standard Proctor densities from both Quarries 1 and 2, even though for the Quarry 1 test mixtures of 25% RCA - 75% crushed rock and 100% RCA, as well as the Quarry 2 test mixtures of 25% RCA - 75% crushed rock and 50% RCA - 50% crushed rock, the field gradations after compaction were slightly finer overall but the proportion passing the 75 μm sieve did not increase significantly.

6.5 California Bearing Ratio Measurements

The CBR values seen below in Table 6-3 are all relatively high, achieving above 100% for most of the subbase test mixtures. Furthermore, the test mixtures with high replacement levels of RCA achieved high bearing capacities, which indicate that the introduction of RCA did not hinder the performance of the subbase material. However, one interesting observation is the lower values achieved by the test mixtures containing RAP. The presence of 30% RAP was seen to reduce the CBR values of the aggregate mixes by 30-40%, when compared to the other test mixtures which contained only natural crushed rock and RCA in varying proportions. Additionally, it is possible that the removal and replacement of oversize particles that are normally present in Granular B Type II class materials (described in Section 5.2) in accordance with the ASTM D1883 procedure may have had an effect on the results of this test, as the altered material would be more similar in composition to a finer class of granular fill, such as a 26.5mm dense graded base material.

Table 6-3. California Bearing Ratio test results

Test Mixture	CBR Results (%)	
	Quarry 1	Quarry 2
100% Crushed Rock	108.5	94
25% RCA – 75% Crushed Rock	108.5	90
50% RCA – 50% Crushed Rock	114.5	91
100% RCA	107.5	114
70% RCA – 30% RAP	78.5	72

6.6 Permeability Measurements

The results of the permeability tests seen in Table 6-4 indicate that the test mixtures are all relatively free-draining granular materials, and the increased amount of reclaimed materials has minimal impact on the overall permeability. The observed permeability values ranging from 10^{-2} cm/s to just under 10^{-3} cm/s indicate consistently good drainage characteristics in all of the test mixtures. At both quarries, each set of five test blends had relatively consistent proportions of particles passing the 75µm sieve. The test blends at Quarry 2 were also faster-draining than most of their respective counterparts at Quarry 1, despite generally higher proportions of particles passing the 75µm sieve.

Table 6-4. Permeability testing results

Test Mixture	Quarry 1		Quarry 2	
	Permeability (cm/s)	Percent Passing 75µm Sieve	Permeability (cm/s)	Percent Passing 75µm Sieve
100% Crushed Rock	1.45E-03	4.7%	6.65E-03	5.8%
25% RCA - 75% Crushed Rock	1.02E-03	4.4%	1.00E-02	8.4%
50% RCA - 50% Crushed Rock	4.65E-03	3.8%	8.65E-03	6.9%
100% RCA	8.95E-04	4.4%	4.75E-03	6.4%
70% RCA - 30% RAP	3.30E-03	4.7%	9.10E-03	6.9%

6.7 Resilient Modulus Measurements

For the analysis of resilient modulus triaxial testing results, the data points obtained from the triaxial testing apparatus were fitted to the k_1-k_3 model (Buchanan, 2007) used in the AASHTO mechanistic-empirical pavement design guide. The following model was used, and the method of least squares regression was then used to calculate the values of k_1, k_2 and k_3.

$$M_r = k_1 P_a \left(\frac{\theta}{P_a} \right)^{k_2} \left[\left(\frac{\tau_{oct}}{P_a} \right) + 1 \right]^{k_3} \qquad (2)$$

Where:

- k_1, k_2, and k_3 = material-specific regression coefficients;
- θ = bulk stress;
- P_a = atmospheric pressure (i.e. 101.3 kPa); and
- τ_{oct} = octahedral shear stress $= \frac{1}{3}\sqrt{(\sigma_1 - \sigma_2)^2 + (\sigma_2 - \sigma_3)^2 + (\sigma_3 - \sigma_1)^2}$

Full data tables and material-specific regression coefficient results may be found in Appendix C.

For all three test samples of each mixture from each quarry, at each of the fifteen loading stages contained in the triaxial testing procedure, the bulk stress was determined and the resilient modulus was calculated using the regression coefficients estimated from the raw data and using Equation (2) above. For each set of three tests on each mixture, the average bulk stress and resilient modulus were determined at each of the fifteen loading stages, and using the average resilient modulus values at each loading stage, the percent deviation was calculated for the respective individual test sample resilient moduli.

Kancherla (2004) gives an approximate tolerable error of 12.5% corresponding to a population of three resilient modulus tests on any given material. However, this limit was calculated based on testing unbound granular materials composed solely of natural aggregates and prepared in a laboratory to the same overall master grain size distribution. Correspondingly, the variability will generally be anticipated to be higher when dealing with production samples containing recycled or reclaimed materials, where the consistency of the material would reasonably be expected to vary to a greater degree. Consequently, a limit of 20% allowable error was chosen for this study, and among each set of three tests on each mix, any samples where the resilient modulus results deviated more than 20% (averaged across all fifteen loading stages) from the overall average profile was excluded as an outlier and the average bulk stress and resilient modulus profile was recalculated using the remaining test samples for that material.

The average resilient modulus vs. bulk stress profiles for each material, excluding outliers as described above, are presented in Figures 6-22 and 6-23. Across all materials from Quarry 1 and Quarry 2, none of the test mixtures had any more than one sample identified and excluded as an outlier; as a result, all of the average profiles in the figures below are based on a total of two to three triaxial tests completed on each test mixture. Among Quarry 1 materials, the 25% RCA - 75% crushed rock and 50% RCA - 50% crushed rock test mixtures were found to have higher average resilient modulus values than the respective 100% crushed rock control test mixture, while the 100% RCA and 70% RCA - 30% RAP test mixtures had similar results to the 100%

crushed rock test mixture. Among Quarry 2 materials, the 25% RCA - 75% crushed rock and 50% RCA - 50% crushed rock test mixtures and the 70% RCA - 30% RAP test mixture were found to have similar average resilient modulus values compared to the 100% crushed rock test mixture, while the 100% RCA test mixture had lower average resilient modulus results at higher levels of bulk stress.

Overall, the average resilient modulus values found for the test mixtures containing RCA and RAP are broadly similar to those obtained from the 100% crushed rock test mixtures, although some variability is apparent between the granular materials which were produced separately at Quarry 1 and at Quarry 2.

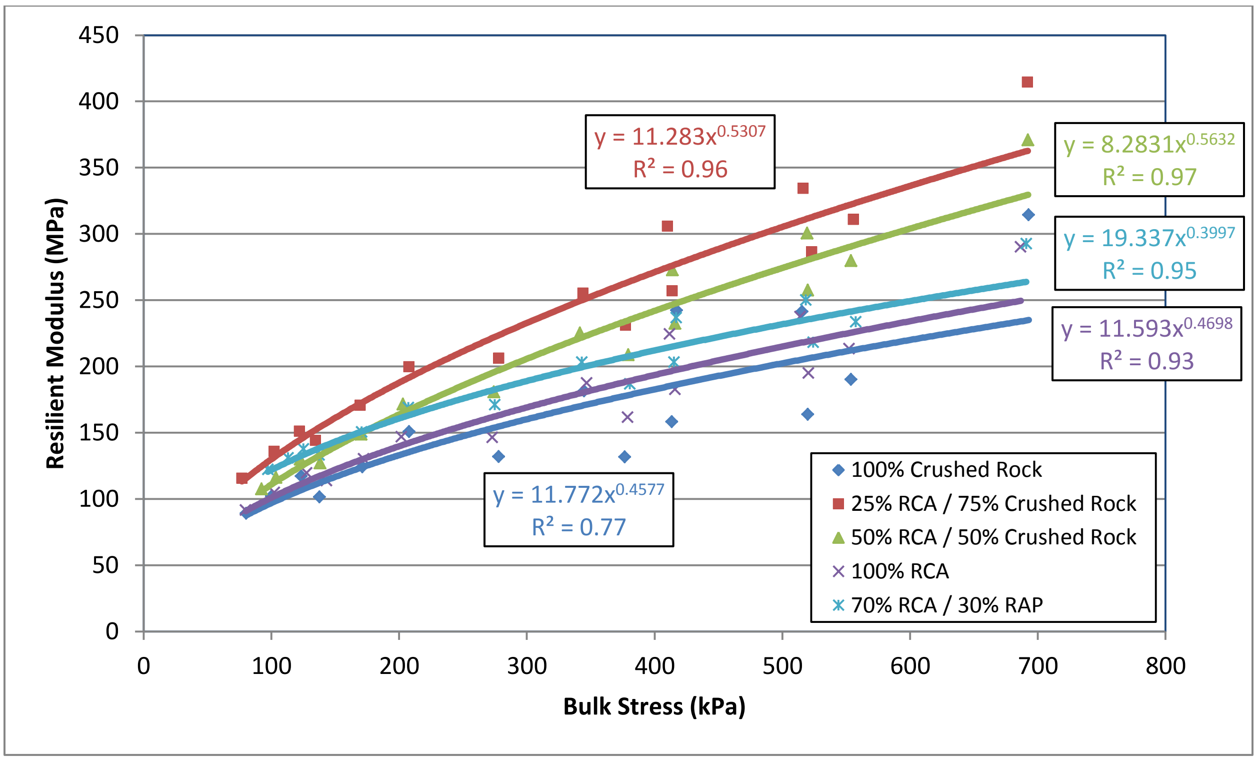

Figure 6-22. Resilient Modulus testing results for subbase test mixtures at Quarry 1

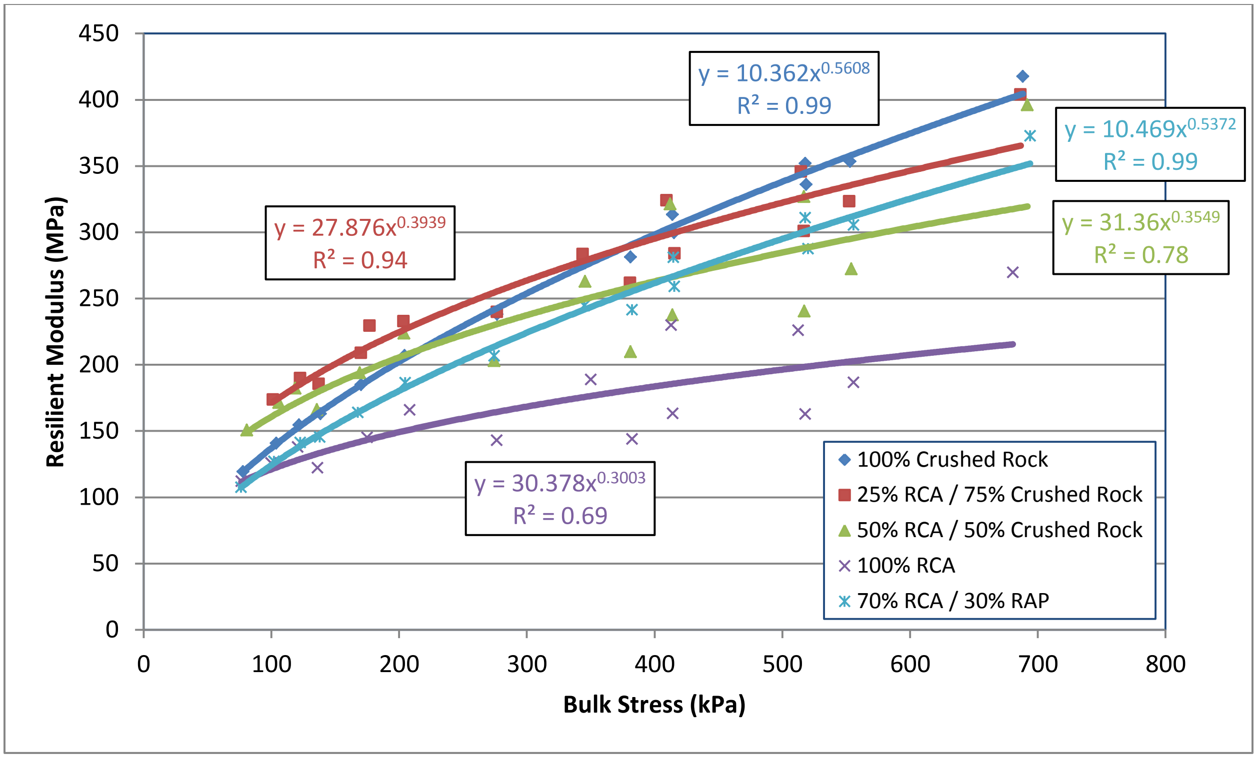

Figure 6-23. Resilient Modulus testing results for subbase test mixtures at Quarry 2

The results in Figures 6-22 and 6-23 also show that the values of the resilient modulus (M_r) increase along with increased bulk stress as expected. The overall bulk stress reflects the state of confinement of the granular material within the pavement structure. In Ontario, the default value of M_r used in AASHTOWare Pavement ME Design software for Granular B Type II material is 200 MPa (Ministry of Transportation of Ontario, 2012). Although this value appears relatively high, it should be noted that it is attained by most of the tested materials at bulk stress levels between 150 and 520 kPa. In the case of Quarry 1, it is the 100% crushed rock test mixture that has the lowest slope of M_r versus bulk stress and the lowest values of M_r overall, where the level of 200 MPa is obtained at approximately 500 kPa bulk stress. In the case of the Quarry 2 materials, it is the 100% RCA test mixture that has the lowest slope and lowest values of M_r, and the 200 MPa level is obtained when the bulk stress reaches approximately 520 kPa. These two test mixtures (100% crushed rock from Quarry 1 and 100% RCA from Quarry 2) showed high variability in the obtained results; however, all of the obtained results across all of the tested materials are relatively good. Even at very low bulk stress states (80 kPa), most of the resilient modulus values obtained were higher than 100 MPa, which is close to the range of values obtained with in-situ LWD testing as described earlier in this report.

CHAPTER 7
STUDY CONCLUSIONS

Based on the results of the field and laboratory testing program carried out in this study, the following conclusions are given:

- Subbase mixtures incorporating RCA and/or RAP demonstrated similar field rolling compactibility relative to the 100% crushed rock OPSS Granular B Type II control mix.
- During field compaction, the 100% crushed rock Granular B Type II at both Quarries 1 and 2 showed a tendency to break down in gradation and generate more material passing the 75µm sieve as measured by particle size analysis after compaction. The gradations of the Quarry 1 test mixtures of 25% RCA with 75% crushed rock and 100% RCA and the Quarry 2 test mixture of 25% RCA with 75% crushed rock were finer overall but the material passing the 75µm sieve did not increase significantly after field compaction. The test mixtures utilizing greater proportions of RCA as well as a combination of RCA and RAP showed minimal increases in material passing the 75µm sieve during compaction.
- Testing using the lightweight deflectometer (LWD) indicated that mixtures using elevated levels of RCA (50% to 100%) with crushed rock resulted in generally lower in-situ moduli of compacted subbase layers compared to 100% crushed rock and blends of 70% RCA with 30% RAP and 25% RCA with 75% crushed rock. However, it should be noted that the LWD measurements can be subject to substantial variability depending on local physical and hydrogeological conditions, as experienced in Quarry 2.
- Optimal moisture for field compaction varied between the two test sites and may be a function of the physical characteristics of the crushed rock, RCA and RAP materials as well as individual test mix gradations.
- Increased moisture is needed when utilizing RCA in dense graded subbase materials, which may be a function of the increased absorption for the recycled material when compared to the equivalent 100% crushed rock Granular B Type II control mixture, as noted by a number of previous studies reviewed in Chapter 3.

- The California Bearing Ratio (CBR) results for the test mixtures incorporating 100% crushed rock and crushed rock blended with RCA were all fairly similar, however both test mixtures of 70% RCA - 30% RAP had approximately 30 to 40% lower CBR values, indicating that the use of RAP at this level results in lower CBR values, as was also observed in the 1989 MTO report referenced in Chapter 3.
- The measured permeability coefficients ranged from 1.0 x 10^{-2} cm/s to 8.95 x 10^{-4} cm/s for all of the test mixtures, indicating consistently good drainage characteristics independent of RCA or RAP content levels.
- Triaxial resilient modulus testing yielded results for blends containing crushed rock with RCA as well as RCA with RAP which were similar overall to average resilient modulus values obtained from the 100% crushed rock Granular B Type II control material.

Based on the conclusions of the field and laboratory testing carried out in this study, it would appear that RCA and RAP are capable of successfully substituting for natural aggregates in test blends for a range of compositional proportions. It is recommended that multiple test sections should be completed in highway construction projects using the different subbase test mixture blends and monitored on an ongoing basis in order to verify their performance in the field and to gain more experience with the use of RCA and RAP in road construction. Contingent upon the success of the field trials, RCA and RAP may be permitted for use in Granular B Type II pavement subbase materials.

PART 2:

FOAM GLASS LIGHTWEIGHT AGGREGATE

CHAPTER 8
INTRODUCTION

In the road and pavement design and construction industry, a number of synthetic lightweight construction materials have been developed for use in a range of applications. Among these possibilities is the potential for roads which are less dense overall than those constructed with natural aggregates. This in turn can be crucial to the reliability of roads in locations where existing subsurface conditions pose challenges which necessitate designs minimizing the impacts of the static and transient loads imparted by both the pavement structure and the traffic upon the road surface.

The current conventional design solution for lightweight fill material in roadway structures within North America is expanded polystyrene (EPS). Polystyrene is a commonplace and well-known polymer material in a range of industries, and EPS blocks are known to be easy to form and to assemble into a pavement structure. However, concerns exist over the long-term strength and performance of layers composed of EPS, in addition to challenges from a sustainability perspective, where EPS blocks are not manufactured from recycled material and are not recyclable in turn. Foamyna Canada Inc. of Toronto, Ontario has proposed the use of foam glass lightweight aggregate (LWA) as a more sustainable lightweight fill solution offering improved strength characteristics as compared to conventional EPS blocks. However, foam glass LWA has not yet gained broader awareness or familiarity as a design solution for pavement structures within Canada and North America.

The purpose of this study is to complete a series of physical properties tests to characterize two foam glass LWA materials supplied by Foamyna Canada Inc. to the Centre for Pavement and Transportation Technology (CPATT) at the University of Waterloo. The results of these tests are analyzed and compared to known properties of conventional EPS to determine the impacts upon pavement design and life cycle costs for structures incorporating foam glass LWA. This work has been conducted in parallel to physicochemical properties testing carried out in partnership with Golder Associates Ltd., which is not detailed in these chapters. The aggregate materials under examination are being evaluated for their performance against standards set out by the Ontario Ministry of Transportation (MTO) for potential future usage in the design and construction of granular base and subbase layers in pavement structures.

CHAPTER 9
LITERATURE REVIEW

A number of studies worldwide have examined the characteristics of lightweight aggregate materials, including foamed glass, to determine their potential as sustainable design solutions in a range of engineering applications. Many recent studies focus on lightweight concrete materials produced using lightweight aggregates, but other studies can be found which center on unbound LWA materials.

In particular, the use of lightweight foam glass aggregates has been well-established in Norway. A 2003 paper by Frydenlund and Aabøe details the local introduction, production and early usage of foam glass as a sustainable alternative fill material. The authors note the economically favourable cost of foam glass materials as well as the chemical stability of the artificial aggregate.

A later 2005 paper by Aabøe, Øiseth and Hägglund presents further research and development work by the Norwegian Public Roads Administration (NPRA) to promote the use of recycled materials in road structures and in design standards and guidelines. Several field monitoring and laboratory testing programs are noted by the authors as demonstrating the successful application of foam glass in pavement construction projects as an alternative to conventional materials.

In Italy, Bernardo et al. (2007) conducted a study into the reutilization and stabilization of wastes in foam glass materials. The testing program found that the foamed glass had low leachability and could be considered chemically stable and environmentally safe. In addition, the inclusion of silicon-carbon (SiC) wastes and a manganese dioxide (MnO_2) oxidizer had positive effects on the homogeneity of the foam structure and thus a corresponding impact on the mechanical strength of the aggregate.

More recently, a 2013 paper by Auvinen, Pekkala and Forsman detailed a construction project carried out in downtown Hämeenlinna, Finland, where a series of bridge approach ramp embankments were constructed with the use of foam glass aggregates during reconstruction work on Highway E12 running through the city. This design option was selected due to poor underlying soil conditions including weak clays and peat. The authors noted that the embankments were constructed and compacted successfully and were able to bear active truck traffic immediately after construction.

In 2015, Arulrajah et al. conducted an investigation into the engineering properties of foamed recycled glass as a design alternative in civil infrastructure applications. The study found a low CBR value for foam glass of 9 to 12%, indicating low shear resistance at small displacement levels, but high values both for cohesion and friction angle. Combined with high Los Angeles (LA) abrasion loss results, the study recommended that foam glass aggregates should be used for applications such as non-structural fills in embankments and backfill, instead of pavement base and subbase layers. The study also noted very low concentrations of contaminants in leachate tests, indicating that the foamed recycled glass is chemically stable and non-hazardous.

Here in North America, a joint American/Canadian study by Hemmings et al. (2009) was conducted to compare physicochemical, microstructural and mineralogical characteristics between an artificial lightweight aggregate known as Versalite and three other commercially available materials including pumice, expanded shale and bottom ash. The study found substantial variations between the materials examined in terms of their total porosity, pore size distribution and structure, and their effects upon unit weight, compressive strength, thermal resistance and thermal conductivity when used in concrete mixes.

More recently, Segui et al. (2016) presented a paper at the 2016 conference of the Transportation Association of Canada on a study into the use of foam glass aggregates as road construction material, focusing on the potential of foam glass LWA for thermal insulation purposes to mitigate damage to roadways caused by freezing and thawing cycles in colder climates. The study found that use of a foam glass aggregate layer was efficient for providing pavement insulation and performed comparably well in this department to conventional expanded polystyrene, while the foam glass material provided good drainage characteristics and did not pose degradation or leaching risks to the environment. Additionally, the field trial showed that despite careful handling requirements, the foam glass aggregates were easy to use on-site and were able to be compacted with conventional densification methods.

CHAPTER 10
EXPERIMENTAL METHODS AND RESULTS

10.1 Tested Materials

In May and June of 2015, CPATT was supplied by Foamyna Canada Inc. with quantities of two distinct foam glass lightweight aggregate (LWA) materials. Both materials were produced by partner companies in Germany by melting down pre-processed recycled glass and mixing it with air and with trace quantities of chemical additives to form a highly porous, rigid foamed glass product with a bulk and absolute density substantially lower than that of water. The resulting material subsequently fractures in the process of cooling to form a coarse, poorly-graded artificial aggregate, which is currently marketed by Foamyna Canada Inc. for usage in a variety of structural, geotechnical and architectural applications.

For the purposes of the physical properties testing detailed in this chapter, the two materials received by CPATT were designated as LWA-A and LWA-B. Both materials possess a highly vesicular structure which is visually similar to pumice or scoria. By relative comparison between the two materials, LWA-A appears darker grey in colour with lighter grey to white on unfractured surfaces, while possessing smaller or finer voids and lower apparent density than LWA-B in hand specimens. Material LWA-B appears a uniform light grey in colour, with larger or coarser voids in its matrix and appearing slightly denser in hand specimens than LWA-A. Both materials appear to be quite brittle and prone to damage if improperly handled, necessitating the use of hand sieving for grain size analysis in lieu of mechanical sieving as described in Section 10.2. LWA-B appears more durable in this regard than LWA-A; a possible reason is that the larger voids in LWA-B appear to correspond with thicker walls between vesicles than those which exist in LWA-A. Further testing and examination of the microstructures of both LWA materials would be needed to confirm this observation.

A visual contrast between the two materials can be seen in Figure 10-1. A sufficient quantity of both materials was obtained and sampled to conduct the tests detailed in this report.

Figure 10-1. Comparison of visual appearance between LWA-A (left) and LWA-B (right)

The results of tests performed on LWA-A and LWA-B are summarized and discussed in the following sections. These results are evaluated against Ontario Provincial Standard Specification document OPSS.MUNI 1010, which includes materials specifications for aggregates in a range of different granular fill materials, designated depending on their respective geotechnical designs and applications. Both LWA-A and LWA-B are considered to be coarse aggregates where applicable in the relevant MTO Laboratory Testing Manual “LS” test methods.

A number of challenges were encountered as a result of LWA-A and LWA-B each having a specific gravity well below 1.0, as many test procedures locally applicable in North America are designed only to accommodate natural aggregates which are more dense than water. Consequently, a number of testing procedures needed to be significantly modified to suit the low-density character of artificial foam glass LWA.

10.2 Grain Size Analysis

Grain size distribution testing and analysis was performed on materials LWA-A and LWA-B based on MTO laboratory standard LS-602, Method of Test for Sieve Analysis of Aggregates.

Since the maximum sieve size of each material was not known, a minimum sample size of 10 kg was adopted, which is equivalent to the minimum mass required under LS-602 to test Granular A type materials. For both materials tested, 10 kg is approximately equivalent in volume to two full standard sized plastic sampling bags.

Due to the large particle size and low density of both LWA-A and LWA-B, it has been found that manual (hand) sieving is the most appropriate method for this type of materials. In total, six samples of a minimum of 10 kg each were obtained and analyzed, including three samples each of LWA-A and LWA-B. After hand sieving, both materials were retained in separated size fractions for the purposes of further testing procedures. As both materials are coarse aggregates, no sieving was performed on material passing the 4.75 mm sieve.

LWA-A and LWA-B were both found to have broadly similar grain size distributions. In both cases, all of the material passed the 75 mm sieve, with the 63 mm sieve being the largest size upon which any material was retained. For both materials, across all samples, less than 10% of the aggregate by mass passed through the 19.0 mm sieve. LWA-A had more material on average passing the 4.75 mm sieve at an average of 3.7% by mass, while LWA-B averaged 2.6% passing the 4.75 mm sieve. Both materials can thus be summarized as relatively coarse and poorly-graded aggregates.

Graphs of the grain size distributions for LWA-A and LWA-B can be found in Figure 10-2 and Figure 10-3 respectively, while the average gradations for both materials are compared against OPSS.MUNI 1010 requirements in Table 10-1. Full grain size analysis data can be found in Tables D-1 and D-2 in Appendix D.

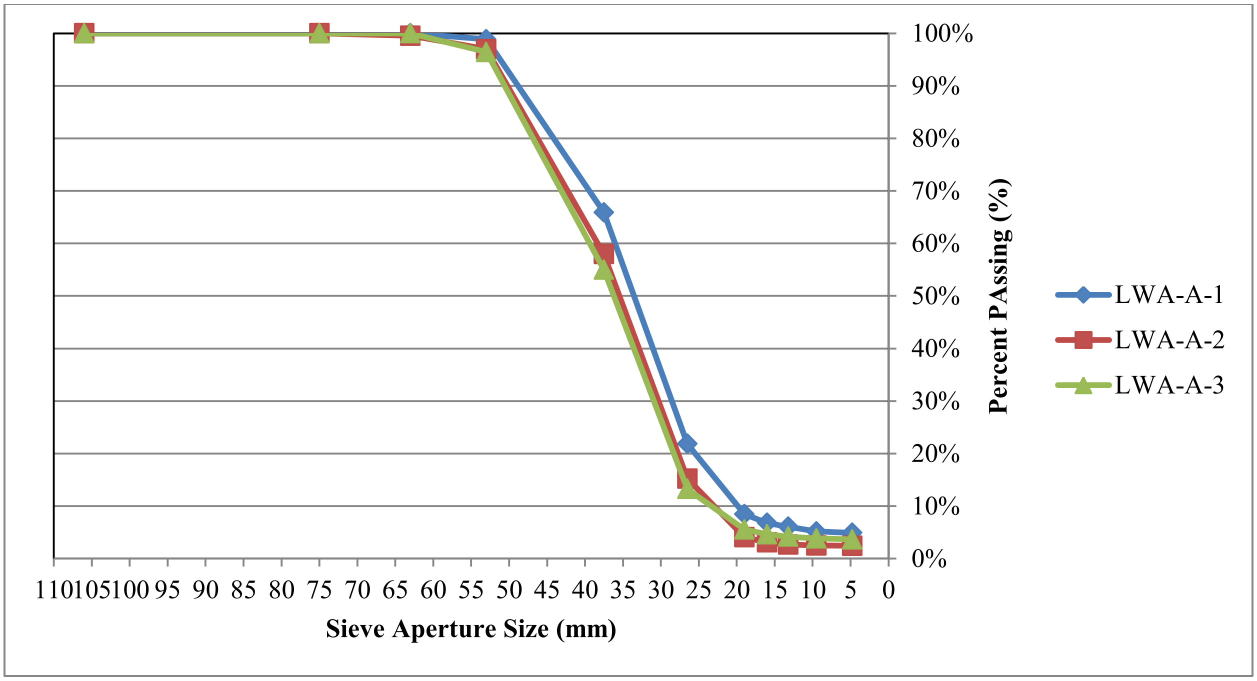

Figure 10-2. Grain size distribution for material LWA-A

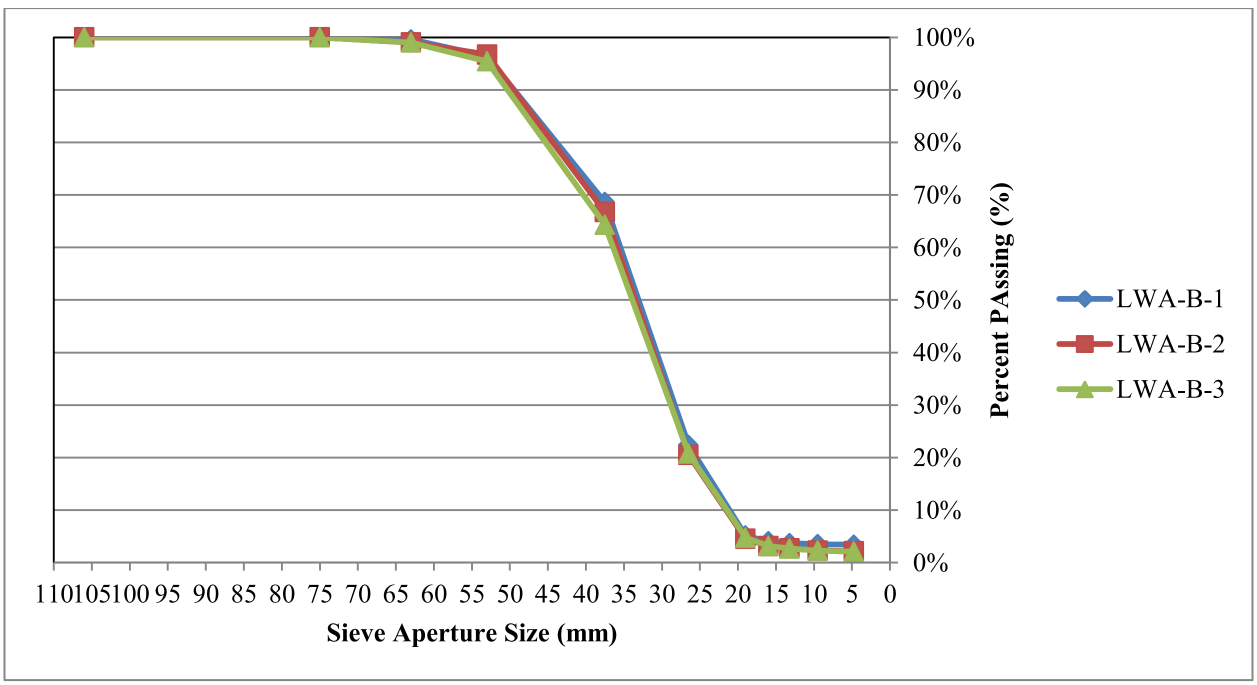

Figure 10-3. Grain size distribution for material LWA-B

Table 10-1. LWA grain size distributions compared against OPSS 1010

Sieve Size	Granular Classification							Select Subgrade Material (SSM)	LWA-A	LWA-B
	A	B			M	O	S			
		Type I	Type II	Type III						
150 mm	-	100	-	100	-	-	-	100	100.0	100.0
106 mm	-	-	100	-	-	-	-	-	100.0	100.0
37.5 mm	-	-	-	-	-	100	-	-	59.6	66.6
26.5 mm	100	50-100	50-100	50-100	-	95-100	100	50-100	16.8	21.2
19.0 mm	85-100	-	-	-	100	80-95	90-100	-	6.0	4.8
13.2 mm	65-90	-	-	-	75-95	60-80	75-100	-	4.3	3.0
9.5 mm	50-73	-	-	32-100	55-80	50-70	60-85	-	3.8	2.7
4.75 mm	35-55	20-100	20-55	20-90	35-55	20-45	40-60	20-100	3.7	2.6

From Table 10-1 above, it can be noted that neither LWA-A nor LWA-B individually satisfies the gradation requirements set out by OPSS 1010 for granular class materials. However, this does not preclude their possible usage in pavement structures, as these gradation ranges are more adapted to natural aggregates and were developed to ensure the stability of the layer and also to prevent frost penetration by limiting the percentages of fine aggregates within specific ranges.

The LWA materials examined in this report are significantly coarser than all of the material classes in OPSS 1010. The LWA materials are, however, not natural in origin and they do not necessarily need to meet the OPSS gradation requirements in order to be used adequately. As these materials are coarse, they will not be frost-sensitive and will not promote upwards capillary movement of groundwater towards granular base layers. They will also ensure good stability due to stone-to-stone contact in the relative absence of smaller fractions of coarse aggregates. Further examination of these strength characteristics in the form of resilient modulus (M_r) testing can be found in Section 10.7.

The LWA materials examined could theoretically be modified in some manner to achieve the overall granular gradation requirements detailed above. This could include such methods as additional crushing after manufacture or otherwise blending the LWA with one or more finer aggregates to create an overall gradation which matches a desired class of granular material. Mechanical crushing would be required to bring the maximum particle size down to the required maximum sizes for Granular A, M, O or S, while blending the existing LWA with a finer material could achieve a grain size distribution suitable for Granular B Type I, II or III or for Select Subgrade Material (SSM). This would, however, negatively impact the function of LWA as lightweight fill materials as it would increase the overall bulk unit weight.

10.3 Crushed Particle Content

Percent crushed particle testing and analysis was performed on materials LWA-A and LWA-B in accordance with MTO laboratory standard LS-607, Method of Test for Determination of Percent Crushed Particles in Processed Coarse Aggregate. As both materials were considered poorly-graded and were already fractionated due to the earlier grain size distribution testing, the samples tested were prepared in accordance with Method B from LS-607. Consequently, the grain size fractions ranging from 19.0 mm to 13.2 mm, from 13.2 mm to 9.5 mm, from 9.5 mm to 6.7 mm and from 6.7 mm to 4.75 mm were not tested as each of these fractions constituted less than 5% of both LWA materials on a mass basis. The percent content of crushed particles was determined solely by examining material from the fraction passing the 26.5mm sieve and retained upon the 19.0mm sieve.

Under sample preparation Method B, MTO standard LS-607 sets a minimum of 200 particles to be examined for the percent crushed particle content from the fraction passing the 26.5mm sieve and retained upon the 19.0mm sieve. For material LWA-A, 200 particles of this size fraction were found to weigh approximately 480 g, so a minimum of 500 g was obtained for each sample examined. For material LWA-B, 200 particles of this size fraction were found to weigh approximately 650 g, so a minimum of 700 g was obtained for each sample examined. Overall, three samples each of the aforementioned weights were obtained and tested from LWA-A and from LWA-B.

Full results can be found in Tables D-3 and D-4 in Appendix D. For material LWA-A, the three samples were found to have crushed particle contents of 99.4%, 99.3% and 99.7% on a mass basis, for an overall average of 99.5% crushed particles. For material LWA-B, all three samples taken consisted of 100% crushed particles. This compares to requirements under OPSS.MUNI

1010 of a minimum of 100% crushed particles for Granular O class materials, 60% for Granular A and Granular M, and 50% for Granular S. No such requirements exist for Granular B Types I, II or III, or for Select Subgrade Material (SSM).

10.4 Flat and Elongated Particle Content

Percent flat and elongated particle content testing and analysis was performed on materials LWA-A and LWA-B in accordance with MTO laboratory standard LS-608, Method of Test for Determination of Percent Flat and Elongated Particles in Coarse Aggregate. Similarly to the crushed particle content testing, the grain size fractions ranging in sieve sizes from 19.0 mm to 13.2 mm, from 13.2 mm to 9.5 mm, from 9.5 mm to 6.7 mm and from 6.7 mm to 4.75 mm were not tested as each fraction constituted less than 5% by mass of the overall gradation in both materials. Consequently, for both materials, this test was performed only on the fractions passing the 37.5 mm sieve and retained upon the 26.5 mm sieve, and passing the 26.5 mm sieve and retained upon the 19.0 mm sieve.

One modification was made to the LS-608 procedure. The mass amount examined for each test was reduced from 3000 g to 1500 g for the fraction passing the 37.5 mm sieve and retained upon the 26.5 mm sieve, and from 2000 g to 1000 g for the fraction passing the 26.5 mm sieve and retained upon the 19.0 mm sieve. This change was followed as the original specified mass amounts would have corresponded to a much greater volume of particles of the lightweight aggregates than would have been the case for a natural aggregate. Overall, three samples each of the aforementioned mass amounts were obtained and tested from both LWA-A and LWA-B.

Full results can be found in Tables D-5 and D-6 in Appendix D. For material LWA-A, the three samples were each found to have flat and elongated particle contents of 0.2% by mass, for an overall average of 0.2%. For material LWA-B, the three samples were found to have flat and elongated particle contents of 0.1%, 0.1% and less than 0.1% by mass for an overall average of 0.1%. No requirements or limits for flat and elongated particle content appear to exist under OPSS 1010; however, this test was completed for physical characterization purposes and to complement the percent crushed particle content testing presented in Section 10.3.

10.5 Abrasion Resistance Testing

Abrasion resistance testing was conducted on materials LWA-A and LWA-B using a Micro-Deval apparatus in the CPATT laboratory at the University of Waterloo. The Micro-Deval testing was based on MTO laboratory standard LS-618, Method of Test for the Resistance of Coarse Aggregate to Degradation by Abrasion in the Micro-Deval Apparatus, with a number of modifications to compensate for the low density of the LWA materials.

The LWA presented a number of challenges due to the greater volume occupied by the specified mass of material as well as the density contrast between the artificial aggregate and the stainless steel balls used during the test. Grading A was selected from LS-618 as both LWA materials are coarse aggregates with a nominal maximum size which is much greater than either 16.0 mm (for Grading B) or 13.2 mm (for Grading C).

Initially, a quantity of natural aggregate was prepared to the mass proportions specified in Grading A of 375 g each from the fraction passing the 19.0 mm sieve and retained upon the 16.0 mm sieve and the fraction passing the 16.0 mm sieve and retained upon the 13.2 mm sieve, combined with 750 g from the fraction passing the 13.2 mm sieve and retained upon the 9.5 mm sieve. An approximately equivalent volume of each LWA material was obtained from the same size fractions, equating to 50 g from each of the two larger size fractions and 100 g from the smallest size fraction for a total of 200 g per portion tested. Three such samples were obtained from LWA-A and from LWA-B.

The steel balls used in this test are intended to simulate the abrasion that would occur within the aggregates over time. The mass of steel balls to be used in testing the LWA should then be reduced by the same proportion as the mass of aggregate used in each test. With the total mass of aggregate reduced from 1500 g in the original procedure to 200 g in each LWA sample, the mass of steel balls used for LWA testing was reduced accordingly from 5000 g to 670 g. The operating procedure of the Micro-Deval apparatus itself was not modified from LS-618.

Full data can be found in Tables D-7, D-8 and D-9 in Appendix D. For LWA-A, percent losses during Micro-Deval tests were 4.6%, 3.7% and 9.2% for an overall average percent loss of 5.9%. For LWA-B, the same sample preparation and testing procedures resulted in percent losses of 1.8%, 3.2% and 4.4% for an overall average percent loss of 3.1%. Under OPSS 1010, the maximum permissible Micro-Deval abrasion loss in coarse aggregates is 21% for Granular O, 25% for Granular A, M and S, and 30% for Granular B (all types) and Select Subgrade Material (SSM).

10.6 Freezing and Thawing Resistance Testing

Freezing and thawing resistance testing was conducted on materials LWA-A and LWA-B based on MTO laboratory standard LS-614, Method of Test for Freezing and Thawing of Coarse Aggregate. This test was conducted using a large walk-in freezer within the Department of Civil and Environmental Engineering at the University of Waterloo. This freezer was programmed to maintain a temperature of approximately minus 20 degrees Celsius for a period of sixteen hours overnight, before returning to room temperature for eight hours during the day.

In accordance with the LS-614 procedure, the freeze-thaw test was conducted on particles from both LWA materials in the fractions ranging from 37.5 mm to 26.5 mm and from 26.5 mm to 19.0 mm. Particles were not tested in the fractions ranging from 19.0 mm to 13.2 mm, from 13.2 mm to 9.5 mm and from 9.5 mm to 4.75 mm, as each of these three fractions constituted less than 5% of each LWA material by mass.

One modification was required to the standard LS-614 procedure. As currently specified, LS-614 requires sample masses for each test of 5000 g for the fraction passing the 37.5 mm sieve and retained upon the 26.5 mm sieve, and of 2500 g for the fraction passing the 26.5 mm sieve and retained upon the 19.0 mm sieve. For both LWA materials, this would have been an impractical volume of aggregate to test, as 5 kg of each material is approximately equal to one full standard granular material sample bag. As an alternative, European Standard BS EN 13055-2 specifies a procedure for testing of freezing and thawing resistance of lightweight aggregates. Annex B of EN 13055-2 requires a sample volume of 1500 mL for freeze-thaw cyclic testing on materials which have a maximum aggregate size of 16 mm to 32 mm; no larger fractions are mentioned.

For each size fraction in each sample of LWA-A and LWA-B tested, a graduated glass beaker was used to obtain a total of approximately 1.5 L of aggregate, which was subsequently weighed and divided into multiple plastic jars. Three such samples were obtained from each LWA material. Saline solution immersion, draining, cyclic freezing and thawing, rinsing, drying and final weighing of the aggregate proceeded in accordance with LS-614.

Full results can be found in Tables D-10 and D-11 in Appendix D. For material LWA-A, percentage losses for each sample were found to be 0.5%, 0.2% and 0.1% by mass, for an overall average of 0.3%. For material LWA-B, percentage losses for each sample were found to be 0.01%, 0.1% and 1.4% by mass, for an overall average of 0.5%. OPSS 1010 specifies a maximum unconfined freeze-thaw percentage loss of 15% by mass solely for Granular O class materials, with no such maximums listed for any other categories of granular fill.

10.7 Resilient Modulus Measurements

Resilient modulus testing was conducted on materials LWA-A and LWA-B based on Ministry of Transportation of Quebec (MTQ) characterization standard LC 22-400, which is in turn based upon the AASHTO T307 resilient modulus testing standard. This procedure determines the resilient moduli by examining the strain response of compacted aggregate specimens under a series of fifteen separate phases of varying confining stresses and applied axial stresses.

The resilient modulus testing on materials LWA-A and LWA-B was carried out at the Department of Civil Engineering at Université Laval in Quebec City, Québec. Only material passing the 26.5 mm sieve was used due to geometric limitations in the size of the testing equipment. For each specimen, a sample of approximately 1500 g of foam glass aggregate was obtained and immersed in water for a period of approximately 24 hours. Upon the conclusion of this period, the water was carefully drained and the surface-saturated LWA material was compacted in a series of seven equal lifts within a cylindrical metal mould with a 152.4 mm interior diameter, which was lightly coated on its inner surface using a release agent. The height per added lift of material was targeted to achieve a final overall specimen height of 300 mm ± 10 mm. The compactive effort on each lift was provided by 30 seconds of vibration using a Hilti TE 505 mechanical hammer mounted vertically in an enclosure and equipped with a 150 mm diameter steel head with a flat contact surface. This apparatus may be seen in Figure 10-4.

Once fully compacted, the specimen was then placed, still inside the mould, within a large chest-style freezer for a period of approximately 24 hours. This freezing period was added to the procedure to help ensure that the specimen would not disintegrate when transferred into the resilient modulus testing apparatus. After the freezing period was completed, the compacted specimen was removed from the mould, measured to determine its exact height, and placed into the resilient modulus testing cell with a paper filter and a permeable geotextile on top and on bottom. The specimen was then surrounded with layer of plastic tarp fabric, followed by two impermeable plastic membranes, in order to avoid puncturing the impermeable membranes during the test procedure. A compacted LWA specimen may be seen prior to transfer in Figure 10-5 and after fabric and membrane application in Figure 10-6.

Figure 10-4. Resilient modulus specimen compaction apparatus at Université Laval

Figure 10-5. Free-standing LWA-B specimen after freezing period and before transfer

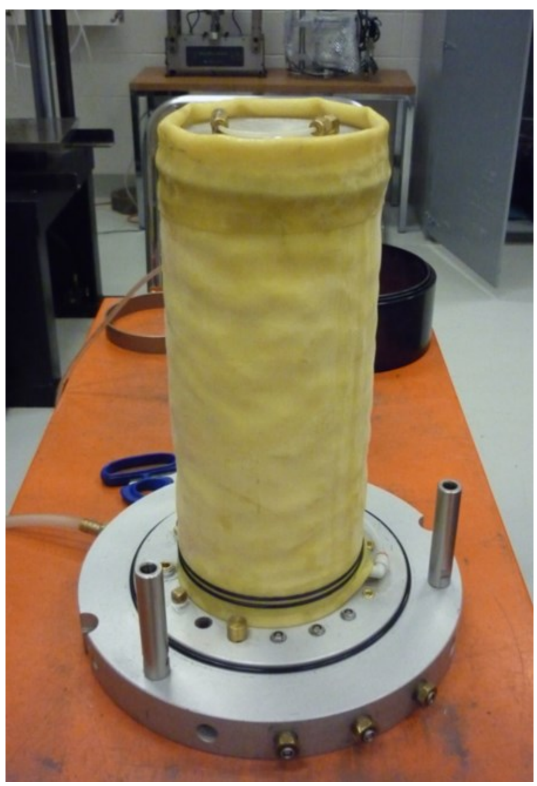

Figure 10-6. LWA specimen after application of fabric and impermeable membranes

After the transfer of the specimen into the resilient modulus testing cell, a further 24-hour period was included prior to testing in order to allow the frozen material to thaw at room temperature and to prevent the freezing process from influencing the results of the resilient modulus test. Proper sealing of the testing cell was confirmed prior to starting the test and allowing the automated cycle to proceed through the conditioning phase and the fifteen prescribed resilient modulus testing phases. The resilient modulus testing apparatus was an IPC UTM-100 Universal Testing Machine (seen in Figure 10-7), connected to an air compressor used to apply the confining stress within the testing cell. A total of six LWA specimens were compacted and tested, including three each from material LWA-A and from material LWA-B.

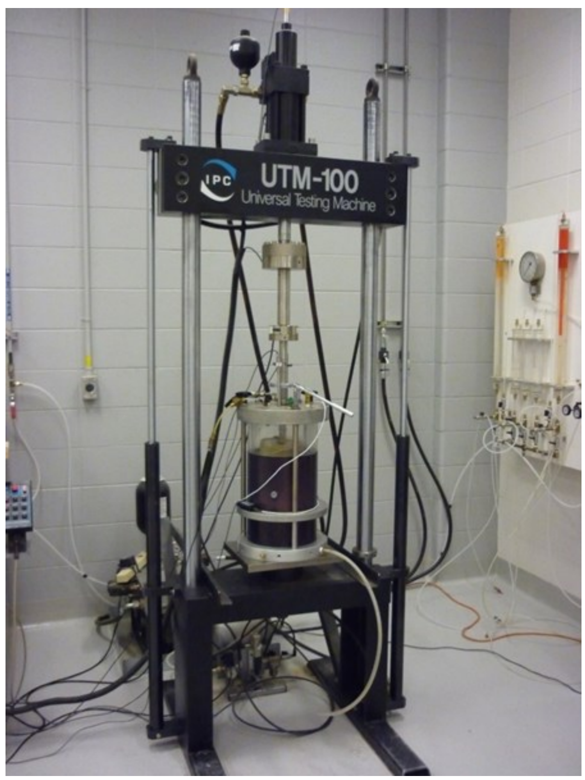

Figure 10-7. Resilient modulus laboratory testing apparatus at Université Laval

In accordance with the testing standard, resilient modulus measurements were determined by analyzing an average composed of the final five loading cycles in each testing phase as measured and recorded electronically by the testing system. The resilient moduli (M_r) at each phase were calculated as a ratio of the total bulk stress (θ) experienced by the specimen to the vertical resilient strain (ε_{vr}) exhibited by that specimen under loading. For each material, the results for each of the three specimens at each testing phase were averaged together to create an overall profile of resilient moduli vs. bulk stress.

Overall, material LWA-B exhibited slightly higher resilient modulus results at each testing phase, varying from 66.14 MPa to 203.36 MPa, relative to material LWA-A, which ranged from 65.41 MPa to 184.75 MPa. No results were considered to be outliers, as across all specimens at all testing phases, the maximum variation of any resilient modulus measurement was 5.7% relative to the average for that material. In addition, no anomalous effects were found to result from the freezing period used in the specimen preparation process.

A summary of the testing results can be seen in Table 10-2 and Figure 10-8. Results for each specimen may be found in Tables D-12 and D-13 in Appendix D.

Table 10-2. Average resilient modulus measurements for LWA-A and LWA-B

Testing Sequence	LWA-A		LWA-B	
	θ (kPa)	M_R (MPa)	θ (kPa)	M_R (MPa)
1	82.33	65.41	82.22	66.14
2	103.12	72.27	103.08	73.84
3	123.87	79.61	123.89	83.39
4	137.88	85.36	137.75	90.75
5	172.20	94.98	172.25	102.64
6	206.96	100.29	206.97	108.47
7	275.70	122.70	275.67	132.96
8	344.96	132.37	344.99	142.28
9	414.08	134.23	413.99	147.19
10	379.50	137.91	379.37	148.75
11	414.05	148.26	414.06	160.16
12	517.84	159.15	517.81	173.84
13	517.91	167.43	518.01	179.91
14	552.33	172.79	552.40	188.02
15	690.67	184.75	690.92	203.36

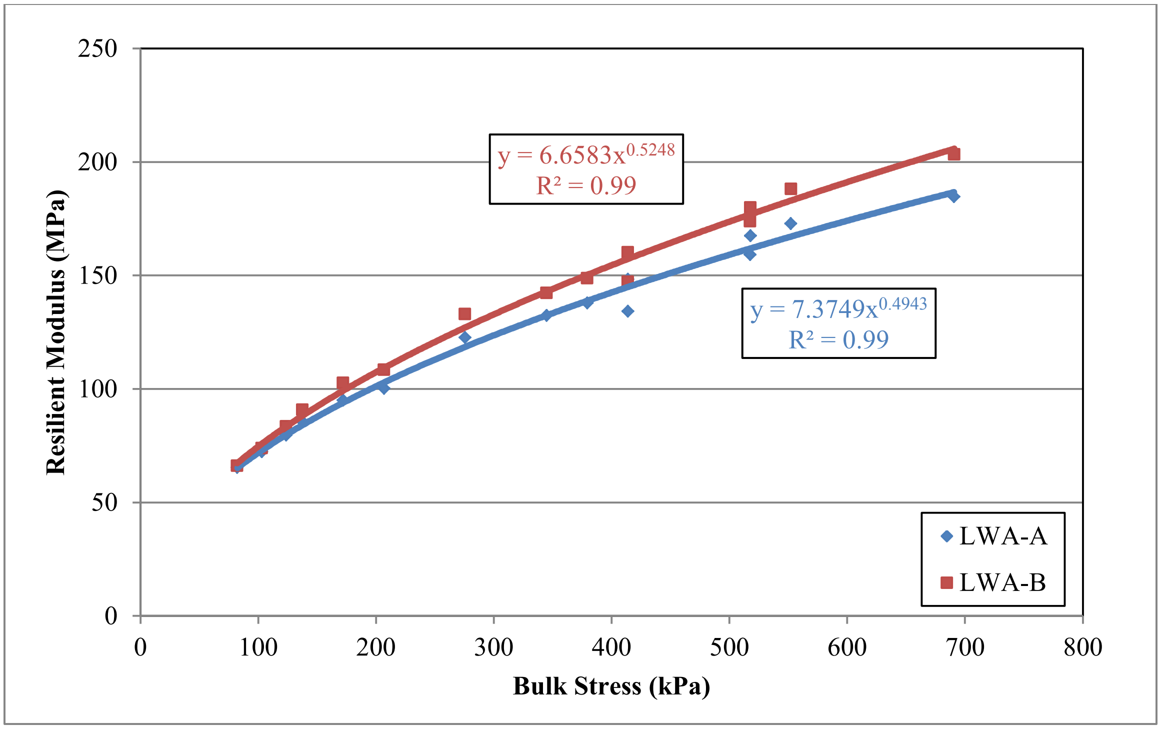

Figure 10-8. Graph of resilient moduli vs. bulk stress for LWA-A and LWA-B

The experimental results presented in Table 10-2 and Figure 10-8 compare favourably with resilient modulus values for conventional materials in granular base, subbase and subgrade layers in pavement structures. Huang (2004) gives a typical range of 15,000 to 45,000 psi (103.5 to 310.5 MPa) for unbound granular fill material elastic moduli, as well as a range of 3000 to 40,000 psi (20.7 to 276 MPa) for fine-grained or natural subgrade material elastic moduli. Amongst natural subgrade materials, typical average resilient or elastic modulus values for predominantly clayey soils are 12,000 psi (82.8 MPa) for stiff clay, 8000 psi (55.2 MPa) for medium clay, 5000 psi (34.5 MPa) for soft clay and 3000 psi (20.7 MPa) for very soft clay. Apart from typical resilient modulus design values, these results can be compared to the AASHTO T307 triaxial resilient modulus testing of OPSS 1010 Granular B Type II subbase mixes detailed in Sections 5.4 and 6.7, where two test mixes incorporating 100% natural rock aggregate materials exhibited resilient modulus values ranging from 89.1 to 314.3 MPa and 150.7 to 396.2 MPa respectively across all fifteen loading stages of the testing procedure (Schneider, Baaj & Lum, 2017).

The resilient modulus values observed for LWA-A and LWA-B can also be compared to expanded polystyrene (EPS), which is currently used by the pavement design and construction industry as a conventional lightweight fill material. Chen et al. (2015) studied two EPS materials of differing densities and found elastic (Young's) modulus values of 2.7 MPa for EPS foam with a density of 13.5 kg/m^3 and 4.8 MPa for EPS foam with a density of 28 kg/m^3. Hazarika (2006) proposed a mathematical relation between the elastic modulus and density of EPS geofoam whereby $E = 0.41\rho - 2.8$ and noted that a number of other studies had found similar moduli and linear relationships with density values ranging from 10 to 35 kg/m^3. Huang and Negussey (2011) note that the most commonly used EPS geofoam density in road pavement applications has been 20 kg/m^3, placing the typical resilient modulus level for such EPS geofoams at well below 10 MPa. By comparison, the lowest observed resilient modulus value for the foam glass LWA materials tested in this study is 65.4 MPa, indicating superior structural properties as compared to conventional EPS.

10.8 Relative Density Measurements

Relative density testing was also conducted on samples of materials LWA-A and LWA-B. However, current locally applicable laboratory testing standards were found to be unsuited to the foam glass LWA materials under examination, as both LWA-A and LWA-B are of sufficiently low density that specimens float in water, making conventional maximum and bulk relative density (MRD and BRD) testing methods impractical. A novel testing procedure needed to be devised in order to provide a suitably accurate and reliable measurement of the densities of both LWA materials while maintaining user safety.

A typical concrete mix air void testing apparatus, shown in Figure 10-9, was obtained from the Structures Laboratory at the University of Waterloo. This apparatus was selected as its design allows it to be filled completely with liquid while leaving an absolute minimum of air bubbles within the sealed container. The concrete air void testing apparatus was first cleaned thoroughly by hand to remove any particles of aggregate and/or concrete which were loose or were likely to dislodge during testing, and was subsequently allowed to dry completely at room temperature.

Figure 10-9. Concrete air void testing apparatus used for relative density measurements

A small valve leading to an upper chamber in the testing apparatus was blocked off with commonly available duct tape to prevent water from escaping through any orifice aside from the two main valves fitted in the lid of the container and was checked to ensure a continued seal before and after each test run. The testing apparatus was first weighed while dry at room temperature to establish its baseline mass while completely empty, which was determined to be 8348.1 g. The concrete air void testing apparatus was then attached to a supply of deionized water by means of a MasterFlex Easy-Load model 7529-30 peristaltic pump equipped with flexible PVC tubing. This pump system was selected for the ability to transfer the deionized water at a relatively steady rate without undue disturbance or turbulence, so as to prevent or minimize the introduction of air bubbles into the enclosed container.

The first step in the testing procedure was to establish the interior volume of the testing apparatus. The peristaltic pump was attached to one of the main valves in the testing apparatus and was operated to fill the container solely with deionized water until only water and no air escaped the unconnected valve on the lid of the apparatus. During this process, the exterior of the apparatus container was agitated using a rubber-headed hammer in order to dislodge any air bubbles inside the container. Once the container was filled, the pump was shut off and disconnected, the two main valves were closed, and the exterior of the apparatus was dried off by hand to remove any adhering water or moisture. The closed apparatus was weighed to establish the total mass and the net weight of the deionized water inside the filled container. The apparatus was then returned to the sink and the lid was removed, before an electronic thermometer was used to determine the temperature of the deionized water. The temperature of the water in degrees Celsius was used to select the density of deionized water at that temperature, which was used to convert the net weight of water into the equivalent volume. Through several trial runs using this method, the interior volume of the container apparatus was determined to be an average of 7143.1 cm^3.

With the interior volume of the container established, a control test was conducted using a selected block of commonly available tool steel, for which a rectangular prism specimen was obtained for ease of measurement. This steel block was measured using a set of electronic calipers to have average dimensions of 131.41 mm by 60.70 mm by 62.60 mm, for a total volume of 499.3 cm^3. The steel block was weighed while dry at room temperature to establish a mass of 3820.5 g and a corresponding reference density of 7.651 g/cm^3. The block was then placed inside the testing apparatus and the remaining space within the container was filled with deionized water as described above. The exterior of the apparatus was again agitated by means of a rubber-headed hammer to promote the escape of any air bubbles during the filling process. Once filling was completed, the pump was disconnected, the exterior valves on the apparatus were closed and the exterior surface was again dried to remove adhering water and moisture. The total mass of the apparatus containing the steel block and water was obtained, with the known masses of the apparatus and the block subtracted to obtain the weight of the deionized water. As before, the water temperature inside the container was then measured using an electronic thermometer before using the temperature to obtain the corresponding density of deionized water and thus the volume of water inside the container. The volume of the deionized water was subtracted from the known internal volume of the apparatus to determine the apparent volume of the steel block, and the known mass of the steel block was divided by the apparent volume to obtain a measured density. Across three such control tests, the average measured density of the steel block was 7.679 g/cm^3, which was slightly high by a proportion of 0.36%. This was due to a slightly lowered apparent volume for the block, which may have been due to a slight excess of water, potentially any remaining drops or moisture on the exterior of the container. Full data measurements can be found in Table D-14 in Appendix D.

Density measurements for materials LWA-A and LWA-B proceeded by the same method. For both LWA materials, four samples of at least 500 g each were obtained from the particles retained on or above the 26.5 mm sieve, which were made available due to the size restrictions for the resilient modulus testing described in Section 10.7. This was done to avoid any finer particles potentially escaping the container, and was considered to be representative of each material as a whole as approximately 80% of both materials by mass were retained upon the 26.5 mm sieve (see Table 10-1 in Section 10.2). Each 500 g sample was weighed while dry at room temperature before being placed into the apparatus. Similar to the water-only and metal block tests, the peristaltic pump was then connected and used to fill the container with deionized water while regularly agitating from the exterior using a rubber-headed hammer to help ensure the escape of any air bubbles. When the container was observed to be completely filled, the valves were shut and the pump was disconnected, before the exterior was dried by hand and the total weight of the apparatus, the water and the LWA was obtained. Views of the test in progress can be seen in Figures 10-10 and 10-11. The known weights of the apparatus and the LWA sample were subtracted to obtain the weight of the deionized water, and the temperature of the deionized water in each test was used to determine its corresponding density at that temperature. The corresponding volume of deionized water was subtracted from the known internal volume of the containing apparatus in order to find the net volume of the LWA sample. Average material densities for LWA-A and for LWA-B were determined from four tests each of 500 g of sample material. Full data measurements can be found in Table D-14 in Appendix D.

Figure 10-10. View of a dry sample of material LWA-B in the density testing apparatus

Figure 10-11. View of a sample of material LWA-A after immersion during density testing

For material LWA-A, the four test samples yielded densities of 0.298, 0.301, 0.297 and 0.291, for an overall average of 0.297 g/cm^3. Based on the results of the metal block control test, the overall apparent average density was reduced by a factor of 0.36% to give a density value for LWA-A of 0.296 g/cm^3. By contrast, when the LWA-A material stockpile was shipped to and received by CPATT, the loose, uncompacted bulk density of the aggregate was approximately 150 kg/m^3 or 0.150 g/cm^3, indicating approximately 50% air voids when uncompacted.

For material LWA-B, the four test samples yielded densities of 0.368, 0.373, 0.385 and 0.385, for an overall apparent average density of 0.378 g/cm^3. As with the first material, this was reduced by a factor of 0.36% to give a density value for LWA-B of 0.376 g/cm^3. By contrast, when the LWA-B material stockpile was shipped to and received by CPATT, the loose, uncompacted bulk density of the aggregate was approximately 187.5 kg/m^3 or 0.1875 g/cm^3, again indicating approximately 50% air voids when uncompacted. For both materials, the large contrast between the maximum density of the pure LWA material and the bulk density of the uncompacted aggregate is expected due to the coarse character of both LWA-A and LWA-B.

CHAPTER 11
PAVEMENT DESIGN

11.1 Design Calculations

A structural pavement design process was undertaken to quantify the effects that could result from the utilization of foam glass LWA in place of conventional EPS geofoam as a lightweight subgrade replacement fill. For this purpose, the standard AASHTO 1993 empirical design method was utilized in combination with an online calculation software tool provided by Pavement Interactive (2008).

For this process, a series of design cases were examined, each structure consisting of a hot mix asphalt (HMA) layer underlain by an unbound granular base fill layer, an unbound granular subbase fill layer, and finally by either foam glass LWA or EPS geofoam acting as the subgrade. The LWA or EPS was considered to be sufficiently vertically extensive (e.g. 5 metres or greater) in the pavement structure so as to leave no significant influence on subgrade resilient modulus from the naturally existing soil in the area of the hypothetical roadway. Additionally, due to the limitations of the AASHTO 1993 empirical design procedure, the granular subbase layer was assumed to be lying directly on top of the artificial lightweight subgrade layer in all cases; this structure would be normal for foam glass LWA, but this would be contrary to typical EPS geofoam construction best practices, where a rigid concrete slab layer is normally placed on top of the EPS geofoam to attenuate and distribute the vertical loading from overlying layers (Huang & Negussey, 2011).

Other design conditions and assumptions are as follows:

- Three different lifetime design 80-kN equivalent single axle load (ESAL) levels were examined, corresponding to low (1 x 10^6 over 20 years), intermediate (10 x 10^6 over 20 years) and high (60 x 10^6 over 30 years) highway traffic.
- The reliability level (R) was assumed to be 85% or 0.85 in the low traffic cases, 90% or 0.90 in the intermediate traffic cases, and 95% or 0.95 in the high traffic cases.

- The combined standard error (S_e) was assumed to be 0.5 in all cases.
- The initial serviceability index was set at 4.5 for a flexible pavement, while the terminal serviceability indices were set at 2.5 for the low traffic cases, 3.0 for the intermediate traffic cases, and 3.5 for the high traffic cases, for overall change-in-serviceability (ΔPSI) values of 2.0, 1.5 and 1.0 respectively.
- The layer coefficient (a_1) of the HMA layer was set at 0.44, corresponding to a standard HMA resilient modulus of 450,000 psi or 3.1 GPa.
- The layer coefficient (a_2) of the granular base layer was set at 0.13, corresponding to a standard granular base layer resilient modulus of 28,000 psi or 193 MPa.
- The layer coefficient (a_3) of the granular subbase layer was set at 0.11, with a standard granular subbase layer resilient modulus of 21,000 psi or 145 MPa.
- Drainage coefficients (m) were set at 1.0 for the HMA layer and 0.8 for the granular base and subbase layers.
- The resilient modulus of the EPS geofoam subgrade was assumed to be 6 MPa or 870 psi, while the resilient modulus of the foam glass LWA subgrade was assumed to be the lowest level observed in this study at 65.4 MPa or 9480 psi.
- According to the above noted traffic ESAL levels, the minimum thickness of the HMA layer was assumed to be 3.0 in (76.2 mm) for the low traffic cases and 4.0 in (101.6 mm) for the intermediate and high traffic cases, while the minimum granular base layer thickness was 6.0 in (152.4 mm) in all cases in accordance with AASHTO procedure minimum thicknesses.

Using the AASHTO 1993 design calculation software, in the design cases utilizing EPS geofoam as the subgrade, the thickness of the HMA layer was increased from its initial calculation output to the nearest half-inch necessary in order to achieve as close as possible to the same granular base and subbase thickness values as in the foam glass LWA subgrade cases, and to minimize the total pavement thickness overall to reduce the static loading applied to the underlying EPS geofoam artificial subgrade. The results of the design calculation procedure can be seen below in Table 11-1.

Table 11-1. Design case results comparing foam glass LWA to EPS geofoam

Design ESALs	1×10^6		10×10^6		60×10^6	
Subgrade Used	LWA	EPS	LWA	EPS	LWA	EPS
HMA Layer Thickness (in.)	5	12.5	7.5	19	12	28
Granular Base Thickness (in.)	6	6	6	6	6	6
Granular Subbase Thickness (in.)	6	6	9	8.5	15.5	14.5
Overall Structural Number (SN)	3.51	6.81	4.87	9.89	7.42	14.38

In each design case examined, the much higher structural number necessitated by the lower resilient modulus of the EPS geofoam artificial subgrade layers resulted in a much higher HMA and total pavement thickness relative to the corresponding pavement structures overlying foam glass LWA artificial subgrade. Manual variation and maximization of the thickness of the HMA relative to the granular layers was unable to produce total pavement thickness levels in the EPS design cases which were as low as those calculated for the LWA subgrade design cases. To achieve the same pavement thickness overlying EPS geofoam, the design would need to utilize HMA and granular fill materials with higher resilient moduli.

11.2 Life Cycle Cost Analysis

As observed in the pavement design calculations in Section 11.1, the usage of foam glass LWA as a lightweight subgrade replacement fill material in place of conventional EPS geofoam can result in substantially lower pavement HMA and granular fill layer thicknesses. This carries direct benefits in terms of requiring smaller quantities of bitumen and aggregates as well as lower labour and equipment costs during production, construction and maintenance of the pavement materials and structure. A life cycle cost analysis (LCCA) procedure is necessary to estimate and quantify these amounts and the differences between both lightweight fill methods.

For this LCCA assessment, each design case presented in Section 11.1 was applied to a hypothetical roadway section of 1 km length. A total structure height of 6 metres was assumed for all cases, whereby the HMA, granular base and granular subbase layer thicknesses are as specified in Table 11-1 and the remainder of the depth is made up of artificial lightweight fill material in the form of either foam glass LWA or EPS geofoam, depending on the specific design case. The roadway width was assumed to be 15 metres in all cases, consisting of two traffic lanes in each direction for a total of four lanes each spanning 3.75 metres.

For material costs, a study by the FWHA was cited by the American firm GeoTech Systems Corporation (2009) placed the typical cost of EPS geofoam at a density of 20 kg/m^3, including installation, at \$65 USD per cubic yard, based on a materials-only cost of \$40-\$45 USD per cubic yard; applying this ratio to an equivalent materials cost in SI units of \$50-\$58 USD per cubic metre yields a total materials and installation cost of \$82.59 USD per cubic metre of EPS geofoam. Applying the current (as of late March 2017) currency conversion rate of \$1 USD to \$1.34 CAD gives a total cost of \$110.67 CAD per cubic metre for EPS geofoam. For foam glass LWA, Foamyna Canada Inc. markets the materials at a cost of \$50 CAD per cubic metre; applying the same ratio per cubic metre as applied to the EPS geofoam figure yields an estimated total cost including installation of \$76.47 CAD per cubic metre for foam glass LWA.

Typical unit density for HMA, granular base and granular subbase was assumed to be 2.35 t/m^3, with overall unit costs summarized below in Table 11-2 based on Holt, Sullivan and Hein (2011). For simplification purposes, excavation costs were not included in this LCCA procedure.

Table 11-2. Unit costs for HMA, granular base and granular subbase used in LCCA

Material	Unit Cost (\$/t)	Unit Cost (\$/m^3)
Hot Mix Asphalt (HMA)	\$110.00	\$258.50
Granular Base	\$18.00	\$42.30
Granular Subbase	\$15.00	\$35.25

The analysis periods used for the LCCA procedure were set at 30 years for the low and intermediate traffic design cases and 50 years for the high traffic design cases. A conventional flexible pavement maintenance schedule was adopted based on El-Hakim (2013) and is summarized in Table 11-3.

Table 11-3. Maintenance schedule for conventional flexible pavement structure

Maintenance Activity	Year
Rout and Crack Sealing (352 m/km)	3
Rout and Crack Sealing (352 m/km)	6
Rout and Crack Sealing (352 m/km)	9
Mill and Patch 5% of HMA to 50 mm	9
Rout and Crack Sealing (704 m/km)	12
Mill and Patch 20% of HMA to 50 mm	15
Rout and Crack Sealing (704 m/km)	18
Tack Coat	20
Mill 50 mm of HMA Throughout	20
Pave 50 mm of HMA Throughout	20
Rout and Crack Sealing (352 m/km)	21
Rout and Crack Sealing (352 m/km)	24
Rout and Crack Sealing (352 m/km)	28
Mill and Patch 20% of HMA to 50 mm	28
Major Rehabilitation of Pavement	30
Rout and Crack Sealing (352 m/km)	33
Rout and Crack Sealing (352 m/km)	36
Rout and Crack Sealing (352 m/km)	39
Mill and Patch 5% of HMA to 50 mm	39
Rout and Crack Sealing (704 m/km)	42
Mill and Patch 20% of HMA to 50 mm	45
Rout and Crack Sealing (704 m/km)	48
Tack Coat	50
Mill 50 mm of HMA Throughout	50
Pave 50 mm of HMA Throughout	50

The major pavement rehabilitation item at the 30-year point above in Table 11-3 was assumed to consist of the milling and replacement of the entirety of the HMA, granular base and granular subbase. The following unit costs in Table 11-4 were used for the rehabilitation activities. The materials and installation costs of replacement HMA, granular base and granular subbase were assumed to be the same as in Table 11-2. The rout, crack seal and HMA milling costs in Table 11-4 were based on Holt, Sullivan and Hein (2011) and the tack coating unit cost was based on an average of figures provided by two major firms active in the HMA industry in Ontario (Capital Paving Inc. and McAsphalt Industries Ltd.).

Table 11-4. Unit costs for flexible pavement rehabilitation activities

Maintenance Activity	Unit Cost
Rout and Crack Seal	\$5.00 / m
HMA Milling	\$15.00 / t (\$35.25 / m^3)
Tack Coat	\$0.50 / m^2

For the LCCA procedure, an annual discount rate of 5% or 0.05 was assumed for converting future rehabilitation costs into Net Present Worth (NPW). The salvage value of the pavement segments was not calculated as it was considered to be the same between both alternatives for each of the three designed traffic levels. The results of the LCCA procedure are summarized below in Table 11-5 (all costs cited are in dollars CAD) and a full breakdown can be found in Table D-15 in Appendix D.

Table 11-5. LCCA comparison between foam glass LWA and EPS geofoam

Design LW Fill	LWA	EPS	LWA	EPS	LWA	EPS
Design ESALs	1×10^6	1×10^6	10×10^6	10×10^6	60×10^6	60×10^6
Initial Cost of HMA	\$492,443	\$1,231,106	\$738,664	\$1,871,282	\$1,181,862	\$2,757,678
Initial Cost of Granular Base	\$96,698	\$96,698	\$96,698	\$96,698	\$96,698	\$96,698
Initial Cost of Subbase	\$80,582	\$80,582	\$120,872	\$114,157	\$208,169	\$194,739
Initial Cost of LW Fill	\$6,387,053	\$8,927,109	\$6,226,809	\$8,547,627	\$5,906,321	\$7,915,158
Total Cost of Construction	\$7,056,775	\$10,335,494	\$7,183,043	\$10,629,764	\$7,393,049	\$10,964,273
Total Cost of Rehabilitation (NPW)	\$342,198	\$536,414	\$425,582	\$720,272	\$610,632	\$1,018,744
Overall Cost (NPW)	\$7,398,973	\$10,871,909	\$7,608,624	\$11,350,036	\$8,003,681	\$11,983,017

From Table 11-5, the use of foam glass LWA as a lightweight artificial subgrade replacement fill resulted in overall cost savings on a NPW basis of 31.9% in the low traffic case, 33.0% in the intermediate traffic case and 33.2% in the high traffic case, calculated relative to the overall cost levels using conventional EPS geofoam. The largest factors in this difference were the higher construction cost of EPS geofoam relative to foam glass LWA, as well as the higher construction and rehabilitation costs associated with the increased HMA layer thickness in pavement structures overlying EPS geofoam.

11.3 Environmental Safety

From an environmental safety perspective, foam glass is chemically stable and, with proper process and quality control measures during the glass recycling process, foam glass is considered unlikely to carry chemical impurities or to release them after manufacture and placement (Bernardo et al., 2007). Additionally, as foam glass does not incorporate hydrocarbons, it does not carry the same inherent risks as expanded polystyrene, which is known to be flammable and also susceptible to dissolution in contact with hydrocarbon solvents such as petroleum. A brief summary comparison of environmental safety properties between foam glass LWA and EPS geofoam can be seen below in Table 11-6.

Table 11-6. Comparison of environmental properties between LWA and EPS.

Criteria	Foam Glass LWA	EPS Geofoam
Post-Consumer Recycled Material	Yes	No
Recyclable Material	Yes	Only where accepted
Biodegradable	No	No
Water-Absorptive	No	Yes
Hydrocarbon-Sensitive	No	Yes
Flammable	No	Yes

Due to the very low density of foam glass LWA materials, measured at 0.296 g/cm^3 for LWA-A and 0.376 g/cm^3 for LWA-B (see Section 10.8), it is strongly recommended that foam glass aggregates should not be used in areas which experience a high risk of large-scale flooding or storm flow conditions, such as in proximity to bridges, culverts and similar structures. Under exposure to flowing water conditions, the high buoyancy and unbound character of the foam glass LWA would accelerate the breakup or wash-out of pavement structures if left unprotected from the incoming water by the absence of other layers consisting of erosion-resistant materials. In such an event, the chemical and physical stability of the foam glass could also contribute to LWA particles being carried a significant distance downstream to accumulate either in an area of obstruction or in a marine environment (whether fluvial, lacustrine or oceanic), incurring additional hazards to wildlife or to downstream infrastructure and necessitating additional costs for cleanup or remediation as compared to denser natural rock aggregates.

CHAPTER 12
STUDY CONCLUSIONS

The laboratory testing detailed in Chapter 10 indicates that both LWA-A and LWA-B have a very consistent and repeatable gradation with high percentages of coarse aggregates. This is highly beneficial to ensure the stability of the aggregate layers and to prevent capillary water movement upward to other granular layers. However, it was found that the grain size distributions of these two tested materials, as currently manufactured, do not satisfy the requirements of OPSS 1010. The existing standards were developed for natural aggregates and, as currently constituted, may not be appropriately adapted to these materials and to other similar lightweight aggregates.

Both LWA-A and LWA-B have very high crushed particle contents, in excess of 99%, and very low flat and elongated particle contents, well below 1% by mass percent. Under Micro-Deval abrasion resistance testing, LWA-A had an average percent loss of 5.9% by mass and LWA-B had an average percent loss of 3.1%, which indicates good abrasion resistance for both the tested materials. Freeze-thaw resistance testing showed average losses by mass of 0.3% for LWA-A and 0.5% for LWA-B. Resilient modulus measurements varied from 65 to 185 MPa for LWA-A, and from 66 to 203 MPa for LWA-B. Density testing yielded average measurements of 0.296 g/cm^3 for LWA-A and 0.376 g/cm^3 for LWA-B.

Pavement design calculations using the AASHTO 1993 procedure and incorporating the above LWA resilient modulus measurements showed that utilizing foam glass LWA as a lightweight subgrade replacement fill material can result in substantially leaner pavement structures as compared to HMA and granular fill layers overlying conventional expanded polystyrene (EPS) geofoam blocks. A life-cycle cost analysis (LCCA) procedure carried out on the pavement designs derived using AASHTO 1993 showed that the use of foam glass LWA as a lightweight fill material underlying pavement can result in overall cost savings of over 30 percent relative to pavement structures which are underlain by conventional EPS geofoam.

In summary, the two tested foam glass LWA materials showed excellent physical and mechanical characteristics and conform to most of the OPSS 1010 requirements for Granular A, M, O or S. Both materials would be suitable for use in pavement structures as innovative lightweight and environmentally-friendly alternative aggregate materials. It is recommended that future studies include more detailed pavement design using commercially-available design software in order to refine or further validate the calculations carried out in this study. Additionally, future studies should undertake the construction of test sections incorporating foam glass LWA fill materials in order to examine their response to compactive effort, to verify their performance in the field, and to gain more experience with the use of foam glass LWA in pavement structures.

CHAPTER 13
CONCLUSIONS

In Part 1 of this thesis, recycled concrete (RCA) and recycled asphalt (RAP) were compared against conventional natural aggregates for potential inclusion in Granular B Type II subbase fill material under OPSS 1010. Though the results of some of the field and laboratory tests were mixed in certain cases, overall it appears that RCA and RAP can successfully substitute for natural aggregates in subbase mixes in a range of volumetric proportions without adversely affecting the physical strength and permeability characteristics of the fill material.

In Part 2, two foam glass lightweight aggregate (LWA) materials were subjected to a series of physical characterization tests to determine their potential as an alternative solution for lightweight pavement construction. The foam glass LWA materials showed good physical characteristics and exhibited substantially improved mechanical properties compared to conventional lightweight expanded polystyrene (EPS) geofoam blocks. This in turn indicated that roadways built with foam glass LWA as a subgrade replacement fill material can achieve substantial life cycle cost savings as compared to roadways constructed using EPS geofoams.

In both studies, recycled or reclaimed materials proved to be capable of serving successfully and economically as construction aggregates for pavement engineering applications. The findings of these studies can be used to further the understanding of RCA, RAP and foam glass LWA as pavement engineering solutions, and may be able to lead to their expanded usage under applicable regulations here in Ontario and in other jurisdictions. Recycled and reclaimed materials are still building awareness and acceptance in the pavement construction industry, and consequently, it is recommended that future work should include the design and construction of test sections in order to demonstrate, examine and verify the longer-term performance of these sustainable materials when utilized in the field. With greater understanding of the characteristics and behaviour of recycled and reclaimed materials, they can be utilized to a greater degree in pavements and roadways and can impart a wide range of both economic and environmental benefits as sustainable engineering solutions.

REFERENCES

Aabøe, R., Øiseth, E., & Hägglund, J. (2005). *Granulated Foamed Glass for Civil Engineering Applications*. Paper published in the 2005 Workshop NR2 – Recycled Materials in Road & Airfield, Oslo, Norway.

Arulrajah, A., Disfani, M.M., Maghoolpilehrood, F., Horpibulsuk, S., Udonchai, A., Imteaz, M., & Du, Y.-J. (2015). *Engineering and environmental properties of foamed recycled glass as a lightweight engineering material*. Journal of Cleaner Production, 94, 369-375.

Aurstad, J., Asknes, J., Dahlhaug, J.E., Berntsen, G., & Uthus, N. (n.d.; 2004 or later). *Unbound crushed concrete in high volume roads – A field and laboratory study*. Trondheim, Norway.

Aurstad, J., Berntsen, G., & Petkovic, G. (n.d.; 2006 or later). *Evaluation of unbound crushed concrete as road building material – Mechanical properties vs. field performance*. Norwegian Public Roads Administration (NPRA), Trondheim, Norway.

Auvinen, T., Pekkala, J., & Forsman, J. (2013). *Covering the Highway E12 in the centre of Hämeenlinna – Innovative Use of Foamed Glass as Light Weight Material of Approach Embankment*. Paper presented at the XXVIII International Baltic Road Conference held in Vilnius, Lithuania.

Bernardo, E., Cedro, R., Florean, M., & Hreglich, S. (2007). *Reutilization and stabilization of wastes by the production of glass foams*. Ceramics International, 33, 963-968.

Buchanan, S. (2007). *Resilient Modulus: What, Why, and How?* Vulcan Materials Company, Birmingham, AL.

Chen, W., Hao, H., Hughes, D., Shi, Y., Cui, J., & Li, Z.-X. (2015). *Static and dynamic mechanical properties of expanded polystyrene*. Materials and Design, 55, 170-180.

Comité Européen de Normalisation (2004). *Lightweight aggregates – Part 2: Lightweight aggregates for bituminous mixtures and surface treatments and for unbound and bound applications* (European Standard EN 13055-2). CEN Management Centre, Brussels, Belgium.

El-Hakim, M. (2013). *A Structural and Economic Evaluation of Perpetual Pavements: A Canadian Perspective* (Doctoral thesis). University of Waterloo, Waterloo, ON, Canada. Retrieved from https://uwspace.uwaterloo.ca/handle/10012/7274

Frydenlund, T.E., & Aabøe, R. (2003). *Foamglass – a New Vision in Road Construction*. Paper published in the 2003 Proceedings of the 22nd PIARC – C12 technical committee on earthworks, drainage and subgrade, Durban, South Africa.

Hanks, A.J., & Magni, E.R. (1989). *The Use of Recovered Bituminous & Concrete Materials in Granular and Earth*. Ministry of Transportation of Ontario, Engineering Materials Office, Downsview, Toronto, ON.

Hazarika, H. (2006). *Stress-strain modeling of EPS geofoam for large-strain applications*. Geotextiles and Geomembranes, 24, 79-90.

Hemmings, R.T., Cornelius, B.J., Yuran, P. & Wu. M. (2009). *Comparative Study of Lightweight Aggregates*. Paper presented at the May 2009 World of Coal Ash (WOCA) Conference, held in Lexington, KY, USA.

Holt, A., Sullivan, S., & Hein, D.K. (2011). *Life Cycle Cost Analysis of Municipal Pavements in Southern and Eastern Ontario*. Paper presented at the September 2011 annual conference of the Transportation Association of Canada (TAC), held in Edmonton, AB, Canada.

Hossain, M.S., & Apeagyei, A.K. (2010). *Evaluation of the lightweight deflectometer for in-situ determination of pavement layer moduli* (Virginia Transportation Research Council Publication No. FHWA/VTRC 10-R6). Virginia Transportation Research Council, Charlottesville, VA. Retrieved from http://www.virginiadot.org/vtrc/main/online_reports/pdf/10-r6.pdf

Huang, X., & Negussey, D. (2011). *EPS Geofoam Design Parameters for Pavement Structures*. American Society of Civil Engineers (ASCE), Geotechnical Special Publication, 211, 4544-4554.

Huang, Y.H. (2004). *Pavement Analysis and Design* (2nd ed.). Pearson Education, Inc., Upper Saddle River, NJ, USA.

Kancherla, A. (2004). *Resilient modulus and permanent deformation testing of unbound granular materials* (Unpublished Master of Science thesis). Texas A&M University. Retrieved October 27, 2015, from http://oaktrust.library.tamu.edu/bitstream/handle/1969.1/2711/etd-tamu-2004B-CVEN-Kancherla.pdf

Kuo, S.-S., Chini, A.R., Mahgoub, H.S., Ortega, J.E., & Monteiro, A.R. (2011, October). *Use of Recycled Concrete made with Florida Limestone Aggregate for a Base Course in Flexible Pavement*. University of Central Florida, Orlando, FL.

Ministère des Transports du Québec (2010). *Détermination du module réversible des matériaux granulaires* (LC-22-400). Laboratory procedure, Ministère des Transports du Québec (MTQ), QC, Canada.

Ministry of Transportation of Ontario (2012). *Ontario's Default Parameters for AASHTOWare Pavement ME Design – Interim Report*. Ministry of Transportation of Ontario, Pavements and Foundations Section, Material Engineering Research Office, Downsview, Toronto, ON.

Moore, T., Jagdat, S., Kazmierowski, T., & Ng, L. (2014, September). *Quality Metrics for Recycled Concrete Aggregates in Municipal Roads*. Paper presented at the Green Technologies – Innovation to Implementation and Evaluation Session of the annual conference of the Transportation Association of Canada (TAC), Montréal, QC.

National Cooperative Highway Research Program (2013). *NCHRP Synthesis 445: Practices for Unbound Aggregate Pavement Layers*. Transportation Research Board, Washington, DC.

Ontario Provincial Standards (2013). *Material Specification for Aggregates – Base, Subbase, Select Subgrade, and Backfill Material* (OPSS 1010). Ministry of Transportation of Ontario, Downsview, Toronto, ON, Canada.

Pavement Interactive (2008). *1993 AASHTO Flexible Pavement Structural Design*. Retrieved from http://www.pavementinteractive.org/article/1993-aashto-flexible-pavement-structural-design/

Recycled Materials Resource Center (2008). *Reclaimed Concrete Material – Material Description*. University of New Hampshire, Durham, NH.

Schneider, A.C., Baaj, H. & Lum, P. (2017). *Evaluation of Reclaimed Materials as Aggregate for OPSS Granular B Type II* (Unpublished research report). University of Waterloo, Waterloo, ON, Canada.

Segui, P., Doré, G., Bilodeau, J.-P., & Morasse, S. (2016). *Innovative materials for road insulation in cold climates: Foam glass aggregates*. Paper presented at the Innovation in Geotechnical and Materials Engineering session of the 2016 annual conference of the Transportation Association of Canada (TAC), held in Toronto, ON, Canada.

Senior, S.A., Szoke, S.I., & Rogers, C.A. (1994, July). *Ontario's Experience with Reclaimed Materials for Use as Aggregates*. Paper published in the International Road Federation / Transportation Association of Canada Conference Proceedings, Volume 6, pp. A31-A55, Calgary, AB.

United States Department of Transportation – Federal Highway Administration (2010). *User Guidelines for Waste and Byproduct Materials in Pavement Construction – Reclaimed Concrete Material*. Publication Number: FHWA-RD-97-148.

Van Wagoner, D.D. (2009). *Frequently Asked Questions*. GeoTech Systems Corporation, Great Falls, VA, USA. Retrieved from http://www.geosyscorp.com/noframes/company/faq.htm

Volovski, M., Arman, M., & Labi, S. (2014). *Developing statistical limits for using the light weight deflectometer (LWD) in construction quality assurance* (Joint Transportation Research Program Publication No. FHWA/IN/JTRP-2014/10). Purdue University, West Lafayette, IN. Retrieved from http://dx.doi.org/10.5703/1288284315504

Yeo, R.E.Y., & Sharp, K.G. (1997, May). *Investigation into the Use of Recycled Crushed Concrete for Road Base Use*. VicRoads, Kew, Victoria, Australia.

APPENDIX A:
DENSOMETER AND PHYSICAL PROPERTIES TESTING DATA TABLES

Table A-1. Compaction measurements at Quarry 1 for 100% crushed rock test mixture

Pass Number	Test Locations					
	Test #1		Test #4		Test #7	
	Density kg/m^3	Moisture Content %	Density kg/m^3	Moisture Content %	Density kg/m^3	Moisture Content %
Subgrade Layer	2214	4.5	2250	3.6	2283	3.2
1			1959	1.8		
2			1980	1.7		
3			2034	2.3		
4			2164	3.2	2146	2.1
5	2198	2.3	2243	2.1	2204	2.3
6	2223	2.4	2246	1.9	2248	2.4
7	2265	3.2	2246	1.9	2228	2.3
8	2270	2.7	2254	2.3	2299	2.7

Table A-2. Compaction measurements at Quarry 1 for 25% RCA - 75% crushed rock test mixture

Pass Number	Test Locations					
	Test #1		Test #4		Test #7	
	Density kg/m^3	Moisture Content %	Density kg/m^3	Moisture Content %	Density kg/m^3	Moisture Content %
Subgrade Layer	2292	3.3	2266	4.6	2171	3.5
1			1925	2.8		
2			1960	4.4		
3			1900	4.6		
4	2008	5.7	2007	4.8	1978	4.6
5	2078	4.2	2078	5.1	2066	3.7
6	2108	4.0	2080	5.0	2062	5.3
7	2067	4.7	2152	6.7	2193	5.3
8	2126	4.6	2161	6.1	2107	5.1

Table A-3. Compaction measurements at Quarry 1 for 50% RCA - 50% crushed rock test mixture

Pass Number	Test Locations					
	Test #1		Test #4		Test #7	
	Density kg/m^3	Moisture Content %	Density kg/m^3	Moisture Content %	Density kg/m^3	Moisture Content %
Subgrade Layer	2292	3.3	2323	5.0	2338	5.7
1			1843	4.5		
2			1951	4.7		
3			1983	5.3		
4	1905	6.3	1986	6.7	2001	4.3
5	2073	6.3	2066	5.9	2011	4.6
6	2036	6.5	2053	5.6	2038	5.9
7	2047	4.4	2001	5.6	2036	6.5
8	2036	6.5	2053	5.6	2038	5.9

Table A-4. Compaction measurements at Quarry 1 for 100% RCA test mixture

Pass Number	Test Locations					
	Test #1		Test #4		Test #7	
	Density kg/m^3	Moisture Content %	Density kg/m^3	Moisture Content %	Density kg/m^3	Moisture Content %
Subgrade Layer	2382	3.7	2326	4.2	2253	3.6
1			1834	4.5		
2			1951	4.7		
3			1983	5.3		
4	1963	6.4	1998	5.9	1993	4.6
5	2003	6.3	1986	6.7	2001	4.3
6	2073	6.3	2206	5.9	2011	4.6
7	2036	6.5	2053	5.6	2038	5.9
8	2047	4.4	2001	5.6	2023	6.1

Table A-5. Compaction measurements at Quarry 1 for 70% RCA - 30% RAP test mixture

Pass Number	Test Locations					
	Test #1		Test #4		Test #8	
	Density kg/m^3	Moisture Content %	Density kg/m^3	Moisture Content %	Density kg/m^3	Moisture Content %
Subgrade Layer	2167	3.5	2224	4.0	2233	2.8
2			1821	9.4		
3			1944	10.1		
4	1913	8.1	1942	10.4	1879	10.2
5	1945	9.9	1968	10.1	1929	8.2
6	1925	10.7	1973	10.7	1976	7.8
7	1925	9.5	1922	10.6	1968	8
8	1970	10.6	1927	11.6	1962	9.6

Table A-6. Compaction measurements at Quarry 2 for 100% crushed rock test mixture

Pass Number	Test Locations			
	Test #1		Test #2	
	Density kg/m^3	Moisture Content %	Density kg/m^3	Moisture Content %
1	2040	2.4	2001	2.0
2	2084	2.2	2042	3.4
3	2209	3.2	2089	3.1
4	2209	3.6	2117	2.8
5	2183	2.7	2191	3.5
6	2208	3.0	2144	2.5
7	2298	3.6	2273	3.3

Table A-7. Compaction measurements at Quarry 2 for 25% RCA - 75% crushed rock test mixture

Pass Number	Test Locations			
	Test #1		Test #2	
	Density kg/m^3	Moisture Content %	Density kg/m^3	Moisture Content %
1	2078	5.8	2122	5.0
2	2101	6.6	2158	5.6
3	2180	5.5	2165	5.3
4	2209	5.8	2224	5.1
5	2189	6.0	2245	5.7

Table A-8. Compaction measurements at Quarry 2 for 50% RCA - 50% crushed rock test mixture

Pass Number	Test Location			
	Test #1		Test #2	
	Density kg/m^3	Moisture Content %	Density kg/m^3	Moisture Content %
1	1983	6.2	1980	6.3
2	2015	7.1	1995	5.9
3	2076	6.9	2081	5.8
4	2058	6.8	2046	6.4

Table A-9. Compaction measurements at Quarry 2 for 100% RCA test mixture

Pass Number	Test Locations			
	Test #1		Test #2	
	Density kg/m^3	Moisture Content %	Density kg/m^3	Moisture Content %
1	1841	8.0	1739	8.0
2	1850	8.6	1769	8.1
3	1886	10.0	1893	7.0
4	1884	8.8	1914	8.4
5	1881	9.3	1943	8.1
6	1969	9.5	1942	8.2
7	1962	9.3	1910	8.5
8	1983	8.6	1962	8.7

Table A-10. Compaction measurements at Quarry 2 for 70% RCA - 30% RAP test mixture

Pass Number	Test Location			
	Test #1		Test #2	
	Density kg/m^3	Moisture Content %	Density kg/m^3	Moisture Content %
1	1920	9.0	1923	7.6
2	1917	9.5	1927	8.4
3	1915	8.9	1935	7.9

Table A-11. Gradation results at Quarry 1 for 100% crushed rock test mixture

Sieve Size (mm)	Before in Stockpile		After Compaction of Pad					Difference
	2-1	Average	2-1	2-2	2-3	2-4	Average	
150	100.0	100.0	100.0	100.0	100.0	100.0	100.0	0.0
106	100.0	100.0	100.0	100.0	100.0	100.0	100.0	0.0
26.5	70.0	70.0	79.8	71.4	77.6	76.7	76.4	6.4
9.5	43.1	43.1	50.5	44.9	51.5	43.7	47.7	4.6
4.75	29.0	29.0	35.4	31.3	36.4	28.3	32.9	3.9
2.36	18.7	18.7	25.9	23.4	25.3	19.7	23.6	4.9
1.18	12.1	12.1	17.8	16.4	16.6	13.8	16.2	4.1
0.6	8.5	8.5	12.6	11.8	11.8	10.3	11.6	3.1
0.3	6.6	6.6	9.8	9.2	9.1	8.3	9.1	2.5
0.15	5.5	5.5	8.0	7.5	7.5	6.9	7.5	2.0
0.075	4.7	4.7	6.6	6.2	6.1	5.7	6.2	1.5

Table A-12. Gradation results at Quarry 1 for 25% RCA - 75% crushed rock test mixture

Sieve Size (mm)	Before in Stockpile		After Compaction of Pad					Difference
	4-1	Average	4-1	4-2	4-3	4-4	Average	
150	100.0	100.0	100.0	100.0	100.0	100.0	100.0	0.0
106	100.0	100.0	100.0	100.0	100.0	100.0	100.0	0.0
26.5	79.1	79.1	87.8	84.3	78.3	83.4	83.5	4.3
9.5	49.6	49.6	62.4	58.2	47.1	52.9	55.2	5.6
4.75	33.9	33.9	44.7	40.9	31.1	36.0	38.2	4.3
2.36	24.3	24.3	31.5	28.1	21.5	26.4	26.9	2.6
1.18	17.4	17.4	21.5	19.5	15.6	19.2	19.0	1.6
0.6	12.5	12.5	14.9	13.8	11.5	13.9	13.5	1.0
0.3	8.9	8.9	10.2	9.8	8.4	10.0	9.6	0.7
0.15	6.3	6.3	7.2	7.0	6.2	7.0	6.9	0.6
0.075	4.4	4.4	5.1	5.1	4.5	5.1	5.0	0.5

Table A-13. Gradation results at Quarry 1 for 50% RCA - 50% crushed rock test mixture

Sieve Size (mm)	Before in Stockpile		After Compaction of Pad					Difference
	3-1	Average	3-1	3-2	3-3	3-4	Average	
150	100.0	100.0	100.0	100.0	100.0	100.0	100.0	0.0
106	100.0	100.0	100.0	100.0	100.0	100.0	100.0	0.0
26.5	77.5	77.5	73.9	78.4	73.0	78.9	76.1	-1.4
9.5	50.9	50.9	48.6	53.2	44.5	51.4	49.4	-1.5
4.75	35.8	35.8	34.6	38.0	31.1	36.5	35.1	-0.8
2.36	25.6	25.6	25.5	28.0	21.0	26.3	25.2	-0.4
1.18	18.6	18.6	18.9	20.8	15.1	19.7	18.6	0.0
0.6	13.1	13.1	13.9	15.2	11.0	14.8	13.7	0.6
0.3	8.7	8.7	9.8	10.6	7.9	10.8	9.8	1.1
0.15	5.6	5.6	6.5	7.0	5.4	7.3	6.6	1.0
0.075	3.8	3.8	4.4	4.7	3.8	5.0	4.5	0.7

Table A-14. Gradation results at Quarry 1 for 100% RCA test mixture

Sieve Size (mm)	Before in Stockpile				After Compaction of Pad					Difference
	1-1	1-2	1-3	Average	1-1	1-2	1-3	1-4	Average	
150	100.0	100.0	100.0	100.0	100.0	100.0	100.0	100.0	100.0	0.0
106	100.0	100.0	100.0	100.0	100.0	100.0	100.0	100.0	100.0	0.0
26.5	77.3	72.8	78.4	76.2	78.2	83.5	80.7	76.8	79.8	3.6
9.5	49.4	47.1	51.5	49.3	56.9	60.5	53.8	52.9	56.0	6.7
4.75	34.3	33.5	37.8	35.2	42.8	44.5	38.8	38.6	41.2	6.0
2.36	26.8	24.3	31.8	27.6	33.0	32.1	28.7	28.1	30.5	2.8
1.18	21.4	17.7	25.7	21.6	24.9	23.1	21.8	20.8	22.7	1.1
0.6	16.5	12.6	19.2	16.1	18.0	16.5	16.3	15.1	16.5	0.4
0.3	11.3	8.4	12.7	10.8	11.8	11.0	11.5	10.5	11.2	0.4
0.15	7.3	5.3	7.6	6.7	7.2	7.0	8.0	6.9	7.3	0.5
0.075	5.1	3.6	4.6	4.4	4.5	4.7	5.7	4.8	4.9	0.5

Table A-15. Gradation results at Quarry 1 for 70% RCA - 30% RAP test mixture

Sieve Size (mm)	Before in Stockpile				After Compaction of Pad					Difference
	5-1	5-2	5-3	Average	5-1	5-2	5-3	5-4	Average	
150	100.0	100.0	100.0	100.0	100.0	100.0	100.0	100.0	100.0	0.0
106	100.0	100.0	100.0	100.0	100.0	100.0	100.0	100.0	100.0	0.0
26.5	81.1	85.2	86.5	84.3	92.9	87.9	88.3	87.4	89.1	4.9
9.5	59.4	64.4	63.7	62.5	68.6	61.0	65.9	60.3	64.0	1.5
4.75	41.3	45.3	44.6	43.7	48.3	41.6	46.8	41.3	44.5	0.8
2.36	27.4	32.1	33.1	30.9	33.6	27.7	31.9	29.1	30.6	-0.3
1.18	18.7	23.5	25.2	22.5	24.9	20.4	22.7	21.4	22.4	-0.1
0.6	12.5	17.5	18.4	16.1	18.6	15.4	16.6	16.0	16.7	0.5
0.3	7.9	11.9	11.8	10.5	12.5	10.6	11.2	10.9	11.3	0.8
0.15	5.2	7.9	7.5	6.9	8.1	7.1	7.5	7.2	7.5	0.6
0.075	3.5	5.5	5.1	4.7	5.4	4.8	5.2	4.8	5.1	0.4

Table A-16. Quarry 1 test mixtures physical properties results

MTO Laboratory Test and Number	100% Crushed Rock	25% RCA - 75% Rock	50% RCA - 50% Rock	100% RCA	70% RCA - 30% RAP	OPSS Gran. B Type II
Micro Deval Abrasion Coarse Aggregate % maximum loss, LS-618	18.0	18.1	18.8	19.8	17.8	30
Micro Deval Abrasion Fine Aggregate % maximum loss, LS-619	18.1	14.1	24.1	20.1	11.2	35
Asphalt Coated Particles % maximum LS-621	0	0	0	0	28.5	0
Amount of Contamination % maximum LS-630	0	Not Tested	Not Tested	Not Tested	Not Tested	0.1 (wood)
Plasticity Index maximum LS-631	NP	Not Tested	Not Tested	NP	Not Tested	NP

Table A-17. Gradation results at Quarry 2 for 100% crushed rock test mixture

Sieve Size (mm)	Before in Stockpile				After Compaction of Pad					Difference
	1-1	1-2	1-3	Average	1-1	1-2	1-3	1-4	Average	
150	100.0	100.0	100.0	100.0	100.0	100.0	100.0	100.0	100.0	0.0
106	100.0	100.0	100.0	100.0	100.0	100.0	100.0	100.0	100.0	0.0
26.5	70.5	71.3	70.2	70.7	70.6	77.9	69.3	75.4	73.3	2.6
9.5	37.3	36.0	34.0	35.8	41.9	47.9	36.8	47.2	43.5	7.7
4.75	26.0	24.4	22.9	24.4	30.5	35.2	26.8	35.3	32.0	7.5
2.36	18.5	19.3	15.7	17.8	23.6	24.6	19.0	25.4	23.2	5.3
1.18	13.1	15.6	10.8	13.2	17.5	18.1	13.7	18.9	17.1	3.9
0.6	9.8	12.9	7.9	10.2	13.5	14.0	10.5	14.6	13.2	3.0
0.3	7.9	10.5	6.4	8.3	11.0	11.3	8.5	11.8	10.7	2.4
0.15	6.8	8.8	5.5	7.0	9.5	9.7	7.4	10.1	9.2	2.1
0.075	5.7	7.2	4.5	5.8	8.0	8.2	6.2	8.5	7.7	1.9

Table A-18. Gradation results at Quarry 2 for 25% RCA - 75% crushed rock test mixture

Sieve Size (mm)	Before in Stockpile				After Compaction of Pad					Difference
	4-1	4-2	4-3	Average	4-1	4-2	4-3	4-4	Average	
150	100.0	100.0	100.0	100.0	100.0	100.0	100.0	100.0	100.0	0.0
106	100.0	100.0	100.0	100.0	100.0	100.0	100.0	100.0	100.0	0.0
26.5	82.6	82.1	77.8	80.8	84.6	83.7	79.2	88.0	83.9	3.0
9.5	50.1	53.1	47.9	50.4	57.1	51.2	50.1	54.4	53.2	2.8
4.75	37.7	40.1	36.4	38.1	43.6	38.6	38.8	42.4	40.9	2.8
2.36	28.8	27.5	26.0	27.4	29.7	27.2	28.6	31.2	29.2	1.7
1.18	21.7	20.4	19.1	20.4	21.1	19.6	20.6	23.0	21.1	0.7
0.6	16.4	15.9	14.4	15.6	15.7	14.9	15.3	17.6	15.9	0.3
0.3	12.6	12.5	11.4	12.2	12.2	11.6	12.0	13.8	12.4	0.2
0.15	10.6	10.4	9.6	10.2	10.3	9.7	10.0	11.5	10.4	0.2
0.075	8.8	8.5	8.0	8.4	8.5	8.1	8.3	9.4	8.6	0.1

Table A-19. Gradation results at Quarry 2 for 50% RCA - 50% crushed rock test mixture

Sieve Size (mm)	Before in Stockpile				After Compaction of Pad					Difference
	5-1	5-2	5-3	Average	5-1	5-2	5-3	5-4	Average	
150	100.0	100.0	100.0	100.0	100.0	100.0	100.0	100.0	100.0	0.0
106	100.0	100.0	100.0	100.0	100.0	100.0	100.0	100.0	100.0	0.0
26.5	80.5	81.4	80.3	80.7	71.9	80.6	74.7	83.2	77.6	-3.1
9.5	46.4	48.5	47.1	47.3	37.9	47.9	45.4	54.8	46.5	-0.8
4.75	33.5	34.9	34.0	34.1	26.5	36.1	34.8	42.7	35.0	0.9
2.36	23.0	25.1	23.6	23.9	19.7	26.8	27.3	31.3	26.3	2.4
1.18	16.8	19.4	17.4	17.9	15.0	20.0	21.9	22.4	19.8	2.0
0.6	12.8	15.3	13.7	13.9	11.8	14.9	16.5	16.0	14.8	0.9
0.3	9.8	11.8	10.6	10.7	9.2	11.4	12.7	12.0	11.3	0.6
0.15	8.0	9.5	8.6	8.7	7.4	9.2	10.3	9.8	9.2	0.5
0.075	6.4	7.5	6.8	6.9	5.9	7.2	8.1	7.9	7.3	0.4

Table A-20. Gradation results at Quarry 2 for 100% RCA test mixture

Sieve Size (mm)	Before in Stockpile				After Compaction of Pad					Difference
	2-1	2-2	2-3	Average	2-1	2-2	2-3	2-4	Average	
150	100.0	100.0	100.0	100.0	100.0	100.0	100.0	100.0	100.0	0.0
106	100.0	100.0	100.0	100.0	100.0	100.0	100.0	100.0	100.0	0.0
26.5	83.3	89.2	86.0	86.2	87.8	89.3	88.1	90.5	88.9	2.8
9.5	51.7	56.5	53.1	53.8	58.1	51.2	52.1	53.2	53.7	-0.1
4.75	38.5	41.8	38.7	39.7	44.6	38.0	36.8	37.4	39.2	-0.5
2.36	28.0	32.3	30.5	30.3	32.0	29.1	26.2	28.8	29.0	-1.2
1.18	21.1	24.2	24.1	23.1	24.1	22.0	18.8	22.6	21.9	-1.3
0.6	15.9	17.3	19.0	17.4	18.3	16.6	13.6	17.5	16.5	-0.9
0.3	11.7	11.9	14.4	12.7	13.7	12.1	9.6	13.1	12.1	-0.5
0.15	8.9	8.7	11.7	9.8	10.7	9.3	7.3	9.9	9.3	-0.5
0.075	5.9	5.8	7.6	6.4	7.9	6.7	5.1	6.6	6.6	0.1

Table A-21. Gradation results at Quarry 2 for 70% RCA - 30% RAP test mixture

Sieve Size (mm)	Before in Stockpile				After Compaction of Pad					Difference
	3-1	3-2	3-3	Average	3-1	3-2	3-3	3-4	Average	
150	100.0	100.0	100.0	100.0	100.0	100.0	100.0	100.0	100.0	0.0
106	100.0	100.0	100.0	100.0	100.0	100.0	100.0	100.0	100.0	0.0
26.5	83.4	94.1	90.6	89.4	95.6	80.6	85.1	91.7	88.3	-1.1
9.5	57.2	66.1	64.0	62.4	68.4	57.9	60.1	63.8	62.6	0.1
4.75	43.6	51.1	50.2	48.3	51.2	45.9	46.9	49.3	48.3	0.0
2.36	34.6	40.6	35.1	36.8	36.9	36.5	33.9	38.3	36.4	-0.4
1.18	25.9	30.2	24.3	26.8	25.7	27.5	24.7	29.0	26.7	-0.1
0.6	18.3	21.0	16.7	18.7	16.7	19.3	17.3	21.5	18.7	0.0
0.3	12.0	14.1	11.1	12.4	10.2	12.7	11.6	15.0	12.4	0.0
0.15	8.9	10.6	8.4	9.3	7.6	9.2	8.6	11.1	9.1	-0.2
0.075	6.5	7.9	6.3	6.9	5.7	6.7	6.3	7.9	6.7	-0.2

Table A-22. Quarry 2 test mixtures physical properties results

MTO Laboratory Test and Number	100% Crushed Rock	25% RCA - 75% Rock	50% RCA - 50% Rock	100% RCA	70% RCA - 30% RAP	OPSS Gran. B Type II
Micro Deval Abrasion Coarse Aggregate % maximum loss, LS-618	12.8	15.7	15.3	15.8	15.0	30
Micro Deval Abrasion Fine Aggregate % maximum loss, LS-619	25.7	17.9	16.3	13.0	10.6	35
Asphalt Coated Particles % maximum LS-621	0	0.5	0.8	3.0	29.3	0
Amount of Contamination % maximum LS-630	0	0.1	0.4	2.7	0.4	0.1 (wood)
Plasticity Index maximum LS-631	NP	NP	NP	NP	NP	NP

APPENDIX B:
LIGHTWEIGHT DEFLECTOMETER DATA TABLES

Table B-1. Quarry 1, Test Pad #1, 26.5mm dense-graded crushed material subgrade layer

Location	PointNo	DropNo	Surface Temp	In-Depth Temp	Radius (mm)	Load (kN)	Deflection (um)	Stress (kPa)	Modulus (MPa)	Average (MPa)
pad1-loc1	1	1	20.6	19.6	150	16.74	625.13			
pad1-loc1	1	2	20.6	19.6	150	16.84	519.36	238.28	94.86	109.09
pad1-loc1	1	3	20.6	19.6	150	16.96	466.06	239.98	106.46	
pad1-loc1	1	4	20.6	19.6	150	17.10	464.92	241.94	107.59	
pad1-loc1	1	5	20.6	19.6	150	17.00	432.98	240.55	114.87	
pad1-loc1	1	6	20.6	19.6	150	17.07	410.30	241.46	121.67	
pad1-loc1	1	7	20.6	19.6	150	15.51	1322.42			
pad1-loc1	1	8	20.6	19.6	150	17.03	653.82			
pad1-loc2	2	1	20.6	19.6	150	17.04	583.07	241.12	85.50	101.14
pad1-loc2	2	2	20.6	19.6	150	17.18	542.66	242.99	92.58	
pad1-loc2	2	3	20.6	19.6	150	17.20	512.98	243.39	98.10	
pad1-loc2	2	4	20.6	19.6	150	16.98	471.08	240.15	105.40	
pad1-loc2	2	5	20.6	19.6	150	16.60	382.47			
pad1-loc2	2	6	20.6	19.6	150	17.25	406.52	243.99	124.09	
pad1-loc3	3	1	20.6	19.6	150	15.60	1448.72			
pad1-loc3	3	2	20.6	19.6	150	17.16	674.55	242.72	74.40	86.34
pad1-loc3	3	3	20.6	19.6	150	17.04	652.83	241.04	76.34	
pad1-loc3	3	4	20.6	19.6	150	17.14	581.42	242.55	86.25	
pad1-loc3	3	5	20.6	19.6	150	17.29	536.59	244.63	94.26	
pad1-loc3	3	6	20.6	19.6	150	17.43	507.43	246.55	100.46	
pad1-loc4	4	1	20.6	19.6	150	14.02	1326.06			
pad1-loc4	4	2	20.6	19.6	150	16.91	605.60	239.17	81.65	103.32
pad1-loc4	4	3	20.6	19.6	150	17.29	498.87	244.63	101.39	
pad1-loc4	4	4	20.6	19.6	150	17.30	475.84	244.68	106.31	
pad1-loc4	4	5	20.6	19.6	150	17.35	459.37	245.40	110.45	
pad1-loc4	4	6	20.6	19.6	150	17.39	435.58	246.08	116.81	
pad1-loc5	5	1	20.6	19.6	150	15.11	1692.74			

pad1-loc5	5	2	20.6	19.6	150	16.81	736.45	237.80	66.76	
pad1-loc5	5	3	20.6	19.6	150	16.89	634.88	238.88	77.79	
pad1-loc5	5	4	20.6	19.6	150	17.22	576.63	243.65	87.36	83.28
pad1-loc5	5	5	20.6	19.6	150	17.21	550.79	243.51	91.41	
pad1-loc5	5	6	20.6	19.6	150	17.25	542.01	243.97	93.07	
pad1-loc6	6	1	20.6	19.6	150	15.15	1466.91			
pad1-loc6	6	2	20.6	19.6	150	17.22	635.47	243.67	79.28	
pad1-loc6	6	3	20.6	19.6	150	17.22	551.79	243.56	91.26	
pad1-loc6	6	4	20.6	19.6	150	17.32	525.48	244.98	96.39	97.38
pad1-loc6	6	5	20.6	19.6	150	17.37	468.73	245.68	108.37	
pad1-loc6	6	6	20.6	19.6	150	17.50	458.77	247.60	111.59	
pad1-loc7	7	1	20.6	19.6	150	13.49	787.00			
pad1-loc7	7	2	20.6	19.6	150	17.17	550.13	242.86	91.27	
pad1-loc7	7	3	20.6	19.6	150	17.37	512.51	245.75	99.14	
pad1-loc7	7	4	20.6	19.6	150	17.37	492.42	245.78	103.20	101.61
pad1-loc7	7	5	20.6	19.6	150	17.42	483.15	246.48	105.48	
pad1-loc7	7	6	20.6	19.6	150	17.42	467.68	246.49	108.97	

Table B-2. Quarry 1, Test Pad #1, 100% crushed rock subbase layer

Location	PointNo	DropNo	Surface Temp	In-Depth Temp	Radius (mm)	Load (kN)	Deflection (um)	Stress (kPa)	Modulus (MPa)	Average (MPa)
pad1-loc1	1	1	26.6	22.5	150	15.26	1415.75			
pad1-loc1	1	2	26.6	22.5	150	17.05	643.99	241.25	77.45	88.73
pad1-loc1	1	3	26.6	22.5	150	17.16	570.20	242.75	88.02	
pad1-loc1	1	4	26.6	22.5	150	17.29	537.96	244.67	94.03	
pad1-loc1	1	5	26.6	22.5	150	17.32	552.28	245.05	91.74	
pad1-loc1	1	6	26.6	22.5	150	17.29	547.57	244.66	92.38	
pad1-loc2	2	1	26.6	22.5	150	17.06	807.25			
pad1-loc2	2	2	26.6	22.5	150	17.16	692.99	242.81	72.44	80.80
pad1-loc2	2	3	26.6	22.5	150	17.34	637.66	245.37	79.56	
pad1-loc2	2	4	26.6	22.5	150	17.33	615.07	245.17	82.41	
pad1-loc2	2	5	26.6	22.5	150	17.37	602.61	245.80	84.33	
pad1-loc2	2	6	26.6	22.5	150	17.43	598.26	246.60	85.23	
pad1-loc3	3	1	26.6	22.5	150	16.91	782.48			
pad1-loc3	3	2	26.6	22.5	150	17.14	665.09	242.55	75.40	82.60
pad1-loc3	3	3	26.6	22.5	150	17.13	623.93	242.37	80.32	
pad1-loc3	3	4	26.6	22.5	150	17.16	597.70	242.76	83.98	
pad1-loc3	3	5	26.6	22.5	150	17.26	579.87	244.22	87.08	
pad1-loc3	3	6	26.6	22.5	150	17.34	588.04	245.26	86.23	
pad1-loc4	4	1	26.6	22.5	150	16.88	672.68			
pad1-loc4	4	2	26.6	22.5	150	17.04	604.98	241.03	82.37	92.40
pad1-loc4	4	3	26.6	22.5	150	16.99	544.41	240.29	91.26	
pad1-loc4	4	4	26.6	22.5	150	17.06	529.50	241.39	94.26	
pad1-loc4	4	5	26.6	22.5	150	17.20	531.39	243.31	94.67	
pad1-loc4	4	6	26.6	22.5	150	17.13	503.85	242.31	99.43	
pad1-loc5	5	1	26.6	22.5	150	14.38	1571.24			
pad1-loc5	5	2	26.6	22.5	150	16.91	764.01	239.19	64.73	77.34
pad1-loc5	5	3	26.6	22.5	150	17.04	670.84	241.06	74.30	

pad1-loc5	5	4	26.6	22.5	150	17.01	630.10	240.71	78.99	
pad1-loc5	5	5	26.6	22.5	150	17.22	607.68	243.68	82.91	
pad1-loc5	5	6	26.6	22.5	150	17.28	589.38	244.52	85.78	
pad1-loc6	6	1	26.6	22.5	150	16.99	727.80			
pad1-loc6	6	2	26.6	22.5	150	17.03	623.39	240.86	79.89	
pad1-loc6	6	3	26.6	22.5	150	17.23	577.62	243.71	87.24	
pad1-loc6	6	4	26.6	22.5	150	17.16	537.56	242.79	93.38	91.35
pad1-loc6	6	5	26.6	22.5	150	17.25	518.24	243.98	97.34	
pad1-loc6	6	6	26.6	22.5	150	17.21	508.82	243.42	98.91	
pad1-loc7	7	1	26.6	22.5	150	16.85	775.53			
pad1-loc7	7	2	26.6	22.5	150	17.11	664.52	242.05	75.31	
pad1-loc7	7	3	26.6	22.5	150	17.14	628.57	242.53	79.78	
pad1-loc7	7	4	26.6	22.5	150	17.22	594.83	243.65	84.69	83.89
pad1-loc7	7	5	26.6	22.5	150	17.34	573.76	245.31	88.40	
pad1-loc7	7	6	26.6	22.5	150	17.23	551.96	243.71	91.29	

Table B-3. Quarry 1, Test Pad #2, 26.5mm dense-graded crushed material subgrade layer

Location	PointNo	DropNo	Surface Temp	In-Depth Temp	Radius (mm)	Load (kN)	Deflection (um)	Stress (kPa)	Modulus (MPa)	Average (MPa)
pad2-loc1	1	1	17.6	18.6	150	17.05	664.06	241.25	75.11	90.74
pad2-loc1	1	2	17.6	18.6	150	17.19	575.10	243.19	87.43	
pad2-loc1	1	3	17.6	18.6	150	17.25	540.90	244.08	93.30	
pad2-loc1	1	4	17.6	18.6	150	17.35	520.92	245.46	97.42	
pad2-loc1	1	5	17.6	18.6	150	17.36	505.42	245.58	100.46	
pad2-loc2	2	1	17.6	18.6	150	13.25	2153.67			
pad2-loc2	2	2	17.6	18.6	150	16.93	600.42	239.50	82.47	94.20
pad2-loc2	2	3	17.6	18.6	150	16.92	549.98	239.42	90.00	
pad2-loc2	2	4	17.6	18.6	150	17.17	513.22	242.94	97.87	
pad2-loc2	2	5	17.6	18.6	150	17.25	508.72	244.06	99.19	
pad2-loc2	2	6	17.6	18.6	150	17.30	498.79	244.81	101.48	
pad2-loc3	3	1	17.6	18.6	150	17.15	670.41	242.56	74.81	87.48
pad2-loc3	3	2	17.6	18.6	150	17.32	591.99	245.09	85.60	
pad2-loc3	3	3	17.6	18.6	150	17.37	567.84	245.74	89.47	
pad2-loc3	3	4	17.6	18.6	150	17.35	556.13	245.48	91.26	
pad2-loc3	3	5	17.6	18.6	150	17.37	527.78	245.70	96.25	
pad2-loc4	4	1	17.6	18.6	150	11.71	927.02			
pad2-loc4	4	2	17.6	18.6	150	15.81	598.10			
pad2-loc4	4	3	17.6	18.6	150	16.80	568.00	237.61	86.49	97.93
pad2-loc4	4	4	17.6	18.6	150	16.99	533.95	240.40	93.09	
pad2-loc4	4	5	17.6	18.6	150	16.15	858.70			
pad2-loc4	4	6	17.6	18.6	150	17.13	493.78	242.40	101.50	
pad2-loc4	4	7	17.6	18.6	150	17.12	483.09	242.27	103.69	
pad2-loc4	4	8	17.6	18.6	150	16.99	473.70	240.35	104.91	
pad2-loc5	5	1	17.6	17.7	150	15.34	1713.06			
pad2-loc5	5	2	17.6	17.7	150	17.02	664.59	240.84	74.92	89.41
pad2-loc5	5	3	17.6	17.7	150	17.05	582.02	241.14	85.66	

pad2-loc5	5	4	17.6	17.7	150	17.22	550.23	243.55	91.52	
pad2-loc5	5	5	17.6	17.7	150	17.27	527.60	244.33	95.75	
pad2-loc5	5	6	17.6	17.7	150	17.24	508.47	243.96	99.20	
pad2-loc6	6	1	17.6	17.7	150	15.63	1073.87			
pad2-loc6	6	2	17.6	17.7	150	16.94	634.93	239.59	78.02	
pad2-loc6	6	3	17.6	17.7	150	16.97	561.34	240.07	88.42	
pad2-loc6	6	4	17.6	17.7	150	17.04	520.09	241.13	95.86	92.18
pad2-loc6	6	5	17.6	17.7	150	16.99	519.66	240.37	95.64	
pad2-loc6	6	6	17.6	17.7	150	16.97	482.09	240.03	102.94	
pad2-loc7	7	1	17.6	17.7	150	15.55	1385.90			
pad2-loc7	7	2	17.6	17.7	150	16.94	670.02	239.67	73.96	
pad2-loc7	7	3	17.6	17.7	150	17.15	607.51	242.61	82.57	
pad2-loc7	7	4	17.6	17.7	150	17.23	577.44	243.72	87.27	86.11
pad2-loc7	7	5	17.6	17.7	150	16.89	546.85	238.97	90.35	
pad2-loc7	7	6	17.6	17.7	150	17.29	524.51	244.57	96.41	

Table B-4. Quarry 1, Test Pad #2, 100% RCA subbase layer

Location	PointNo	DropNo	Surface Temp	In-Depth Temp	Radius (mm)	Load (kN)	Deflection (um)	Stress (kPa)	Modulus (MPa)	Average (MPa)
pad2-loc1	1	1	24.2	21.8	150	16.77	846.73			
pad2-loc1	1	2	24.2	21.8	150	17.05	750.26	241.24	66.48	70.34
pad2-loc1	1	3	24.2	21.8	150	17.11	723.76	242.05	69.14	
pad2-loc1	1	4	24.2	21.8	150	16.91	702.34	239.22	70.42	
pad2-loc1	1	5	24.2	21.8	150	17.16	697.22	242.78	72.00	
pad2-loc1	1	6	24.2	21.8	150	17.12	680.02	242.23	73.65	
pad2-loc2	2	1	24.2	21.8	150	16.61	930.58			
pad2-loc2	2	2	24.2	21.8	150	16.76	858.17	237.09	57.12	60.95
pad2-loc2	2	3	24.2	21.8	150	16.82	807.88	237.93	60.89	
pad2-loc2	2	4	24.2	21.8	150	16.74	793.20	236.84	61.74	
pad2-loc2	2	5	24.2	21.8	150	16.34	786.63	231.11	60.75	
pad2-loc2	2	6	24.2	21.8	150	16.89	768.37	238.88	64.28	
pad2-loc3	3	1	24.2	21.8	150	14.17	2184.41			
pad2-loc3	3	2	24.2	21.8	150	16.62	974.59	235.13	49.88	56.85
pad2-loc3	3	3	24.2	21.8	150	16.82	885.19	237.92	55.57	
pad2-loc3	3	4	24.2	21.8	150	16.85	848.12	238.39	58.11	
pad2-loc3	3	5	24.2	21.8	150	16.85	828.90	238.40	59.47	
pad2-loc3	3	6	24.2	21.8	150	16.99	811.53	240.36	61.24	
pad2-loc4	4	1	24.2	21.8	150	16.88	982.48			
pad2-loc4	4	2	24.2	21.8	150	17.00	907.10	240.54	54.83	61.21
pad2-loc4	4	3	24.2	21.8	150	17.02	833.44	240.78	59.73	
pad2-loc4	4	4	24.2	21.8	150	17.11	803.49	242.11	62.30	
pad2-loc4	4	5	24.2	21.8	150	17.20	778.43	243.37	64.64	
pad2-loc4	4	6	24.2	21.8	150	17.13	775.74	242.27	64.57	
pad2-loc5	5	1	24.2	21.8	150	16.65	1035.80			
pad2-loc5	5	2	24.2	21.8	150	16.90	939.14	239.02	52.62	55.08
pad2-loc5	5	3	24.2	21.8	150	16.86	904.34	238.59	54.55	

pad2-loc5	5	4	24.2	21.8	150	16.95	877.41	239.85	56.52	
pad2-loc5	5	5	24.2	21.8	150	16.86	862.31	238.56	57.20	
pad2-loc5	5	6	24.2	21.8	150	16.40	879.54	231.97	54.53	
pad2-loc6	6	1	24.2	21.8	150	16.78	992.75			
pad2-loc6	6	2	24.2	21.8	150	16.81	902.38	237.79	54.48	
pad2-loc6	6	3	24.2	21.8	150	16.98	822.43	240.22	60.39	
pad2-loc6	6	4	24.2	21.8	150	17.03	803.94	240.86	61.95	60.39
pad2-loc6	6	5	24.2	21.8	150	17.02	798.11	240.77	62.37	
pad2-loc6	6	6	24.2	21.8	150	17.01	792.62	240.60	62.76	
pad2-loc7	7	1	24.2	21.8	150	14.33	1633.00			
pad2-loc7	7	2	24.2	21.8	150	16.78	985.50	237.34	49.79	
pad2-loc7	7	3	24.2	21.8	150	16.41	1007.31	232.21	47.66	
pad2-loc7	7	4	24.2	21.8	150	16.59	877.77	234.65	55.27	54.71
pad2-loc7	7	5	24.2	21.8	150	16.89	817.85	238.98	60.41	
pad2-loc7	7	6	24.2	21.8	150	16.46	796.58	232.83	60.43	

Table B-5. Quarry 1, Test Pad #3, 26.5mm dense-graded crushed material subgrade layer

Location	PointNo	DropNo	Surface Temp	In-Depth Temp	Radius (mm)	Load (kN)	Deflection (um)	Stress (kPa)	Modulus (MPa)	Average (MPa)
pad3-loc1	1	1	18.4	19.2	150	14.20	1594.34			
pad3-loc1	1	2	18.4	19.2	150	16.97	626.91	240.06	79.17	98.56
pad3-loc1	1	3	18.4	19.2	150	17.14	525.92	242.47	95.32	
pad3-loc1	1	4	18.4	19.2	150	17.23	498.38	243.69	101.09	
pad3-loc1	1	5	18.4	19.2	150	17.28	477.52	244.47	105.85	
pad3-loc1	1	6	18.4	19.2	150	17.26	453.42	244.21	111.36	
pad3-loc2	2	1	18.4	19.2	150	14.41	1923.92			
pad3-loc2	2	2	18.4	19.2	150	17.07	604.16	241.51	82.65	95.47
pad3-loc2	2	3	18.4	19.2	150	17.21	552.93	243.51	91.06	
pad3-loc2	2	4	18.4	19.2	150	17.21	516.08	243.42	97.52	
pad3-loc2	2	5	18.4	19.2	150	17.21	496.59	243.52	101.39	
pad3-loc2	2	6	18.4	19.2	150	17.15	478.99	242.60	104.72	
pad3-loc3	3	1	18.4	19.2	150	15.14	1260.00			
pad3-loc3	3	2	18.4	19.2	150	17.20	394.48	243.32	127.53	135.56
pad3-loc3	3	3	18.4	19.2	150	17.31	390.08	244.93	129.82	
pad3-loc3	3	4	18.4	19.2	150	17.44	371.13	246.66	137.41	
pad3-loc3	3	5	18.4	19.2	150	17.43	366.03	246.65	139.32	
pad3-loc3	3	6	18.4	19.2	150	17.22	350.45	243.62	143.73	
pad3-loc4	4	1	18.4	19.2	150	13.76	1133.61			
pad3-loc4	4	2	18.4	19.2	150	16.90	700.61	239.10	70.56	83.13
pad3-loc4	4	3	18.4	19.2	150	17.04	635.86	241.01	78.37	
pad3-loc4	4	4	18.4	19.2	150	17.20	612.78	243.28	82.08	
pad3-loc4	4	5	18.4	19.2	150	17.18	542.76	242.99	92.56	
pad3-loc4	4	6	18.4	19.2	150	17.24	547.52	243.89	92.10	
pad3-loc5	5	1	18.4	19.2	150	14.06	1092.77			
pad3-loc5	5	2	18.4	19.2	150	17.13	564.19	242.39	88.83	106.33
pad3-loc5	5	3	18.4	19.2	150	17.36	521.97	245.66	97.31	

pad3-loc5	5	4	18.4	19.2	150	17.36	460.98	245.62	110.16	
pad3-loc5	5	5	18.4	19.2	150	17.45	448.57	246.84	113.78	
pad3-loc5	5	6	18.4	19.2	150	17.45	419.94	246.89	121.55	
pad3-loc6	6	1	18.4	19.2	150	14.42	975.04			
pad3-loc6	6	2	18.4	19.2	150	16.46	346.73			
pad3-loc6	6	3	18.4	19.2	150	16.14	801.68	228.36	58.89	
pad3-loc6	6	4	18.4	19.2	150	16.26	748.07	230.05	63.58	
pad3-loc6	6	5	18.4	19.2	150	16.64	697.47	235.36	69.77	63.89
pad3-loc6	6	6	18.4	19.2	150	16.59	782.17	234.64	62.02	
pad3-loc6	6	7	18.4	19.2	150	16.80	754.05	237.71	65.18	
pad3-loc7	7	1	18.4	19.2	150	14.01	1613.10			
pad3-loc7	7	2	18.4	19.2	150	16.13	935.21	228.20	50.45	
pad3-loc7	7	3	18.4	19.2	150	16.30	824.74	230.55	57.80	
pad3-loc7	7	4	18.4	19.2	150	16.41	885.27	232.14	54.22	57.25
pad3-loc7	7	5	18.4	19.2	150	16.47	786.62	232.99	61.24	
pad3-loc7	7	6	18.4	19.2	150	16.56	774.25	234.30	62.57	

Table B-6. Quarry 1, Test Pad #3, 50% RCA - 50% crushed rock subbase layer

Location	PointNo	DropNo	Surface Temp	In-Depth Temp	Radius (mm)	Load (kN)	Deflection (um)	Stress (kPa)	Modulus (MPa)	Average (MPa)
pad3-loc1	1	1	25.8	20.9	150	16.65	820.02	235.58	59.40	68.74
pad3-loc1	1	2	25.8	20.9	150	16.88	743.22	238.75	66.42	
pad3-loc1	1	3	25.8	20.9	150	16.94	705.30	239.63	70.24	
pad3-loc1	1	4	25.8	20.9	150	16.95	680.30	239.83	72.89	
pad3-loc1	1	5	25.8	20.9	150	17.01	665.42	240.61	74.76	
pad3-loc2	2	1	25.8	20.9	150	16.97	858.91	240.01	57.77	67.75
pad3-loc2	2	2	25.8	20.9	150	17.08	774.29	241.60	64.51	
pad3-loc2	2	3	25.8	20.9	150	17.11	719.90	242.07	69.52	
pad3-loc2	2	4	25.8	20.9	150	17.21	686.35	243.43	73.33	
pad3-loc2	2	5	25.8	20.9	150	17.17	682.35	242.87	73.59	
pad3-loc3	3	1	25.8	20.9	150	16.77	1050.51	237.25	46.69	54.27
pad3-loc3	3	2	25.8	20.9	150	16.89	947.82	238.97	52.13	
pad3-loc3	3	3	25.8	20.9	150	16.94	885.07	239.63	55.98	
pad3-loc3	3	4	25.8	20.9	150	17.00	858.60	240.56	57.93	
pad3-loc3	3	5	25.8	20.9	150	16.96	845.97	239.92	58.64	
pad3-loc4	4	1	25.8	20.9	150	17.08	829.04	241.57	60.25	71.30
pad3-loc4	4	2	25.8	20.9	150	17.17	736.72	242.91	68.17	
pad3-loc4	4	3	25.8	20.9	150	17.25	691.23	243.99	72.98	
pad3-loc4	4	4	25.8	20.9	150	17.29	663.11	244.55	76.25	
pad3-loc4	4	5	25.8	20.9	150	17.37	644.42	245.70	78.83	
pad3-loc5	5	1	25.8	20.9	150	16.49	1268.13	233.35	38.05	40.00
pad3-loc5	5	2	25.8	20.9	150	16.54	1211.61	234.03	39.94	
pad3-loc5	5	3	25.8	20.9	150	16.47	1216.35	232.97	39.60	
pad3-loc5	5	4	25.8	20.9	150	16.47	1181.57	232.96	40.76	
pad3-loc5	5	5	25.8	20.9	150	16.54	1161.86	234.01	41.64	
pad3-loc6	6	1	25.8	20.9	150	16.40	1252.55			
pad3-loc6	6	2	25.8	20.9	150	16.69	1080.71	236.10	45.17	49.57

pad3-loc6	6	3	25.8	20.9	150	16.85	979.58	238.39	50.32	
pad3-loc6	6	4	25.8	20.9	150	16.87	964.10	238.63	51.18	
pad3-loc6	6	5	25.8	20.9	150	16.75	967.76	236.95	50.62	
pad3-loc6	6	6	25.8	20.9	150	16.80	972.21	237.68	50.55	
pad3-loc7	7	1	25.8	20.9	150	16.67	850.41			
pad3-loc7	7	2	25.8	20.9	150	16.88	755.15	238.74	65.37	
pad3-loc7	7	3	25.8	20.9	150	16.88	709.14	238.87	69.65	
pad3-loc7	7	4	25.8	20.9	150	16.90	693.30	239.13	71.31	71.25
pad3-loc7	7	5	25.8	20.9	150	17.02	675.76	240.81	73.68	
pad3-loc7	7	6	25.8	20.9	150	17.04	653.55	241.07	76.27	

Table B-7. Quarry 1, Test Pad #4, 26.5mm dense-graded crushed material subgrade layer

Location	PointNo	DropNo	Surface Temp	In-Depth Temp	Radius (mm)	Load (kN)	Deflection (um)	Stress (kPa)	Modulus (MPa)	Average (MPa)
pad4-loc1	1	1	17.6	17.2	150	14.46	810.96			
pad4-loc1	1	2	17.6	17.2	150	17.07	516.28	241.54	96.73	
pad4-loc1	1	3	17.6	17.2	150	17.13	500.04	242.28	100.18	
pad4-loc1	1	4	17.6	17.2	150	17.24	488.90	243.94	103.16	102.38
pad4-loc1	1	5	17.6	17.2	150	17.22	479.01	243.68	105.18	
pad4-loc1	1	6	17.6	17.2	150	17.24	472.75	243.85	106.65	
pad4-loc2	2	1	17.6	17.2	150	15.75	958.98			
pad4-loc2	2	2	17.6	17.2	150	17.06	583.13	241.41	85.59	
pad4-loc2	2	3	17.6	17.2	150	17.15	538.16	242.58	93.20	
pad4-loc2	2	4	17.6	17.2	150	17.25	513.93	244.05	98.18	95.54
pad4-loc2	2	5	17.6	17.2	150	17.22	507.50	243.67	99.27	
pad4-loc2	2	6	17.6	17.2	150	17.28	498.34	244.51	101.44	
pad4-loc3	3	1	17.6	17.2	150	14.66	1248.21			
pad4-loc3	3	2	17.6	17.2	150	17.19	499.46	243.20	100.68	
pad4-loc3	3	3	17.6	17.2	150	17.31	461.09	244.91	109.82	
pad4-loc3	3	4	17.6	17.2	150	17.32	417.29	245.01	121.40	118.13
pad4-loc3	3	5	17.6	17.2	150	17.34	398.94	245.31	127.13	
pad4-loc3	3	6	17.6	17.2	150	17.32	384.88	245.07	131.65	
pad4-loc4	4	1	17.6	17.2	150	15.42	1560.47			
pad4-loc4	4	2	17.6	17.2	150	17.27	558.91	244.36	90.40	
pad4-loc4	4	3	17.6	17.2	150	17.24	489.06	243.95	103.13	
pad4-loc4	4	4	17.6	17.2	150	17.33	448.05	245.16	113.13	110.89
pad4-loc4	4	5	17.6	17.2	150	17.34	418.62	245.26	121.13	
pad4-loc4	4	6	17.6	17.2	150	17.35	400.77	245.50	126.65	
pad4-loc5	5	1	17.6	17.2	150	14.78	776.71			
pad4-loc5	5	2	17.6	17.2	150	17.28	478.99	244.42	105.50	115.60
pad4-loc5	5	3	17.6	17.2	150	17.26	436.78	244.12	115.56	

pad4-loc5	5	4	17.6	17.2	150	17.38	435.90	245.88	116.62	
pad4-loc5	5	5	17.6	17.2	150	17.34	429.84	245.26	117.97	
pad4-loc5	5	6	17.6	17.2	150	17.48	417.96	247.35	122.36	
pad4-loc6	6	1	17.6	17.2	150	14.20	1254.74			
pad4-loc6	6	2	17.6	17.2	150	17.19	603.70	243.13	83.27	
pad4-loc6	6	3	17.6	17.2	150	17.24	535.72	243.94	94.15	
pad4-loc6	6	4	17.6	17.2	150	17.36	501.58	245.54	101.22	99.03
pad4-loc6	6	5	17.6	17.2	150	17.45	478.46	246.89	106.69	
pad4-loc6	6	6	17.6	17.2	150	17.42	463.87	246.40	109.83	
pad4-loc7	7	1	17.6	17.2	150	14.49	1541.09			
pad4-loc7	7	2	17.6	17.2	150	16.88	734.17	238.76	67.24	
pad4-loc7	7	3	17.6	17.2	150	17.06	638.38	241.38	78.18	
pad4-loc7	7	4	17.6	17.2	150	17.14	602.12	242.43	83.24	80.77
pad4-loc7	7	5	17.6	17.2	150	17.21	580.09	243.44	86.77	
pad4-loc7	7	6	17.6	17.2	150	17.14	567.07	242.46	88.40	

Table B-8. Quarry 1, Test Pad #4, 25% RCA - 75% crushed rock subbase layer

Location	PointNo	DropNo	Surface Temp	In-Depth Temp	Radius (mm)	Load (kN)	Deflection (um)	Stress (kPa)	Modulus (MPa)	Average (MPa)
pad4-loc1	1	1	22.8	20.0	150	14.57	1911.40			
pad4-loc1	1	2	22.8	20.0	150	17.04	704.01	241.13	70.82	
pad4-loc1	1	3	22.8	20.0	150	17.17	595.51	242.87	84.32	
pad4-loc1	1	4	22.8	20.0	150	17.24	557.40	243.88	90.46	87.39
pad4-loc1	1	5	22.8	20.0	150	17.24	530.90	243.84	94.96	
pad4-loc1	1	6	22.8	20.0	150	17.39	527.64	246.02	96.40	
pad4-loc2	2	1	22.8	20.0	150	14.57	2003.09			
pad4-loc2	2	2	22.8	20.0	150	16.52	772.60			
pad4-loc2	2	3	22.8	20.0	150	16.67	625.14			
pad4-loc2	2	4	22.8	20.0	150	15.03	1873.75			
pad4-loc2	2	5	22.8	20.0	150	17.04	671.82	241.04	74.18	
pad4-loc2	2	6	22.8	20.0	150	17.06	605.94	241.36	82.36	
pad4-loc2	2	7	22.8	20.0	150	17.04	576.71	241.07	86.43	84.57
pad4-loc2	2	8	22.8	20.0	150	17.20	558.84	243.39	90.05	
pad4-loc2	2	9	22.8	20.0	150	17.20	560.04	243.29	89.82	
pad4-loc3	3	1	22.8	20.0	150	16.84	801.87	238.25	61.43	
pad4-loc3	3	2	22.8	20.0	150	16.56	692.61	234.34	69.96	
pad4-loc3	3	3	22.8	20.0	150	17.16	610.97	242.75	82.15	76.67
pad4-loc3	3	4	22.8	20.0	150	17.09	604.77	241.76	82.65	
pad4-loc3	3	5	22.8	20.0	150	17.27	579.34	244.28	87.18	
pad4-loc4	4	1	22.8	20.0	150	14.95	1785.05			
pad4-loc4	4	2	22.8	20.0	150	16.96	814.21	239.93	60.93	
pad4-loc4	4	3	22.8	20.0	150	17.02	704.66	240.73	70.63	
pad4-loc4	4	4	22.8	20.0	150	17.16	626.25	242.69	80.12	77.73
pad4-loc4	4	5	22.8	20.0	150	17.16	609.02	242.71	82.40	
pad4-loc4	4	6	22.8	20.0	150	17.23	532.82	243.70	94.57	
pad4-loc5	5	1	22.8	20.0	150	16.95	725.78	239.83	68.32	85.87

pad4-loc5	5	2	22.8	20.0	150	17.16	614.10	242.72	81.72	
pad4-loc5	5	3	22.8	20.0	150	17.22	554.00	243.63	90.92	
pad4-loc5	5	4	22.8	20.0	150	17.01	536.12	240.65	92.81	
pad4-loc5	5	5	22.8	20.0	150	17.34	530.89	245.37	95.56	
pad4-loc6	6	1	22.8	20.0	150	16.59	841.05	234.65	57.68	
pad4-loc6	6	2	22.8	20.0	150	16.94	739.99	239.68	66.97	
pad4-loc6	6	3	22.8	20.0	150	17.16	646.57	242.79	77.64	73.13
pad4-loc6	6	4	22.8	20.0	150	17.20	631.56	243.37	79.67	
pad4-loc6	6	5	22.8	20.0	150	17.21	601.72	243.50	83.67	
pad4-loc7	7	1	22.8	20.0	150	16.84	841.72	238.17	58.50	
pad4-loc7	7	2	22.8	20.0	150	16.96	714.52	239.93	69.43	
pad4-loc7	7	3	22.8	20.0	150	17.09	686.71	241.77	72.79	71.51
pad4-loc7	7	4	22.8	20.0	150	17.02	648.40	240.80	76.78	
pad4-loc7	7	5	22.8	20.0	150	17.03	622.07	240.90	80.07	

Table B-9. Quarry 1, Test Pad #5, 26.5mm dense-graded crushed material subgrade layer

Location	PointNo	DropNo	Surface Temp	In-Depth Temp	Radius (mm)	Load (kN)	Deflection (um)	Stress (kPa)	Modulus (MPa)	Average (MPa)
pad5-loc1	1	1	16.8	16.6	150	14.91	1490.87			
pad5-loc1	1	2	16.8	16.6	150	16.95	627.78	239.86	79.00	
pad5-loc1	1	3	16.8	16.6	150	17.08	521.52	241.67	95.81	
pad5-loc1	1	4	16.8	16.6	150	17.17	508.38	242.90	98.79	97.00
pad5-loc1	1	5	16.8	16.6	150	17.17	476.02	242.86	105.48	
pad5-loc1	1	6	16.8	16.6	150	17.25	476.45	244.03	105.90	
pad5-loc2	2	1	16.8	16.6	150	13.18	960.28			
pad5-loc2	2	2	16.8	16.6	150	16.92	614.92	239.33	80.47	
pad5-loc2	2	3	16.8	16.6	150	17.13	541.08	242.39	92.62	
pad5-loc2	2	4	16.8	16.6	150	17.19	513.98	243.14	97.81	96.03
pad5-loc2	2	5	16.8	16.6	150	17.30	489.10	244.76	103.47	
pad5-loc2	2	6	16.8	16.6	150	17.28	477.71	244.47	105.81	
pad5-loc3	3	1	16.8	16.6	150	13.61	1637.32			
pad5-loc3	3	2	16.8	16.6	150	16.80	656.81	237.66	74.81	
pad5-loc3	3	3	16.8	16.6	150	17.01	525.05	240.64	94.76	
pad5-loc3	3	4	16.8	16.6	150	17.07	479.18	241.50	104.20	98.83
pad5-loc3	3	5	16.8	16.6	150	17.05	462.12	241.15	107.89	
pad5-loc3	3	6	16.8	16.6	150	17.10	444.70	241.94	112.49	
pad5-loc4	4	1	16.8	16.6	150	14.96	1631.54			
pad5-loc4	4	2	16.8	16.6	150	17.25	607.29	244.09	83.10	
pad5-loc4	4	3	16.8	16.6	150	17.34	505.30	245.26	100.35	
pad5-loc4	4	4	16.8	16.6	150	17.35	469.46	245.52	108.13	104.93
pad5-loc4	4	5	16.8	16.6	150	17.32	444.53	245.00	113.95	
pad5-loc4	4	6	16.8	16.6	150	17.43	428.05	246.59	119.11	
pad5-loc5	5	1	16.8	16.6	150	14.54	1157.37			
pad5-loc5	5	2	16.8	16.6	150	17.10	529.30	241.85	94.47	111.87
pad5-loc5	5	3	16.8	16.6	150	17.25	470.80	244.04	107.17	

pad5-loc5	5	4	16.8	16.6	150	17.36	442.08	245.58	114.86	
pad5-loc5	5	5	16.8	16.6	150	17.29	423.05	244.56	119.52	
pad5-loc5	5	6	16.8	16.6	150	17.48	414.62	247.30	123.32	
pad5-loc6	6	1	16.8	16.6	150	14.16	1247.96			
pad5-loc6	6	2	16.8	16.6	150	16.93	581.58	239.53	85.15	
pad5-loc6	6	3	16.8	16.6	150	17.07	511.00	241.56	97.74	
pad5-loc6	6	4	16.8	16.6	150	17.26	472.83	244.13	106.75	103.01
pad5-loc6	6	5	16.8	16.6	150	17.27	453.47	244.30	111.38	
pad5-loc6	6	6	16.8	16.6	150	17.35	445.07	245.46	114.03	
pad5-loc7	7	1	16.8	16.6	150	13.69	1643.70			
pad5-loc7	7	2	16.8	16.6	150	16.94	783.73	239.60	63.21	
pad5-loc7	7	3	16.8	16.6	150	17.17	691.75	242.87	72.59	
pad5-loc7	7	4	16.8	16.6	150	17.19	646.39	243.14	77.77	76.19
pad5-loc7	7	5	16.8	16.6	150	17.21	610.97	243.49	82.40	
pad5-loc7	7	6	16.8	16.6	150	17.23	593.16	243.75	84.96	

Table B-10. Quarry 1, Test Pad #5, 70% RCA - 30% RAP subbase layer

Location	PointNo	DropNo	Surface Temp	In-Depth Temp	Radius (mm)	Load (kN)	Deflection (um)	Stress (kPa)	Modulus (MPa)	Average (MPa)
pad5-loc1	1	1	23.2	19.8	150	16.77	855.96	237.26	57.31	69.60
pad5-loc1	1	2	23.2	19.8	150	16.93	742.25	239.58	66.74	
pad5-loc1	1	3	23.2	19.8	150	17.08	693.38	241.63	72.05	
pad5-loc1	1	4	23.2	19.8	150	17.15	672.21	242.68	74.64	
pad5-loc1	1	5	23.2	19.8	150	17.12	648.17	242.13	77.24	
pad5-loc2	2	1	23.2	19.8	150	13.01	970.04			
pad5-loc2	2	2	23.2	19.8	150	16.58	725.92	234.50	66.79	77.06
pad5-loc2	2	3	23.2	19.8	150	16.77	666.08	237.19	73.63	
pad5-loc2	2	4	23.2	19.8	150	17.00	628.43	240.56	79.14	
pad5-loc2	2	5	23.2	19.8	150	16.97	610.50	240.07	81.31	
pad5-loc2	2	6	23.2	19.8	150	17.01	589.15	240.58	84.43	
pad5-loc3	3	1	23.2	19.8	150	16.83	715.71	238.04	68.77	82.58
pad5-loc3	3	2	23.2	19.8	150	17.02	628.30	240.77	79.23	
pad5-loc3	3	3	23.2	19.8	150	17.09	592.97	241.79	84.31	
pad5-loc3	3	4	23.2	19.8	150	17.18	567.41	243.00	88.55	
pad5-loc3	3	5	23.2	19.8	150	17.08	542.76	241.62	92.04	
pad5-loc4	4	1	23.2	19.8	150	13.96	1191.04			
pad5-loc4	4	2	23.2	19.8	150	16.56	702.30	234.32	68.98	78.79
pad5-loc4	4	3	23.2	19.8	150	16.66	665.40	235.73	73.25	
pad5-loc4	4	4	23.2	19.8	150	16.99	619.69	240.38	80.20	
pad5-loc4	4	5	23.2	19.8	150	17.09	591.18	241.79	84.56	
pad5-loc4	4	6	23.2	19.8	150	17.11	575.45	242.08	86.98	
pad5-loc5	5	1	23.2	19.8	150	14.18	1679.61			
pad5-loc5	5	2	23.2	19.8	150	16.32	913.77	230.85	52.23	68.18
pad5-loc5	5	3	23.2	19.8	150	16.86	777.12	238.51	63.46	
pad5-loc5	5	4	23.2	19.8	150	16.97	690.65	240.02	71.85	
pad5-loc5	5	5	23.2	19.8	150	17.09	659.73	241.81	75.78	

pad5-loc5	5	6	23.2	19.8	150	17.02	641.76	240.77	77.57	
pad5-loc6	6	1	23.2	19.8	150	15.67	1453.01			
pad5-loc6	6	2	23.2	19.8	150	16.88	702.25	238.76	70.29	
pad5-loc6	6	3	23.2	19.8	150	17.13	630.27	242.37	79.51	
pad5-loc6	6	4	23.2	19.8	150	17.08	565.13	241.65	88.41	84.61
pad5-loc6	6	5	23.2	19.8	150	17.12	549.36	242.15	91.14	
pad5-loc6	6	6	23.2	19.8	150	17.16	535.77	242.78	93.69	
pad5-loc7	7	1	23.2	19.8	150	16.87	796.02	238.73	62.01	
pad5-loc7	7	2	23.2	19.8	150	17.00	727.68	240.56	68.35	
pad5-loc7	7	3	23.2	19.8	150	17.03	691.83	240.96	72.01	70.32
pad5-loc7	7	4	23.2	19.8	150	17.08	676.08	241.64	73.90	
pad5-loc7	7	5	23.2	19.8	150	17.10	664.12	241.94	75.32	

Table B-11. Quarry 2, Test Pad #1, dense-graded crushed material subgrade layer

Location	PointNo	DropNo	Surface Temp	In-Depth Temp	Radius (mm)	Load (kN)	Deflection (um)	Stress (kPa)	Modulus (MPa)	Average (MPa)
pad1-loc1	1	1	18.2	17.7	150	15.63	1593.04			
pad1-loc1	1	2	18.2	17.7	150	17.07	694.73	241.45	71.86	
pad1-loc1	1	3	18.2	17.7	150	17.15	616.97	242.56	81.29	
pad1-loc1	1	4	18.2	17.7	150	17.13	571.59	242.36	87.67	85.08
pad1-loc1	1	5	18.2	17.7	150	17.26	558.58	244.19	90.39	
pad1-loc1	1	6	18.2	17.7	150	17.35	538.60	245.44	94.22	
pad1-loc2	2	1	18.2	17.7	150	15.66	1603.74			
pad1-loc2	2	2	18.2	17.7	150	17.07	702.74	241.52	71.06	
pad1-loc2	2	3	18.2	17.7	150	17.04	644.36	241.10	77.36	
pad1-loc2	2	4	18.2	17.7	150	17.02	621.68	240.77	80.07	79.22
pad1-loc2	2	5	18.2	17.7	150	17.13	606.45	242.32	82.61	
pad1-loc2	2	6	18.2	17.7	150	17.19	591.69	243.18	84.98	
pad1-loc3	3	1	18.2	17.7	150	16.46	646.65			
pad1-loc3	3	2	18.2	17.7	150	17.07	462.77	241.56	107.92	
pad1-loc3	3	3	18.2	17.7	150	16.96	431.09	239.93	115.07	
pad1-loc3	3	4	18.2	17.7	150	17.19	431.17	243.19	116.61	114.35
pad1-loc3	3	5	18.2	17.7	150	17.05	425.97	241.19	117.07	
pad1-loc3	3	6	18.2	17.7	150	16.98	431.47	240.18	115.09	
pad1-loc4	4	1	18.2	17.7	150	15.90	420.96			
pad1-loc4	4	2	18.2	17.7	150	16.87	319.16			
pad1-loc4	4	3	18.2	17.7	150	17.09	310.59	241.83	160.98	
pad1-loc4	4	4	18.2	17.7	150	17.31	298.09	244.89	169.85	
pad1-loc4	4	5	18.2	17.7	150	17.43	303.65	246.52	167.85	168.42
pad1-loc4	4	6	18.2	17.7	150	17.25	294.76	243.99	171.15	
pad1-loc4	4	7	18.2	17.7	150	17.40	295.53	246.22	172.26	
pad1-loc5	5	1	18.2	17.7	150	15.02	1214.21			
pad1-loc5	5	2	18.2	17.7	150	0.93	80.04			

pad1-loc5	5	3	18.2	17.7	150	16.92	571.41	239.33	86.60	
pad1-loc5	5	4	18.2	17.7	150	16.99	530.80	240.42	93.65	
pad1-loc5	5	5	18.2	17.7	150	17.14	513.70	242.50	97.60	95.58
pad1-loc5	5	6	18.2	17.7	150	17.31	508.26	244.85	99.60	
pad1-loc5	5	7	18.2	17.7	150	17.31	504.05	244.89	100.45	
pad1-loc6	6	1	18.2	17.7	150	14.13	878.67			
pad1-loc6	6	2	18.2	17.7	150	16.54	768.05	233.94	62.98	
pad1-loc6	6	3	18.2	17.7	150	16.63	741.74	235.31	65.59	
pad1-loc6	6	4	18.2	17.7	150	16.67	744.43	235.84	65.50	65.94
pad1-loc6	6	5	18.2	17.7	150	16.61	717.84	235.05	67.70	
pad1-loc6	6	6	18.2	17.7	150	16.66	717.06	235.66	67.95	
pad1-loc7	7	1	18.2	17.7	150	13.72	852.37			
pad1-loc7	7	2	18.2	17.7	150	16.58	1.59			
pad1-loc7	7	3	18.2	17.7	150	15.10	1144.91			
pad1-loc7	7	4	18.2	17.7	150	16.86	586.37	238.56	84.12	
pad1-loc7	7	5	18.2	17.7	150	16.77	551.43	237.29	88.97	
pad1-loc7	7	6	18.2	17.7	150	16.81	527.88	237.87	93.17	92.97
pad1-loc7	7	7	18.2	17.7	150	16.98	508.35	240.20	97.69	
pad1-loc7	7	8	18.2	17.7	150	17.06	494.44	241.33	100.91	

Table B-12. Quarry 2, Test Pad #1, 100% crushed rock subbase layer

Location	PointNo	DropNo	Surface Temp	In-Depth Temp	Radius (mm)	Load (kN)	Deflection (um)	Stress (kPa)	Modulus (MPa)	Average (MPa)
pad1-loc1	1	1	26.4	23.7	150	15.18	1027.08			
pad1-loc1	1	2	26.4	23.7	150	17.14	590.67	242.44	84.86	100.33
pad1-loc1	1	3	26.4	23.7	150	17.25	535.34	244.11	94.28	
pad1-loc1	1	4	26.4	23.7	150	17.21	460.79	243.49	109.25	
pad1-loc1	1	5	26.4	23.7	150	17.24	479.88	243.87	105.07	
pad1-loc1	1	6	26.4	23.7	150	17.31	468.01	244.86	108.17	
pad1-loc2	2	1	26.4	23.7	150	17.06	908.77			
pad1-loc2	2	2	26.4	23.7	150	17.17	792.79	242.96	63.36	71.91
pad1-loc2	2	3	26.4	23.7	150	17.32	732.44	245.07	69.18	
pad1-loc2	2	4	26.4	23.7	150	17.29	697.16	244.57	72.53	
pad1-loc2	2	5	26.4	23.7	150	17.38	664.74	245.88	76.48	
pad1-loc2	2	6	26.4	23.7	150	17.37	651.36	245.76	78.01	
pad1-loc3	3	1	26.4	23.7	150	15.96	1457.74			
pad1-loc3	3	2	26.4	23.7	150	17.30	695.10	244.69	72.78	83.07
pad1-loc3	3	3	26.4	23.7	150	17.28	632.37	244.49	79.94	
pad1-loc3	3	4	26.4	23.7	150	17.48	599.37	247.22	85.28	
pad1-loc3	3	5	26.4	23.7	150	17.43	582.88	246.53	87.45	
pad1-loc3	3	6	26.4	23.7	150	17.44	567.46	246.76	89.91	
pad1-loc4	4	1	26.4	23.7	150	15.69	1513.71			
pad1-loc4	4	2	26.4	23.7	150	17.25	681.18	244.09	74.09	84.29
pad1-loc4	4	3	26.4	23.7	150	17.38	619.48	245.87	82.06	
pad1-loc4	4	4	26.4	23.7	150	17.35	592.25	245.48	85.70	
pad1-loc4	4	5	26.4	23.7	150	17.37	570.98	245.72	88.98	
pad1-loc4	4	6	26.4	23.7	150	17.43	562.53	246.62	90.64	
pad1-loc5	5	1	26.4	23.7	150	16.92	835.06			
pad1-loc5	5	2	26.4	23.7	150	17.14	735.26	242.45	68.18	73.86
pad1-loc5	5	3	26.4	23.7	150	17.17	699.02	242.92	71.85	

pad1-loc5	5	4	26.4	23.7	150	17.31	676.64	244.87	74.82	
pad1-loc5	5	5	26.4	23.7	150	17.19	655.13	243.22	76.76	
pad1-loc5	5	6	26.4	23.7	150	17.28	650.81	244.48	77.67	
pad1-loc6	6	1	26.4	23.7	150	16.61	1051.14			
pad1-loc6	6	2	26.4	23.7	150	16.92	960.67	239.32	51.51	
pad1-loc6	6	3	26.4	23.7	150	17.01	907.29	240.63	54.83	
pad1-loc6	6	4	26.4	23.7	150	17.03	872.43	240.87	57.08	56.91
pad1-loc6	6	5	26.4	23.7	150	16.99	830.37	240.36	59.85	
pad1-loc6	6	6	26.4	23.7	150	17.06	814.54	241.35	61.26	
pad1-loc7	7	1	26.4	23.7	150	16.39	1276.18			
pad1-loc7	7	2	26.4	23.7	150	16.58	1226.29	234.54	39.55	
pad1-loc7	7	3	26.4	23.7	150	16.54	1207.17	233.97	40.07	
pad1-loc7	7	4	26.4	23.7	150	16.63	1191.88	235.26	40.81	40.56
pad1-loc7	7	5	26.4	23.7	150	16.60	1186.94	234.86	40.91	
pad1-loc7	7	6	26.4	23.7	150	16.54	1167.78	234.05	41.44	

Table B-13. Quarry 2, Test Pad #2, dense-graded crushed material subgrade layer

Location	PointNo	DropNo	Surface Temp	In-Depth Temp	Radius (mm)	Load (kN)	Deflection (um)	Stress (kPa)	Modulus (MPa)	Average (MPa)
pad2-loc1	1	1	26.4	18.6	150	14.76	755.24			
pad2-loc1	1	2	26.4	18.6	150	16.42	751.64	232.27	63.89	
pad2-loc1	1	3	26.4	18.6	150	16.51	774.23	233.53	62.36	
pad2-loc1	1	4	26.4	18.6	150	16.62	733.08	235.17	66.33	63.24
pad2-loc1	1	5	26.4	18.6	150	16.61	786.94	235.00	61.74	
pad2-loc1	1	6	26.4	18.6	150	16.70	789.17	236.21	61.89	
pad2-loc2	2	1	26.4	18.6	150	14.91	943.11			
pad2-loc2	2	2	26.4	18.6	150	16.88	435.14	238.78	113.45	
pad2-loc2	2	3	26.4	18.6	150	16.97	416.30	240.03	119.21	
pad2-loc2	2	4	26.4	18.6	150	16.95	397.22	239.75	124.79	122.94
pad2-loc2	2	5	26.4	18.6	150	17.12	389.84	242.19	128.45	
pad2-loc2	2	6	26.4	18.6	150	17.21	390.94	243.48	128.77	
pad2-loc3	3	1	26.4	18.6	150	15.59	1172.21			
pad2-loc3	3	2	26.4	18.6	150	16.88	710.17	238.82	69.53	
pad2-loc3	3	3	26.4	18.6	150	16.77	673.42	237.23	72.84	
pad2-loc3	3	4	26.4	18.6	150	16.73	646.21	236.70	75.73	76.52
pad2-loc3	3	5	26.4	18.6	150	16.81	600.98	237.88	81.84	
pad2-loc3	3	6	26.4	18.6	150	16.85	596.24	238.37	82.66	
pad2-loc4	4	1	26.4	18.6	150	16.22	195.00			
pad2-loc4	4	2	26.4	18.6	150	16.82	183.73	237.92	267.74	
pad2-loc4	4	3	26.4	18.6	150	17.17	209.14	242.96	240.19	
pad2-loc4	4	4	26.4	18.6	150	16.96	211.46	239.95	234.61	243.76
pad2-loc4	4	5	26.4	18.6	150	16.81	203.81	237.76	241.19	
pad2-loc4	4	6	26.4	18.6	150	16.84	209.48	238.18	235.08	
pad2-loc5	5	1	26.4	18.6	150	15.30	267.28			
pad2-loc5	5	2	26.4	18.6	150	16.27	205.99			
pad2-loc5	5	3	26.4	18.6	150	17.12	244.82	242.24	204.58	207.23

pad2-loc5	5	4	26.4	18.6	150	16.76	237.46	237.04	206.40	
pad2-loc5	5	5	26.4	18.6	150	16.82	242.35	237.98	203.03	
pad2-loc5	5	6	26.4	18.6	150	16.89	234.55	238.96	210.64	
pad2-loc5	5	7	26.4	18.6	150	16.99	234.95	240.35	211.51	
pad2-loc6	6	1	26.4	18.6	150	15.96	255.27			
pad2-loc6	6	2	26.4	18.6	150	16.74	136.52			
pad2-loc6	6	3	26.4	18.6	150	16.82	165.73			
pad2-loc6	6	4	26.4	18.6	150	16.58	181.36			
pad2-loc6	6	5	26.4	18.6	150	1.50	5243.33			
pad2-loc6	6	6	26.4	18.6	150	15.02	1046.75			
pad2-loc6	6	7	26.4	18.6	150	16.31	580.32			
pad2-loc6	6	8	26.4	18.6	150	16.40	534.17	232.06	89.82	
pad2-loc6	6	9	26.4	18.6	150	16.64	516.18	235.42	94.30	
pad2-loc6	6	10	26.4	18.6	150	16.34	435.60			98.12
pad2-loc6	6	11	26.4	18.6	150	16.41	495.30	232.17	96.92	
pad2-loc6	6	12	26.4	18.6	150	16.48	468.72	233.21	102.87	
pad2-loc6	6	13	26.4	18.6	150	16.42	450.30	232.34	106.68	
pad2-loc7	7	1	26.4	18.6	150	15.65	806.92			
pad2-loc7	7	2	26.4	18.6	150	16.37	437.72	231.52	109.36	
pad2-loc7	7	3	26.4	18.6	150	16.86	408.51	238.51	120.71	
pad2-loc7	7	4	26.4	18.6	150	16.44	392.04	232.51	122.62	121.50
pad2-loc7	7	5	26.4	18.6	150	16.45	383.22	232.72	125.56	
pad2-loc7	7	6	26.4	18.6	150	16.90	382.35	239.03	129.26	

Table B-14. Quarry 2, Test Pad #2, 100% RCA subbase layer

Location	PointNo	DropNo	Surface Temp	In-Depth Temp	Radius (mm)	Load (kN)	Deflection (um)	Stress (kPa)	Modulus (MPa)	Average (MPa)
pad2-loc1	1	1	26.8	22.7	150	15.77	1845.54			
pad2-loc1	1	2	26.8	22.7	150	15.96	1761.91	225.77	26.49	27.54
pad2-loc1	1	3	26.8	22.7	150	16.03	1727.35	226.80	27.15	
pad2-loc1	1	4	26.8	22.7	150	16.04	1696.31	226.87	27.65	
pad2-loc1	1	5	26.8	22.7	150	16.07	1669.88	227.30	28.14	
pad2-loc1	1	6	26.8	22.7	150	16.05	1661.03	227.12	28.27	
pad2-loc2	2	1	26.8	22.7	150	16.98	853.63			
pad2-loc2	2	2	26.8	22.7	150	17.16	775.55	242.77	64.72	69.77
pad2-loc2	2	3	26.8	22.7	150	17.12	734.56	242.13	68.15	
pad2-loc2	2	4	26.8	22.7	150	17.16	716.17	242.82	70.10	
pad2-loc2	2	5	26.8	22.7	150	17.22	697.99	243.56	72.15	
pad2-loc2	2	6	26.8	22.7	150	17.15	680.52	242.66	73.72	
pad2-loc3	3	1	26.8	22.7	150	16.92	991.61			
pad2-loc3	3	2	26.8	22.7	150	17.01	866.31	240.67	57.44	62.63
pad2-loc3	3	3	26.8	22.7	150	17.10	821.01	241.96	60.93	
pad2-loc3	3	4	26.8	22.7	150	17.14	792.07	242.42	63.28	
pad2-loc3	3	5	26.8	22.7	150	17.16	780.70	242.81	64.30	
pad2-loc3	3	6	26.8	22.7	150	17.19	748.58	243.22	67.18	
pad2-loc4	4	1	26.8	22.7	150	17.04	872.23			
pad2-loc4	4	2	26.8	22.7	150	17.17	762.71	242.95	65.86	71.37
pad2-loc4	4	3	26.8	22.7	150	17.17	733.39	242.88	68.47	
pad2-loc4	4	4	26.8	22.7	150	17.25	699.91	244.01	72.08	
pad2-loc4	4	5	26.8	22.7	150	17.27	679.20	244.30	74.37	
pad2-loc4	4	6	26.8	22.7	150	17.30	665.19	244.77	76.08	
pad2-loc5	5	1	26.8	22.7	150	16.94	899.40			
pad2-loc5	5	2	26.8	22.7	150	17.16	782.61	242.75	64.13	69.49
pad2-loc5	5	3	26.8	22.7	150	17.15	757.42	242.57	66.22	

pad2-loc5	5	4	26.8	22.7	150	17.13	714.82	242.40	70.11	
pad2-loc5	5	5	26.8	22.7	150	17.26	693.21	244.24	72.85	
pad2-loc5	5	6	26.8	22.7	150	17.29	682.02	244.58	74.15	
pad2-loc6	6	1	26.8	22.7	150	16.99	847.93			
pad2-loc6	6	2	26.8	22.7	150	17.17	763.85	242.88	65.74	
pad2-loc6	6	3	26.8	22.7	150	17.20	725.39	243.40	69.38	
pad2-loc6	6	4	26.8	22.7	150	17.27	691.26	244.39	73.10	72.13
pad2-loc6	6	5	26.8	22.7	150	17.14	667.40	242.51	75.13	
pad2-loc6	6	6	26.8	22.7	150	17.37	657.20	245.75	77.31	
pad2-loc7	7	1	26.8	22.7	150	15.07	1651.56			
pad2-loc7	7	2	26.8	22.7	150	17.08	745.60			
pad2-loc7	7	3	26.8	22.7	150	17.21	664.51	243.41	75.73	
pad2-loc7	7	4	26.8	22.7	150	17.27	637.75	244.34	79.22	
pad2-loc7	7	5	26.8	22.7	150	13.27	556.35	187.67	69.74	79.43
pad2-loc7	7	6	26.8	22.7	150	17.38	601.58	245.88	84.51	
pad2-loc7	7	7	26.8	22.7	150	17.31	575.77	244.93	87.95	

Table B-15. Quarry 2, Test Pad #3, dense-graded crushed material subgrade layer

Location	PointNo	DropNo	Surface Temp	In-Depth Temp	Radius (mm)	Load (kN)	Deflection (um)	Stress (kPa)	Modulus (MPa)	Average (MPa)
pad3-loc1	1	1	22.6	22.0	150	14.73	1015.17			
pad3-loc1	1	2	22.6	22.0	150	16.57	653.25	234.42	74.20	
pad3-loc1	1	3	22.6	22.0	150	16.60	596.22	234.86	81.44	
pad3-loc1	1	4	22.6	22.0	150	16.37	614.70	231.65	77.92	79.19
pad3-loc1	1	5	22.6	22.0	150	16.55	596.44	234.13	81.16	
pad3-loc1	1	6	22.6	22.0	150	16.45	592.57	232.76	81.21	
pad3-loc2	2	1	22.6	22.0	150	15.45	1576.53			
pad3-loc2	2	2	22.6	22.0	150	17.01	681.96	240.62	72.95	
pad3-loc2	2	3	22.6	22.0	150	17.12	625.96	242.15	79.98	
pad3-loc2	2	4	22.6	22.0	150	17.19	596.89	243.23	84.25	82.38
pad3-loc2	2	5	22.6	22.0	150	17.18	582.29	243.11	86.32	
pad3-loc2	2	6	22.6	22.0	150	17.22	569.86	243.59	88.38	
pad3-loc3	3	1	22.6	22.0	150	16.20	926.49			
pad3-loc3	3	2	22.6	22.0	150	17.14	543.92	242.52	92.19	
pad3-loc3	3	3	22.6	22.0	150	17.19	494.04	243.26	101.80	
pad3-loc3	3	4	22.6	22.0	150	17.39	473.45	246.02	107.44	104.50
pad3-loc3	3	5	22.6	22.0	150	17.35	459.69	245.39	110.37	
pad3-loc3	3	6	22.6	22.0	150	17.27	456.30	244.30	110.69	
pad3-loc4	4	1	22.6	22.0	150	15.81	1250.01			
pad3-loc4	4	2	22.6	22.0	150	17.21	600.08	243.44	83.88	
pad3-loc4	4	3	22.6	22.0	150	17.26	543.28	244.13	92.91	
pad3-loc4	4	4	22.6	22.0	150	17.41	528.50	246.34	96.37	94.20
pad3-loc4	4	5	22.6	22.0	150	17.39	516.46	246.05	98.50	
pad3-loc4	4	6	22.6	22.0	150	17.47	514.25	247.09	99.34	
pad3-loc5	5	1	22.6	22.0	150	15.84	556.42			
pad3-loc5	5	2	22.6	22.0	150	17.28	375.88	244.46	134.47	137.28
pad3-loc5	5	3	22.6	22.0	150	17.36	368.50	245.57	137.79	

pad3-loc5	5	4	22.6	22.0	150	17.30	371.26	244.76	136.31	
pad3-loc5	5	5	22.6	22.0	150	17.37	359.31	245.70	141.38	
pad3-loc5	5	6	22.6	22.0	150	17.42	373.43	246.49	136.47	
pad3-loc6	6	1	22.6	22.0	150	16.40	331.41			
pad3-loc6	6	2	22.6	22.0	150	17.29	294.79	244.58	171.54	
pad3-loc6	6	3	22.6	22.0	150	17.31	279.54	244.88	181.12	
pad3-loc6	6	4	22.6	22.0	150	17.29	273.53	244.54	184.84	181.09
pad3-loc6	6	5	22.6	22.0	150	17.30	276.62	244.80	182.98	
pad3-loc6	6	6	22.6	22.0	150	17.27	273.16	244.35	184.95	
pad3-loc7	7	1	22.6	22.0	150	16.06	465.04			
pad3-loc7	7	2	22.6	22.0	150	17.51	337.62	247.68	151.68	
pad3-loc7	7	3	22.6	22.0	150	17.44	324.71	246.76	157.13	
pad3-loc7	7	4	22.6	22.0	150	17.46	318.88	247.05	160.18	159.91
pad3-loc7	7	5	22.6	22.0	150	17.53	310.10	247.97	165.33	
pad3-loc7	7	6	22.6	22.0	150	17.55	310.64	248.29	165.26	

Table B-16. Quarry 2, Test Pad #3, 70% RCA - 30% RAP subbase layer

Location	PointNo	DropNo	Surface Temp	In-Depth Temp	Radius (mm)	Load (kN)	Deflection (um)	Stress (kPa)	Modulus (MPa)	Average (MPa)
pad3-loc1	1	1	24.4	23.3	150	15.35	1287.09			
pad3-loc1	1	2	24.4	23.3	150	17.04	709.93	241.12	70.22	
pad3-loc1	1	3	24.4	23.3	150	17.23	646.16	243.71	77.98	
pad3-loc1	1	4	24.4	23.3	150	17.21	607.14	243.49	82.92	80.35
pad3-loc1	1	5	24.4	23.3	150	17.27	596.90	244.32	84.63	
pad3-loc1	1	6	24.4	23.3	150	17.21	585.25	243.47	86.01	
pad3-loc2	2	1	24.4	23.3	150	16.86	856.07			
pad3-loc2	2	2	24.4	23.3	150	17.07	713.17	241.48	70.01	
pad3-loc2	2	3	24.4	23.3	150	17.16	647.14	242.76	77.56	
pad3-loc2	2	4	24.4	23.3	150	17.20	614.25	243.34	81.91	80.79
pad3-loc2	2	5	24.4	23.3	150	17.22	585.57	243.60	86.01	
pad3-loc2	2	6	24.4	23.3	150	17.23	569.71	243.77	88.47	
pad3-loc3	3	1	24.4	23.3	150	16.12	1079.81			
pad3-loc3	3	2	24.4	23.3	150	17.19	595.83	243.15	84.37	
pad3-loc3	3	3	24.4	23.3	150	17.23	555.47	243.72	90.72	
pad3-loc3	3	4	24.4	23.3	150	17.24	533.04	243.95	94.62	93.58
pad3-loc3	3	5	24.4	23.3	150	17.30	515.71	244.80	98.14	
pad3-loc3	3	6	24.4	23.3	150	17.29	505.63	244.64	100.03	
pad3-loc4	4	1	24.4	23.3	150	15.08	1897.32			
pad3-loc4	4	2	24.4	23.3	150	16.68	1038.71	235.91	46.96	
pad3-loc4	4	3	24.4	23.3	150	16.74	985.66	236.78	49.67	
pad3-loc4	4	4	24.4	23.3	150	16.77	964.00	237.18	50.87	49.94
pad3-loc4	4	5	24.4	23.3	150	16.85	962.03	238.40	51.24	
pad3-loc4	4	6	24.4	23.3	150	16.77	962.41	237.24	50.97	
pad3-loc5	5	1	24.4	23.3	150	15.31	2114.30			
pad3-loc5	5	2	24.4	23.3	150	16.89	933.52			
pad3-loc5	5	3	24.4	23.3	150	17.05	867.92	241.23	57.47	59.74

pad3-loc5	5	4	24.4	23.3	150	17.05	849.12	241.19	58.73	
pad3-loc5	5	5	24.4	23.3	150	17.03	821.76	240.90	60.61	
pad3-loc5	5	6	24.4	23.3	150	17.08	813.09	241.63	61.44	
pad3-loc5	5	7	24.4	23.3	150	17.03	823.71	240.92	60.47	
pad3-loc6	6	1	24.4	23.3	150	17.05	775.87			
pad3-loc6	6	2	24.4	23.3	150	17.26	641.09	244.19	78.75	
pad3-loc6	6	3	24.4	23.3	150	17.36	589.71	245.53	86.08	
pad3-loc6	6	4	24.4	23.3	150	17.30	555.02	244.79	91.19	89.97
pad3-loc6	6	5	24.4	23.3	150	17.36	537.16	245.53	94.50	
pad3-loc6	6	6	24.4	23.3	150	17.33	510.44	245.19	99.32	
pad3-loc7	7	1	24.4	23.3	150	15.74	2412.89			
pad3-loc7	7	2	24.4	23.3	150	17.01	507.90	240.63	97.95	
pad3-loc7	7	3	24.4	23.3	150	17.18	460.24	243.04	109.18	
pad3-loc7	7	4	24.4	23.3	150	17.22	437.51	243.58	115.11	113.48
pad3-loc7	7	5	24.4	23.3	150	17.35	418.68	245.45	121.21	
pad3-loc7	7	6	24.4	23.3	150	17.32	408.59	244.98	123.97	

Table B-17. Quarry 2, Test Pad #4, dense-graded crushed material subgrade layer

Location	PointNo	DropNo	Surface Temp	In-Depth Temp	Radius (mm)	Load (kN)	Deflection (um)	Stress (kPa)	Modulus (MPa)	Average (MPa)
pad4-loc1	1	1	26.2	25.7	150	16.81	333.76			
pad4-loc1	1	2	26.2	25.7	150	17.62	243.69	249.28	211.50	229.51
pad4-loc1	1	3	26.2	25.7	150	17.59	225.66	248.84	227.99	
pad4-loc1	1	4	26.2	25.7	150	17.74	221.77	250.99	233.99	
pad4-loc1	1	5	26.2	25.7	150	17.71	219.54	250.54	235.95	
pad4-loc1	1	6	26.2	25.7	150	17.71	217.54	250.54	238.12	
pad4-loc2	2	1	26.2	25.7	150	16.72	172.18			
pad4-loc2	2	2	26.2	25.7	150	17.56	186.69	248.38	275.08	274.41
pad4-loc2	2	3	26.2	25.7	150	17.49	185.79	247.45	275.38	
pad4-loc2	2	4	26.2	25.7	150	17.61	187.91	249.12	274.11	
pad4-loc2	2	5	26.2	25.7	150	17.57	189.30	248.60	271.53	
pad4-loc2	2	6	26.2	25.7	150	17.65	187.07	249.67	275.94	
pad4-loc3	3	1	26.2	25.7	150	14.58	1459.85			
pad4-loc3	3	2	26.2	25.7	150	17.18	584.64	243.02	85.94	95.96
pad4-loc3	3	3	26.2	25.7	150	17.35	535.31	245.47	94.81	
pad4-loc3	3	4	26.2	25.7	150	17.40	520.91	246.21	97.72	
pad4-loc3	3	5	26.2	25.7	150	17.40	508.07	246.17	100.18	
pad4-loc3	3	6	26.2	25.7	150	17.34	501.44	245.35	101.17	
pad4-loc4	4	1	26.2	25.7	150	16.56	599.85			
pad4-loc4	4	2	26.2	25.7	150	17.51	348.41	247.78	147.04	158.59
pad4-loc4	4	3	26.2	25.7	150	17.49	325.86	247.39	156.97	
pad4-loc4	4	4	26.2	25.7	150	17.62	321.14	249.28	160.49	
pad4-loc4	4	5	26.2	25.7	150	17.59	315.15	248.79	163.22	
pad4-loc4	4	6	26.2	25.7	150	17.65	312.39	249.65	165.23	
pad4-loc5	5	1	26.2	25.7	150	16.95	310.94			
pad4-loc5	5	2	26.2	25.7	150	17.64	189.06	249.53	272.89	289.13
pad4-loc5	5	3	26.2	25.7	150	17.65	179.28	249.73	288.00	

pad4-loc5	5	4	26.2	25.7	150	17.72	177.10	250.74	292.73	
pad4-loc5	5	5	26.2	25.7	150	17.67	173.44	250.01	298.03	
pad4-loc5	5	6	26.2	25.7	150	17.64	175.49	249.56	294.01	
pad4-loc6	6	1	26.2	25.7	150	16.00	158.41			
pad4-loc6	6	2	26.2	25.7	150	17.59	166.12	248.82	309.70	
pad4-loc6	6	3	26.2	25.7	150	17.65	153.63	249.72	336.08	
pad4-loc6	6	4	26.2	25.7	150	17.67	153.98	249.99	335.67	330.58
pad4-loc6	6	5	26.2	25.7	150	17.63	151.92	249.42	339.46	
pad4-loc6	6	6	26.2	25.7	150	17.59	159.79			
pad4-loc6	6	7	26.2	25.7	150	17.65	155.51	249.71	332.00	
pad4-loc7	7	1	26.2	25.7	150	16.59	458.78			
pad4-loc7	7	2	26.2	25.7	150	16.75	241.44			
pad4-loc7	7	3	26.2	25.7	150	17.03	334.79			
pad4-loc7	7	4	26.2	25.7	150	17.42	250.76	246.50	203.25	
pad4-loc7	7	5	26.2	25.7	150	17.48	234.51	247.36	218.08	
pad4-loc7	7	6	26.2	25.7	150	17.51	244.94	247.66	209.05	214.33
pad4-loc7	7	7	26.2	25.7	150	17.47	228.54	247.11	223.56	
pad4-loc7	7	8	26.2	25.7	150	17.49	234.95	247.42	217.73	

Table B-18. Quarry 2, Test Pad #4, 25% RCA - 75% crushed rock subbase layer

Location	PointNo	DropNo	Surface Temp	In-Depth Temp	Radius (mm)	Load (kN)	Deflection (um)	Stress (kPa)	Modulus (MPa)	Average (MPa)
pad4-loc1	1	1	23.4	22.5	150	17.36	655.59			
pad4-loc1	1	2	23.4	22.5	150	17.47	559.90	247.14	91.26	97.20
pad4-loc1	1	3	23.4	22.5	150	13.37	470.06	189.17	83.21	
pad4-loc1	1	4	23.4	22.5	150	17.45	502.82	246.93	101.53	
pad4-loc1	1	5	23.4	22.5	150	17.58	494.97	248.64	103.86	
pad4-loc1	1	6	23.4	22.5	150	17.56	483.89	248.39	106.13	
pad4-loc2	2	1	23.4	22.5	150	15.73	1666.98			
pad4-loc2	2	2	23.4	22.5	150	17.24	569.69	243.83	88.49	97.52
pad4-loc2	2	3	23.4	22.5	150	17.24	512.16	243.83	98.43	
pad4-loc2	2	4	23.4	22.5	150	13.28	456.05	187.87	85.17	
pad4-loc2	2	5	23.4	22.5	150	17.35	474.45	245.39	106.94	
pad4-loc2	2	6	23.4	22.5	150	17.36	467.65	245.56	108.57	
pad4-loc3	3	1	23.4	22.5	150	15.56	2019.04			
pad4-loc3	3	2	23.4	22.5	150	17.24	802.07	243.96	62.89	71.58
pad4-loc3	3	3	23.4	22.5	150	17.29	705.31	244.64	71.71	
pad4-loc3	3	4	23.4	22.5	150	17.32	676.23	245.00	74.91	
pad4-loc3	3	5	23.4	22.5	150	17.41	636.07	246.34	80.07	
pad4-loc3	3	6	23.4	22.5	150	13.64	584.01	192.99	68.33	
pad4-loc4	4	1	23.4	22.5	150	15.26	2031.70			
pad4-loc4	4	2	23.4	22.5	150	17.16	746.83	242.81	67.22	76.48
pad4-loc4	4	3	23.4	22.5	150	13.26	608.30	187.66	63.78	
pad4-loc4	4	4	23.4	22.5	150	17.25	620.98	244.06	81.26	
pad4-loc4	4	5	23.4	22.5	150	17.38	603.75	245.92	84.21	
pad4-loc4	4	6	23.4	22.5	150	17.34	590.28	245.29	85.92	
pad4-loc5	5	1	23.4	22.5	150	17.19	705.05			
pad4-loc5	5	2	23.4	22.5	150	17.44	613.33	246.66	83.15	87.36
pad4-loc5	5	3	23.4	22.5	150	13.48	540.60	190.66	72.92	

pad4-loc5	5	4	23.4	22.5	150	17.44	560.56	246.76	91.02	
pad4-loc5	5	5	23.4	22.5	150	17.40	543.19	246.19	93.71	
pad4-loc5	5	6	23.4	22.5	150	17.41	530.34	246.25	96.00	
pad4-loc6	6	1	23.4	22.5	150	17.15	777.91			
pad4-loc6	6	2	23.4	22.5	150	17.24	686.22	243.85	73.47	
pad4-loc6	6	3	23.4	22.5	150	17.26	41.42			
pad4-loc6	6	4	23.4	22.5	150	17.36	629.63	245.56	80.64	76.21
pad4-loc6	6	5	23.4	22.5	150	13.42	569.71	189.89	68.91	
pad4-loc6	6	6	23.4	22.5	150	13.56	563.70	191.82	70.36	
pad4-loc6	6	7	23.4	22.5	150	17.44	581.78	246.69	87.67	
pad4-loc7	7	1	23.4	22.5	150	15.42	1894.12			
pad4-loc7	7	2	23.4	22.5	150	17.25	645.61	243.98	78.13	
pad4-loc7	7	3	23.4	22.5	150	17.18	575.05	243.00	87.37	
pad4-loc7	7	4	23.4	22.5	150	17.38	547.54	245.94	92.87	90.92
pad4-loc7	7	5	23.4	22.5	150	17.34	523.45	245.32	96.90	
pad4-loc7	7	6	23.4	22.5	150	17.35	510.88	245.48	99.35	

Table B-19. Quarry 2, Test Pad #5, dense-graded crushed material subgrade layer

Location	PointNo	DropNo	Surface Temp	In-Depth Temp	Radius (mm)	Load (kN)	Deflection (um)	Stress (kPa)	Modulus (MPa)	Average (MPa)
pad5-loc1	1	1	26.8	22.5	150	15.45	1138.35			
pad5-loc1	1	2	26.8	22.5	150	16.97	472.84	240.04	104.96	
pad5-loc1	1	3	26.8	22.5	150	17.14	487.99	242.42	102.71	
pad5-loc1	1	4	26.8	22.5	150	17.28	449.58	244.51	112.45	107.72
pad5-loc1	1	5	26.8	22.5	150	17.29	467.18	244.56	108.23	
pad5-loc1	1	6	26.8	22.5	150	17.34	460.03	245.28	110.24	
pad5-loc2	2	1	26.8	22.5	150	14.55	946.98			
pad5-loc2	2	2	26.8	22.5	150	16.67	779.28			
pad5-loc2	2	3	26.8	22.5	150	16.84	654.42	238.23	75.27	
pad5-loc2	2	4	26.8	22.5	150	16.64	758.19	235.39	64.19	
pad5-loc2	2	5	26.8	22.5	150	16.86	647.24	238.45	76.17	76.00
pad5-loc2	2	6	26.8	22.5	150	16.87	664.71	238.73	74.26	
pad5-loc2	2	7	26.8	22.5	150	17.10	555.05	241.98	90.14	
pad5-loc3	3	1	26.8	22.5	150	14.79	1862.54			
pad5-loc3	3	2	26.8	22.5	150	16.80	711.59			
pad5-loc3	3	3	26.8	22.5	150	17.15	584.26	242.66	85.87	
pad5-loc3	3	4	26.8	22.5	150	17.06	548.30	241.29	90.99	
pad5-loc3	3	5	26.8	22.5	150	17.26	513.83	244.22	98.27	95.96
pad5-loc3	3	6	26.8	22.5	150	17.17	515.66	242.92	97.40	
pad5-loc3	3	7	26.8	22.5	150	17.33	472.64	245.21	107.27	
pad5-loc4	4	1	26.8	22.5	150	14.85	664.63			
pad5-loc4	4	2	26.8	22.5	150	17.32	466.91	245.02	108.50	
pad5-loc4	4	3	26.8	22.5	150	17.48	459.89	247.30	111.18	
pad5-loc4	4	4	26.8	22.5	150	17.41	435.33	246.36	117.01	116.29
pad5-loc4	4	5	26.8	22.5	150	17.55	422.79	248.34	121.44	
pad5-loc4	4	6	26.8	22.5	150	17.54	415.97	248.07	123.30	
pad5-loc5	5	1	26.8	22.5	150	16.41	357.41			

pad5-loc5	5	2	26.8	22.5	150	17.46	307.39	247.00	166.14	
pad5-loc5	5	3	26.8	22.5	150	17.52	284.96	247.79	179.79	
pad5-loc5	5	4	26.8	22.5	150	17.54	278.47	248.16	184.25	181.13
pad5-loc5	5	5	26.8	22.5	150	17.60	273.80	248.92	187.97	
pad5-loc5	5	6	26.8	22.5	150	17.58	274.22	248.71	187.52	
pad5-loc6	6	1	26.8	22.5	150	16.81	438.93			
pad5-loc6	6	2	26.8	22.5	150	17.61	342.79	249.14	150.27	
pad5-loc6	6	3	26.8	22.5	150	17.64	325.36	249.61	158.62	
pad5-loc6	6	4	26.8	22.5	150	17.62	317.85	249.29	162.16	161.22
pad5-loc6	6	5	26.8	22.5	150	17.65	310.22	249.77	166.47	
pad5-loc6	6	6	26.8	22.5	150	17.62	305.70	249.23	168.57	
pad5-loc7	7	1	26.8	22.5	150	16.11	600.87			
pad5-loc7	7	2	26.8	22.5	150	17.54	388.02	248.18	132.24	
pad5-loc7	7	3	26.8	22.5	150	17.58	367.71	248.66	139.82	
pad5-loc7	7	4	26.8	22.5	150	17.54	362.08	248.10	141.67	141.15
pad5-loc7	7	5	26.8	22.5	150	17.57	352.60	248.50	145.72	
pad5-loc7	7	6	26.8	22.5	150	17.61	352.19	249.19	146.29	

Table B-20. Quarry 2, Test Pad #5, 50% RCA - 50% crushed rock subbase layer

Location	PointNo	DropNo	Surface Temp	In-Depth Temp	Radius (mm)	Load (kN)	Deflection (um)	Stress (kPa)	Modulus (MPa)	Average (MPa)
pad5-loc1	1	1	21.6	21.9	150	15.44	2118.52			
pad5-loc1	1	2	21.6	21.9	150	15.64	1927.46	221.21	23.73	26.11
pad5-loc1	1	3	21.6	21.9	150	15.76	1811.67	222.96	25.45	
pad5-loc1	1	4	21.6	21.9	150	15.91	1754.85	225.06	26.52	
pad5-loc1	1	5	21.6	21.9	150	15.71	1685.83	222.20	27.25	
pad5-loc1	1	6	21.6	21.9	150	15.98	1693.13	226.07	27.61	
pad5-loc2	2	1	21.6	21.9	150	16.44	1175.21			
pad5-loc2	2	2	21.6	21.9	150	16.63	1109.51	235.26	43.84	47.40
pad5-loc2	2	3	21.6	21.9	150	16.71	1057.40	236.42	46.23	
pad5-loc2	2	4	21.6	21.9	150	16.75	1035.69	236.90	47.29	
pad5-loc2	2	5	21.6	21.9	150	16.75	996.30	237.00	49.18	
pad5-loc2	2	6	21.6	21.9	150	16.81	974.53	237.75	50.44	
pad5-loc3	3	1	21.6	21.9	150	16.10	1534.66			
pad5-loc3	3	2	21.6	21.9	150	16.36	1384.31	231.44	34.57	38.29
pad5-loc3	3	3	21.6	21.9	150	16.40	1285.62	231.99	37.31	
pad5-loc3	3	4	21.6	21.9	150	16.56	1255.80	234.22	38.56	
pad5-loc3	3	5	21.6	21.9	150	16.58	1217.80	234.53	39.82	
pad5-loc3	3	6	21.6	21.9	150	16.56	1175.85	234.30	41.20	
pad5-loc4	4	1	21.6	21.9	150	15.20	1837.45			
pad5-loc4	4	2	21.6	21.9	150	17.04	769.63	241.04	64.75	75.34
pad5-loc4	4	3	21.6	21.9	150	17.15	689.06	242.63	72.80	
pad5-loc4	4	4	21.6	21.9	150	17.18	653.06	242.98	76.93	
pad5-loc4	4	5	21.6	21.9	150	17.28	631.32	244.51	80.07	
pad5-loc4	4	6	21.6	21.9	150	17.20	612.42	243.27	82.13	
pad5-loc5	5	1	21.6	21.9	150	17.01	780.21			
pad5-loc5	5	2	21.6	21.9	150	17.23	686.51	243.75	73.41	83.25
pad5-loc5	5	3	21.6	21.9	150	17.31	631.91	244.88	80.12	

pad5-loc5	5	4	21.6	21.9	150	17.37	597.28	245.79	85.08	
pad5-loc5	5	5	21.6	21.9	150	17.34	579.07	245.25	87.57	
pad5-loc5	5	6	21.6	21.9	150	17.42	565.69	246.37	90.05	
pad5-loc6	6	1	21.6	21.9	150	17.14	811.95			
pad5-loc6	6	2	21.6	21.9	150	17.22	721.01	243.67	69.87	
pad5-loc6	6	3	21.6	21.9	150	17.25	662.46	244.10	76.18	
pad5-loc6	6	4	21.6	21.9	150	17.37	638.08	245.71	79.62	78.01
pad5-loc6	6	5	21.6	21.9	150	17.32	625.07	244.98	81.03	
pad5-loc6	6	6	21.6	21.9	150	17.43	611.49	246.54	83.36	
pad5-loc7	7	1	21.6	21.9	150	17.07	746.57			
pad5-loc7	7	2	21.6	21.9	150	17.22	656.98	243.54	76.65	
pad5-loc7	7	3	21.6	21.9	150	17.34	605.92	245.31	83.70	
pad5-loc7	7	4	21.6	21.9	150	17.30	572.94	244.72	88.31	86.28
pad5-loc7	7	5	21.6	21.9	150	17.33	560.14	245.22	90.51	
pad5-loc7	7	6	21.6	21.9	150	17.24	546.98	243.96	92.22	

APPENDIX C:
RESILIENT MODULUS DATA TABLES

Table C-1. Quarry 1, 100% crushed rock test mixture, Test #1

Seq. No.	Chamber Confining Pressure (kPa)	Actual Applied Max. Axial Stress (kPa)	Resilient Modulus (MPa)	Bulk Stress (kPa)	Calculated Resilient Modulus (MPa)	Squared Difference Between the Real and Calculated Resilient Modulus (MPa)
1	20.02	19.47	49.81	79.53	69.44737816	385.6266211
2	20.12	40.37	72.95	100.73	82.78080219	96.64467172
3	20.3	63.66	102.39	124.56	98.53608051	14.85269542
4	34.36	35.67	67.97	138.75	85.23008369	297.910489
5	34.5	71.04	111.47	174.54	109.0960045	5.635854779
6	34.17	107.37	154.18	209.88	135.8568818	335.7366592
7	68.9	74.16	113.86	280.86	120.944257	50.18669779
8	69.15	138.16	184.21	345.61	171.3794748	164.6223766
9	69.08	215.33	254.82	422.57	241.6947749	172.2715335
10	103.99	62.28	100.11	374.25	119.357405	370.4625993
11	104.12	100.08	146.14	412.44	148.1887317	4.197301685
12	103.95	200.46	256.86	512.31	236.9606215	395.9852642
13	138.82	106.51	163.36	522.97	159.643614	13.8115248
14	138.8	136.57	199.1	552.97	185.3151192	190.0229374
15	138.77	275.6	295.49	691.91	324.0530939	815.8503304
					Sum of Squares:	3313.817557

Regression Coefficients		
k1	k2	k3
625.70146	0.18126884	1.555165

Table C-2. Quarry 1, 100% crushed rock test mixture, Test #2

Seq. No.	Chamber Confining Pressure (kPa)	Actual Applied Max. Axial Stress (kPa)	Resilient Modulus (MPa)	Bulk Stress (kPa)	Calculated Resilient Modulus (MPa)	Squared Difference Between the Real and Calculated Resilient Modulus (MPa)
1	19.78	21.63	77.52	80.97	108.7101598	972.826067
2	19.51	41.15	110.07	99.68	121.4152643	128.7150219
3	19.78	62.91	147.02	122.25	136.0018068	121.4005819
4	34.03	34.28	100.21	136.37	118.0273904	317.4594002
5	33.93	66.25	148.01	168.04	139.2807194	76.20033931
6	33.69	104.47	194.87	205.54	165.8119765	844.368729
7	68.53	69.27	148.37	274.86	143.0189185	28.63407286
8	68.77	137.83	218.94	344.14	191.6598605	744.2060117
9	68.72	205.67	238.06	411.83	243.2075272	26.49703673
10	103.48	68.83	128.67	379.27	143.8774214	231.2656642
11	103.48	103.89	178.98	414.33	168.3342098	113.3328481
12	103.71	207.33	248.02	518.46	245.8940091	4.519837204
13	138.31	102.04	158.1	516.97	167.9637189	97.29294972
14	138.35	139.66	199.89	554.71	195.2972159	21.09366563
15	138.52	278.4	288.9	693.96	304.5620381	245.2994385
					Sum of Squares:	3973.111664

Regression Coefficients		
k1	k2	k3
949.63499	0.02498029	1.328908

Table C-3. Quarry 1, 100% crushed rock test mixture, Test #3

(This test was excluded as an outlier.)

Seq. No.	Chamber Confining Pressure (kPa)	Actual Applied Max. Axial Stress (kPa)	Resilient Modulus (MPa)	Bulk Stress (kPa)	Calculated Resilient Modulus (MPa)	Squared Difference Between the Real and Calculated Resilient Modulus (MPa)
1	20.49	19.45	116.86	80.92	137.037455	407.12969
2	20.69	41.71	152.36	103.78	155.5312626	10.05690635
3	20.57	64.38	190.27	126.09	174.2827251	255.5929587
4	34.35	33.59	138.15	136.64	155.01224	284.3351385
5	34.22	69.8	194.49	172.46	184.4289904	101.2239136
6	34.25	97.86	215.11	200.61	207.7285038	54.48648649
7	68.94	69.92	195.25	276.74	194.7606254	0.239487529
8	69.27	138.5	271.67	346.31	252.3434763	373.5145175
9	68.91	202.96	292.81	409.69	308.357318	241.719097
10	103.9	73.35	205.72	385.05	204.8895822	0.689593717
11	103.99	100.63	224.19	412.6	227.7365765	12.5782048
12	103.96	210.02	340.78	521.9	322.806488	323.0471338
13	138.87	103.45	230.89	520.06	236.1034327	27.17988093
14	138.82	138.58	265.18	555.04	266.3866743	1.456062944
15	138.89	282.74	385.67	699.41	396.0049658	106.8115181
					Sum of Squares:	2200.06059

Regression Coefficients		
k1	k2	k3
1263.248	0.11429345	1.082118

Table C-4. Quarry 1, 100% RCA test mixture, Test #1

Seq. No.	Chamber Confining Pressure (kPa)	Actual Applied Max. Axial Stress (kPa)	Resilient Modulus (MPa)	Bulk Stress (kPa)	Calculated Resilient Modulus (MPa)	Squared Difference Between the Real and Calculated Resilient Modulus (MPa)
1	20.1	24.01	83.66	84.31	79.20228911	19.87118641
2	19.98	44.65	104.8	104.59	91.80457335	168.8811139
3	20.17	73.3	125.71	133.81	109.1114732	275.5110917
4	34.31	36.76	96.04	139.69	105.8431076	96.10091951
5	33.89	72.42	133.66	174.09	125.4133966	68.00646694
6	34.2	104.45	152.32	207.05	143.4174021	79.25625013
7	68.85	67.59	125.86	274.14	158.742983	1081.290572
8	68.91	143.04	188.05	349.77	198.4431684	108.0179486
9	68.71	204.69	218.75	410.82	230.1944731	130.9759653
10	103.62	66.39	181.21	377.25	187.9190034	45.01072681
11	103.53	106.3	205.89	416.89	208.8389165	8.696108727
12	103.63	206.3	254.93	517.19	260.68788	33.15318255
13	138.45	104.41	251.38	519.76	234.3812886	288.956189
14	138.37	134.55	262.35	549.66	250.2117168	147.3379181
15	138.4	273.56	327.1	688.76	321.9987551	26.0226997
					Sum of Squares:	2577.088339

Regression Coefficients		
k1	k2	k3
826.947145	0.53371969	0.393755

Table C-5. Quarry 1, 100% RCA test mixture, Test #2

Seq. No.	Chamber Confining Pressure (kPa)	Actual Applied Max. Axial Stress (kPa)	Resilient Modulus (MPa)	Bulk Stress (kPa)	Calculated Resilient Modulus (MPa)	Squared Difference Between the Real and Calculated Resilient Modulus (MPa)
1	19.87	15.08	110.44	74.69	103.4772592	48.4797591
2	19.65	40.94	96.54	99.89	118.1705145	467.8791576
3	19.72	63.49	128.18	122.65	131.2205623	9.245018988
4	33.84	52.89	138.44	154.41	125.8706676	157.9881165
5	33.65	68.68	128.38	169.63	135.0161215	44.03810795
6	33.73	96.54	151.81	197.73	151.4287952	0.145317132
7	68.46	65.62	130.77	271	134.5415543	14.22462184
8	68.57	137.95	196.33	343.66	177.6720903	348.1175959
9	68.52	205.73	229.05	411.29	219.8387249	84.84758838
10	103.54	65.32	129.62	375.94	135.2558709	31.76304035
11	103.29	106.55	161.19	416.42	159.6134462	2.485521756
12	103.43	198.43	222.56	508.72	216.2212819	40.17934664
13	137.99	103.84	156.97	517.81	158.7042573	3.007648216
14	138	138.14	179.2	552.14	179.4862146	0.081918807
15	138.24	269.69	248.16	684.41	262.8991125	217.2414367
					Sum of Squares:	1469.724196

Regression Coefficients		
k1	k2	k3
947.53689	0.02007254	1.191737

Table C-6. Quarry 1, 100% RCA test mixture, Test #3

Seq. No.	Chamber Confining Pressure (kPa)	Actual Applied Max. Axial Stress (kPa)	Resilient Modulus (MPa)	Bulk Stress (kPa)	Calculated Resilient Modulus (MPa)	Squared Difference Between the Real and Calculated Resilient Modulus (MPa)
1	19.88	21.14	95.81	80.78	92.03768496	14.23036079
2	20.15	42.22	99.37	102.67	104.8496836	30.02693268
3	20.08	66.12	125.24	126.36	118.7293863	42.38809044
4	34.51	32.15	115.69	135.68	109.5197528	38.07195105
5	34.38	70.12	129.25	173.26	130.6029894	1.830580372
6	34.11	98.68	149.98	201.01	146.3234934	13.37004086
7	69.14	66.68	126.59	274.1	146.2566126	386.7756503
8	69.33	139.51	189.49	347.5	186.2186605	10.7016624
9	68.75	207.12	220.71	413.37	223.30348	6.726138749
10	104.11	71.04	153.28	383.37	161.8932718	74.18845101
11	103.61	104.12	180.97	414.95	179.9840027	0.972190764
12	103.84	204.48	235.33	516	235.791031	0.212549547
13	139.81	104.68	201.29	524.11	191.8375322	89.34914827
14	138.85	138.51	217.63	555.06	210.5885121	49.58255221
15	138.15	272.44	283.46	686.89	285.9222951	6.062897337
					Sum of Squares:	764.4891968

Regression Coefficients		
k1	k2	k3
897.269217	0.267285	0.774629

Table C-7. Quarry 1, 25% RCA - 75% crushed rock test mixture, Test #1

Seq. No.	Chamber Confining Pressure (kPa)	Actual Applied Max. Axial Stress (kPa)	Resilient Modulus (MPa)	Bulk Stress (kPa)	Calculated Resilient Modulus (MPa)	Squared Difference Between the Real and Calculated Resilient Modulus (MPa)
1	19.99	7.81	236.7	67.78	150.2691587	7470.290322
2	19.75	42.6	140.39	101.85	175.9411875	1263.886929
3	20.16	63.62	158.7	124.1	191.0354569	1045.581775
4	33.98	35.01	178.22	136.95	179.0173421	0.635754352
5	34.07	69.78	209.51	171.99	202.5489418	48.45633126
6	34.12	104.26	237	206.62	225.2496713	138.0702253
7	68.89	71.88	180.82	278.55	216.913475	1302.738937
8	68.45	142.26	248.64	347.61	261.4611674	164.3823332
9	68.55	210.17	287.96	415.82	303.3541675	236.9803935
10	103.52	65.81	200.29	376.37	222.2039046	480.2192142
11	103.6	108.51	241.84	419.31	249.5189257	58.96590049
12	103.6	204.41	307.31	515.21	308.9570679	2.71283255
13	138.44	107.1	278.62	522.42	256.0131627	511.069093
14	138.27	144.3	308.57	559.11	279.4182508	849.8244786
15	138.62	273.52	371.43	689.38	358.188345	175.341426
					Sum of Squares:	13749.15595

Regression Coefficients		
k1	k2	k3
1523.41915	0.13114853	0.718952

Table C-8. Quarry 1, 25% RCA - 75% crushed rock test mixture, Test #2

Seq. No.	Chamber Confining Pressure (kPa)	Actual Applied Max. Axial Stress (kPa)	Resilient Modulus (MPa)	Bulk Stress (kPa)	Calculated Resilient Modulus (MPa)	Squared Difference Between the Real and Calculated Resilient Modulus (MPa)
1	19.99	22.29	77.39	82.26	95.28364878	320.1826667
2	19.75	42.43	93.46	101.68	112.3414642	356.5096907
3	20.16	63.73	115.35	124.21	131.2327503	252.2617562
4	33.98	30.86	112.01	132.8	138.9218229	724.2462126
5	34.07	64.97	154.57	167.18	165.9084885	128.5613208
6	34.12	105.13	206.04	207.49	195.8992507	102.8347956
7	68.89	69.34	277.12	276.01	246.3718446	945.449062
8	68.45	136.74	323.34	342.09	289.8399012	1122.25662
9	68.55	200.29	337.03	405.94	329.9682873	49.86778687
10	103.52	69.14	321.92	379.7	316.9446714	24.75389496
11	103.6	103.02	352.18	413.82	337.9737254	201.8182383
12	103.6	205.65	426.26	516.45	398.8982795	748.6637491
13	138.44	110.92	389.93	526.24	408.2743586	336.5154935
14	138.27	137.91	403.5	552.72	423.3026079	392.1432785
15	138.62	276.75	477.39	692.61	500.3576264	527.511863
					Sum of Squares:	6233.576429

Regression Coefficients		
k1	k2	k3
1112.187	0.78967403	-0.03294

Table C-9. Quarry 1, 25% RCA - 75% crushed rock test mixture, Test #3

Seq. No.	Chamber Confining Pressure (kPa)	Actual Applied Max. Axial Stress (kPa)	Resilient Modulus (MPa)	Bulk Stress (kPa)	Calculated Resilient Modulus (MPa)	Squared Difference Between the Real and Calculated Resilient Modulus (MPa)
1	19.99	21.11	89.26	81.08	100.9463954	136.5718365
2	19.75	44.07	118.91	103.32	119.1344604	0.050382455
3	20.16	57.93	135.11	118.41	130.7529726	18.98368794
4	33.98	32.64	109.23	134.58	114.4116296	26.84928514
5	34.07	67.8	158.79	170.01	143.3001956	239.9340405
6	34.12	106.66	201.92	209.02	177.8920063	577.3444798
7	68.89	73.3	177.84	279.97	155.4595957	500.8824955
8	68.45	136.95	224.75	342.3	214.6308383	102.3974331
9	68.55	203.49	240.15	409.14	284.0926002	1930.952111
10	103.52	65.62	148.5	376.18	153.9424259	29.61999937
11	103.6	97.82	183.82	408.62	182.9846529	0.697804797
12	103.6	207.29	261.86	518.09	295.2229106	1113.083805
13	138.44	105.55	190.28	520.87	194.7574137	20.04723305
14	138.27	140.83	225.05	555.64	229.5945623	20.65304648
15	138.62	278.41	421.55	694.27	385.1528799	1324.750354
					Sum of Squares:	6042.817994

Regression Coefficients		
k1	k2	k3
885.054004	0.10492251	1.511071

Table C-10. Quarry 1, 50% RCA - 50% crushed rock test mixture, Test #1

Seq. No.	Chamber Confining Pressure (kPa)	Actual Applied Max. Axial Stress (kPa)	Resilient Modulus (MPa)	Bulk Stress (kPa)	Calculated Resilient Modulus (MPa)	Squared Difference Between the Real and Calculated Resilient Modulus (MPa)
1	19.22	53.66	86.21	111.32	114.3355181	791.0447687
2	19.53	44.15	83.01	102.74	108.5779255	653.7188119
3	19.63	66.41	118.45	125.3	122.8005929	18.92765833
4	33.5	35.98	82.21	136.48	116.5036383	1176.05363
5	33.09	69.71	122.83	168.98	136.5576877	188.4494109
6	33.21	96.77	139.19	196.4	152.9304398	188.7996867
7	68.41	69.44	226.29	274.67	160.006714	4393.473997
8	68.33	134.47	257.93	339.46	198.2784698	3558.305054
9	68.37	206.13	298.61	411.24	240.793322	3342.768255
10	103.09	72.76	220.18	382.03	179.7329352	1635.965054
11	103.22	108.3	186.41	417.96	200.9334631	210.9309817
12	103.05	212.65	254.58	521.8	263.1606554	73.62764767
13	138.1	103.82	178.92	518.12	213.4736736	1193.956357
14	138.03	136.91	199.89	551	233.515834	1130.696713
15	138.28	285.47	296.8	700.31	323.7427493	725.9117414
					Sum of Squares:	19282.62977

Regression Coefficients		
k1	k2	k3
935.030003	0.32758427	0.704615

Table C-11. Quarry 1, 50% RCA - 50% crushed rock test mixture, Test #2

Seq. No.	Chamber Confining Pressure (kPa)	Actual Applied Max. Axial Stress (kPa)	Resilient Modulus (MPa)	Bulk Stress (kPa)	Calculated Resilient Modulus (MPa)	Squared Difference Between the Real and Calculated Resilient Modulus (MPa)
1	20.41	23.19	111.43	84.42	123.1424353	137.1811402
2	20.53	41.52	124.89	103.11	135.9605763	122.5576605
3	20.07	59.27	139.89	119.48	148.2709193	70.23980854
4	34.26	37.49	135.43	140.27	136.9547926	2.324992469
5	34.41	68.01	160.72	171.24	158.10752	6.825051909
6	34.09	100.71	192.7	202.98	181.1243788	133.9950055
7	68.69	69.65	173.35	275.72	165.4011023	63.18497502
8	68.82	137.41	237.85	343.87	213.7418633	581.2022572
9	68.93	206.93	267.56	413.72	265.2956544	5.127261126
10	103.78	63.85	155.79	375.19	165.7325446	98.85419248
11	103.82	103.87	198.16	415.33	194.1041598	16.44983962
12	103.97	210.8	290.61	522.71	273.1479105	304.9245682
13	138.38	103.78	191.29	518.92	197.5804832	39.57017904
14	138.47	142.01	220.94	557.42	225.5278916	21.04874892
15	138.7	275.45	306.39	691.55	327.204655	433.249864
					Sum of Squares:	2036.735545

Regression Coefficients		
k1	k2	k3
1099.87448	0.08113276	1.116782

Table C-12. Quarry 1, 50% RCA - 50% crushed rock test mixture, Test #3

Seq. No.	Chamber Confining Pressure (kPa)	Actual Applied Max. Axial Stress (kPa)	Resilient Modulus (MPa)	Bulk Stress (kPa)	Calculated Resilient Modulus (MPa)	Squared Difference Between the Real and Calculated Resilient Modulus (MPa)
1	20.41	20.21	79.19	81.44	85.00914305	33.86242581
2	20.53	43.46	95.71	105.05	104.1517988	71.26396713
3	20.07	63.33	110.95	123.54	118.6916922	59.93379743
4	34.26	35.29	123.44	138.07	127.8936797	19.83526294
5	34.41	67.11	149.71	170.34	151.8288447	4.489503008
6	34.09	107.71	182.92	209.98	180.3846478	6.428010897
7	68.69	66.46	229.8	272.53	217.2118658	158.461123
8	68.82	135.04	275.08	341.5	263.3984623	136.4583236
9	68.93	209.96	318.93	416.75	312.3079559	43.85146746
10	103.78	69.54	277.99	380.88	280.6606974	7.132624449
11	103.82	103.05	304.65	414.51	302.5574332	4.378835747
12	103.97	201.93	366.99	513.84	365.716826	1.620972138
13	138.38	107.92	358.51	523.06	361.7943553	10.78698973
14	138.47	137.45	377.05	552.86	380.5669094	12.36865159
15	138.7	269.23	455.63	685.33	462.0660665	41.42295199
					Sum of Squares:	612.294907

Regression Coefficients		
k1	k2	k3
982.542705	0.76250112	0.095273

Table C-13. Quarry 1, 70% RCA - 30% RAP test mixture, Test #1

(This test was excluded as an outlier.)

Seq. No.	Chamber Confining Pressure (kPa)	Actual Applied Max. Axial Stress (kPa)	Resilient Modulus (MPa)	Bulk Stress (kPa)	Calculated Resilient Modulus (MPa)	Squared Difference Between the Real and Calculated Resilient Modulus (MPa)
1	20	19.13	64.95	79.13	85.57369643	425.3368544
2	19.83	43.58	97.84	103.07	94.51196407	11.07582313
3	20.13	64.52	117.67	124.91	101.9019	248.6329771
4	33.73	33.14	86.33	134.33	96.76835644	108.9592851
5	34.11	68.6	123.61	170.93	108.430348	230.4218343
6	34.02	99.66	136.07	201.72	118.0208503	325.7718043
7	68.5	72.7	125.51	278.2	118.8831406	43.91526514
8	68.39	148.96	184.85	354.13	140.7245472	1947.055586
9	68.56	156.23	75.44	361.91	142.7706563	4533.417272
10	103.42	67.86	114.97	378.12	124.2238516	85.63376893
11	103.47	109.1	126.82	419.51	136.1173457	86.44063644
12	103.39	219.2	148.85	529.37	165.9376825	291.9888945
13	138.36	100.76	146.41	515.84	139.1031816	53.38959523
14	138.37	141.69	161.02	556.8	150.5390843	109.849594
15	138.25	275.74	198.27	690.49	185.6121808	160.220386
					Sum of Squares:	8662.109577

Regression Coefficients		
k1	k2	k3
841.657268	0.17304119	0.539723

Table C-14. Quarry 1, 70% RCA - 30% RAP test mixture, Test #2

Seq. No.	Chamber Confining Pressure (kPa)	Actual Applied Max. Axial Stress (kPa)	Resilient Modulus (MPa)	Bulk Stress (kPa)	Calculated Resilient Modulus (MPa)	Squared Difference Between the Real and Calculated Resilient Modulus (MPa)
1	20.38	52.09	139.4	113.23	131.1438586	68.1638709
2	20.47	59.59	122.89	121	135.7824623	166.2155843
3	20.56	65.13	124.22	126.81	139.1929759	224.1900069
4	34.21	34.36	106.61	136.99	132.4931557	669.9377473
5	34.43	67.99	139.93	171.28	151.9645507	144.8304099
6	34.33	101.68	163.72	204.67	170.7127439	48.89846733
7	69.15	69.94	213.84	277.39	173.9462371	1591.51232
8	69.16	137.32	245.77	344.8	209.7847878	1294.935496
9	68.92	210.4	268.14	417.16	247.5746586	422.9332677
10	103.91	68.66	197.59	380.39	189.0086705	73.63921526
11	103.84	104.26	209.49	415.78	207.9692676	2.312626964
12	104.02	211.22	277.21	523.28	263.6006453	185.2145356
13	138.44	110.14	201.32	525.46	224.0806052	518.0451508
14	138.67	146.31	228.07	562.32	243.2652031	230.8941981
15	138.58	281.08	289.54	696.82	312.2906646	517.5927412
					Sum of Squares:	6159.315638

Regression Coefficients		
k1	k2	k3
1101.33976	0.27160986	0.6042

Table C-15. Quarry 1, 70% RCA - 30% RAP test mixture, Test #3

Seq. No.	Chamber Confining Pressure (kPa)	Actual Applied Max. Axial Stress (kPa)	Resilient Modulus (MPa)	Bulk Stress (kPa)	Calculated Resilient Modulus (MPa)	Squared Difference Between the Real and Calculated Resilient Modulus (MPa)
1	20.41	20.21	138.61	81.44	113.2844378	641.3840995
2	20.53	43.46	108.51	105.05	126.278497	315.7194841
3	20.07	63.33	126.48	123.54	136.1661692	93.82187447
4	34.26	35.29	107.88	138.07	133.7393321	668.7050568
5	34.41	67.11	136.85	170.34	149.020822	148.1289085
6	34.09	107.71	166.88	209.98	167.1055146	0.050856849
7	68.69	66.46	204.41	272.53	168.3889255	1297.517805
8	68.82	135.04	199.47	341.5	196.8066196	7.093595081
9	68.93	209.96	244.18	416.75	225.9981747	330.5787705
10	103.78	69.54	187.51	380.88	184.7253517	7.754266085
11	103.82	103.05	188.41	414.51	198.4379414	100.559608
12	103.97	201.93	264.41	513.84	236.7410263	765.5721057
13	138.38	107.92	211.88	523.06	212.3436403	0.214962352
14	138.47	137.45	209.51	552.86	223.9844696	209.51027
15	138.7	269.23	249.28	685.33	272.8437959	555.252476
					Sum of Squares:	5141.864139

Regression Coefficients		
k1	k2	k3
1137.44467	0.26218464	0.443899

Table C-16. Quarry 2, 100% crushed rock test mixture, Test #1

(This test was excluded as an outlier.)

Seq. No.	Chamber Confining Pressure (kPa)	Actual Applied Max. Axial Stress (kPa)	Resilient Modulus (MPa)	Bulk Stress (kPa)	Calculated Resilient Modulus (MPa)	Squared Difference Between the Real and Calculated Resilient Modulus (MPa)
1	19.32	24.24	326.96	82.2	316.2448593	114.8142398
2	19.28	41.65	346.7	99.49	337.6956864	81.07766336
3	19.25	61.5	359.19	119.25	359.6593385	0.220278581
4	33.2	32.14	357.11	131.74	367.0521925	98.84719253
5	33.43	71.39	400.24	171.68	403.9133297	13.49335138
6	33.59	101.97	421.87	202.74	429.2870051	55.01196495
7	68.13	71.37	469.7	275.76	467.7047899	3.980863509
8	68.21	134.47	510.67	339.1	507.9597361	7.34553022
9	68.13	204.68	534.76	409.07	547.5947761	164.7314782
10	102.85	66.65	505.53	375.2	513.6652825	66.18282116
11	102.78	105.44	537.93	413.78	535.8744299	4.225368543
12	103.29	216.66	606.75	526.53	593.6392514	171.8917295
13	137.91	105.19	574.24	518.92	574.7235361	0.233807151
14	138.15	138.88	599.48	553.33	591.7551905	59.67268118
15	138.12	274.04	649.13	688.4	652.5372445	11.60931541
					Sum of Squares:	853.3382855

Regression Coefficients		
k1	k2	k3
3296.20475	0.30944064	0.093322

Table C-17. Quarry 2, 100% crushed rock test mixture, Test #2

Seq. No.	Chamber Confining Pressure (kPa)	Actual Applied Max. Axial Stress (kPa)	Resilient Modulus (MPa)	Bulk Stress (kPa)	Calculated Resilient Modulus (MPa)	Squared Difference Between the Real and Calculated Resilient Modulus (MPa)
1	19.86	15.4	95.51	74.98	107.8906907	153.2815015
2	20.04	41.97	122.06	102.09	131.0263646	80.39569329
3	19.97	61.88	143.21	121.79	146.9003082	13.61837443
4	33.59	35.69	147.17	136.46	151.9917084	23.24887216
5	33.93	67.86	172.3	169.65	176.3777457	16.62801015
6	33.6	101.07	199.5	201.87	199.4169643	0.006894936
7	68.52	67.95	236.68	273.51	227.6834097	80.93863638
8	68.51	137.93	284.17	343.46	272.8897812	127.2433362
9	68.63	209.01	323.69	414.9	317.1512924	42.75469665
10	103.35	68.49	280.24	378.54	271.0080584	85.22874544
11	103.47	103.84	305.42	414.25	293.5106335	141.8330097
12	103.52	209.64	380.57	520.2	358.0427686	507.4761524
13	138.52	102.21	314.3	517.77	330.2157324	253.3105391
14	138.15	137.75	341.73	552.2	351.6716374	98.83615456
15	138.44	270.66	411.7	685.98	430.344059	347.6009372
					Sum of Squares:	1972.401554

Regression Coefficients		
k1	k2	k3
1227.52151	0.53442682	0.2688

Table C-18. Quarry 2, 100% crushed rock test mixture, Test #3

Seq. No.	Chamber Confining Pressure (kPa)	Actual Applied Max. Axial Stress (kPa)	Resilient Modulus (MPa)	Bulk Stress (kPa)	Calculated Resilient Modulus (MPa)	Squared Difference Between the Real and Calculated Resilient Modulus (MPa)
1	19.66	21.81	138.51	80.79	130.8711133	58.35259019
2	19.66	46.51	122.66	105.49	150.6850099	785.4011818
3	19.67	62.33	158.61	121.34	162.3191477	13.757777
4	34.11	38.11	168.22	140.44	173.8458468	31.65015264
5	33.81	69.51	191.54	170.94	193.3756577	3.369639289
6	33.85	105.41	208.84	206.96	214.5448477	32.54528683
7	69.51	71.22	266.51	279.75	248.250262	333.4180321
8	69.66	139.51	301.51	348.49	281.013002	420.1269268
9	68.77	206.58	318.85	412.89	309.3758315	89.759869
10	103.81	72.44	299.81	383.87	291.4651023	69.63731749
11	103.88	104.65	307.61	416.29	305.6016675	4.033399581
12	103.91	203.81	359.67	515.54	346.0573785	185.3034634
13	138.61	103.61	328.51	519.44	341.7883255	176.3139273
14	138	139.88	342.56	553.88	355.3488274	163.5541067
15	138.42	275.47	391.48	690.73	405.0942124	185.3467788
					Sum of Squares:	2552.570449

Regression Coefficients		
k1	k2	k3
1440.10231	0.50640527	0.05935

Table C-19. Quarry 2, 100% RCA test mixture, Test #1

Seq. No.	Chamber Confining Pressure (kPa)	Actual Applied Max. Axial Stress (kPa)	Resilient Modulus (MPa)	Bulk Stress (kPa)	Calculated Resilient Modulus (MPa)	Squared Difference Between the Real and Calculated Resilient Modulus (MPa)
1	20.56	21.47	113.14	83.15	145.2705055	1032.369384
2	20.23	41.92	149.47	102.61	156.7527618	53.03861971
3	20.16	64.31	184.09	124.79	169.3242749	218.0266378
4	34.15	34.64	131.05	137.09	150.934316	395.3860235
5	34.53	67.65	177.68	171.24	169.6382013	64.67052589
6	34.03	103.03	213.1	205.12	189.7256543	546.3600348
7	69.27	68.26	172.65	276.07	167.4560572	26.97704135
8	69.28	143.96	252.96	351.8	210.4533863	1806.812204
9	69.08	206.07	244.53	413.31	245.5074302	0.955369755
10	103.96	68.87	145.58	380.75	166.1189046	421.8466007
11	103.91	103.66	189.53	415.39	185.9071616	13.12495773
12	103.93	205.69	244.05	517.48	243.5498201	0.250179918
13	138.73	104.77	180.92	520.96	185.2223253	18.51000286
14	138.81	137.03	216.05	553.46	203.4659356	158.358676
15	138.89	269.81	248.54	686.48	278.0678569	871.8943326
					Sum of Squares:	5628.580591

Regression Coefficients		
k1	k2	k3
1295.41891	-0.0316108	0.997286

Table C-20. Quarry 2, 100% RCA test mixture, Test #2

(This test was excluded as an outlier.)

Seq. No.	Chamber Confining Pressure (kPa)	Actual Applied Max. Axial Stress (kPa)	Resilient Modulus (MPa)	Bulk Stress (kPa)	Calculated Resilient Modulus (MPa)	Squared Difference Between the Real and Calculated Resilient Modulus (MPa)
1	20	46.21	132.99	106.21	128.5886251	19.37210111
2	19.86	45.41	128.38	104.99	127.5405851	0.70461732
3	20.3	61.92	137.74	122.82	142.7843724	25.44569334
4	34.11	34.43	155.71	136.76	152.2399145	12.04149337
5	34.13	72.06	189.93	174.45	182.1332655	60.78906873
6	33.93	102.75	200.63	204.54	204.9607927	18.75576546
7	69.02	67.07	247.25	274.13	247.7590372	0.259118898
8	68.95	136.8	293.18	343.65	295.0381518	3.45272816
9	68.63	212.84	346.19	418.73	343.7877067	5.771013076
10	103.91	65.43	284.34	377.16	308.0567759	562.4854586
11	103.91	104.39	337.08	416.12	333.3919049	13.60204582
12	103.92	207.52	400	519.28	397.8908128	4.448670462
13	138.68	107.54	393.73	523.58	390.4941068	10.47100455
14	138.74	141.15	428.46	557.37	411.2382196	296.58972
15	138.78	278.96	484.11	695.3	492.7796944	75.16360031
					Sum of Squares:	1109.352099

Regression Coefficients		
k1	k2	k3
1207.29833	0.68435326	0.090397

Table C-21. Quarry 2, 100% RCA test mixture, Test #3

Seq. No.	Chamber Confining Pressure (kPa)	Actual Applied Max. Axial Stress (kPa)	Resilient Modulus (MPa)	Bulk Stress (kPa)	Calculated Resilient Modulus (MPa)	Squared Difference Between the Real and Calculated Resilient Modulus (MPa)
1	19.39	11.57	44.22	69.74	79.00930394	1210.295669
2	19.47	38.58	75.71	96.99	94.70570059	360.836641
3	19.56	57.63	96.48	116.31	106.2773617	95.9882972
4	33.6	34.32	66.73	135.12	93.63168247	723.7005196
5	33.44	78.62	136.83	178.94	120.8164122	256.4349937
6	33.62	110.86	180.25	211.72	142.0530573	1459.006435
7	68.41	71.67	116.55	276.9	118.7247075	4.729352522
8	68.28	143.6	207.04	348.44	167.218232	1585.773203
9	68.65	206.74	234.34	412.69	214.3314996	400.3400899
10	103.44	73.56	109.4	383.88	121.5306921	147.1536901
11	103.56	102.33	143.01	413.01	140.4070069	6.775573293
12	103.56	196.77	224.78	507.45	208.6259027	260.9548596
13	138.28	100.09	125.4	514.93	140.2159989	219.5138233
14	138.4	142.83	192.65	558.03	169.9816709	513.8531431
15	138.1	260.2	207.73	674.5	261.2404553	2863.36883
					Sum of Squares:	10108.72512

Regression Coefficients		
k1	k2	k3
732.408319	0.04159185	1.487118

Table C-22. Quarry 2, 25% RCA - 75% crushed rock test mixture, Test #1

Seq. No.	Chamber Confining Pressure (kPa)	Actual Applied Max. Axial Stress (kPa)	Resilient Modulus (MPa)	Bulk Stress (kPa)	Calculated Resilient Modulus (MPa)	Squared Difference Between the Real and Calculated Resilient Modulus (MPa)
1	20.02	116.55	165.8	176.61	233.2155017	4544.849874
2	19.9	38.92	190.26	98.62	184.7627238	30.22004513
3	19.98	64.11	226.22	124.05	201.2590325	623.0498981
4	33.94	33.9	188.37	135.72	190.2735858	3.623638954
5	34.09	69.57	235.16	171.84	212.3189693	521.7126843
6	33.68	103.91	265.82	204.95	232.3353258	1121.223409
7	68.87	68.26	230.06	274.87	224.9692203	25.91603839
8	68.62	138.42	283.39	344.28	263.9733104	377.0078348
9	68.72	203.38	289.06	409.54	298.2711886	84.84599554
10	103.6	69.02	211.84	379.82	234.9259884	532.9628592
11	103.61	107.16	259.17	417.99	256.2421803	8.572128181
12	103.61	201.58	244.43	512.41	306.2386018	3820.303257
13	138.21	103.11	233.51	517.74	261.4528704	780.8040061
14	138.37	136.55	320.54	551.66	279.6497775	1672.010295
15	138.4	270.55	386.51	685.75	348.1164092	1474.067817
					Sum of Squares:	15621.16978

Regression Coefficients		
k1	k2	k3
1658.05296	0.12901309	0.59123

Table C-23. Quarry 2, 25% RCA - 75% crushed rock test mixture, Test #2

Seq. No.	Chamber Confining Pressure (kPa)	Actual Applied Max. Axial Stress (kPa)	Resilient Modulus (MPa)	Bulk Stress (kPa)	Calculated Resilient Modulus (MPa)	Squared Difference Between the Real and Calculated Resilient Modulus (MPa)
1	20.02	117.04	223.49	177.1	220.518432	8.830216388
2	19.9	44.26	159.21	103.96	159.7738171	0.317889692
3	19.98	61.58	173.7	121.52	175.0077614	1.710240002
4	33.94	35.64	166.19	137.46	176.445941	105.1843257
5	34.09	65.28	188	167.55	200.5775006	158.1935208
6	33.68	100.88	225.02	201.92	227.7137694	7.256393837
7	68.87	71.86	261.11	278.47	249.0919155	144.4343558
8	68.62	137.53	305.85	343.39	296.1749088	93.60739002
9	68.72	203.26	340.6	409.42	342.1953197	2.545044973
10	103.6	71.1	293.82	381.9	282.9356	118.470164
11	103.61	101.81	307.57	412.64	304.9586655	6.819067776
12	103.61	205.78	396.25	516.61	377.1231306	365.837133
13	138.21	101.87	321.96	516.5	334.1575036	148.7790932
14	138.37	137.93	351.9	553.04	359.7326369	61.35020026
15	138.4	271.41	439.51	686.61	450.3861882	118.2914697
					Sum of Squares:	1341.626505

Regression Coefficients		
k1	k2	k3
1440.59172	0.40692919	0.426175

Table C-24. Quarry 2, 25% RCA - 75% crushed rock test mixture, Test #3

Seq. No.	Chamber Confining Pressure (kPa)	Actual Applied Max. Axial Stress (kPa)	Resilient Modulus (MPa)	Bulk Stress (kPa)	Calculated Resilient Modulus (MPa)	Squared Difference Between the Real and Calculated Resilient Modulus (MPa)
1	20.02	117.55	201.23	177.61	234.4207042	1101.825021
2	19.9	41.85	180.64	101.55	176.2167941	19.59744523
3	19.98	62.33	206.72	122.27	192.8440143	192.589662
4	33.94	36.51	183.27	138.33	189.8022732	42.60850774
5	34.09	68.71	218.73	170.98	213.9342977	23.0430405
6	33.68	102.89	253.72	203.93	237.9645882	248.1989648
7	68.87	70.55	253.89	277.16	245.126074	76.7976246
8	68.62	138.32	304.58	344.18	290.005258	212.4996679
9	68.72	203.16	325.48	409.32	331.4459239	35.63962087
10	103.6	70.55	261.38	381.35	267.6047465	38.75381518
11	103.61	105.44	292.95	416.27	290.725196	4.95957218
12	103.61	204.2	331.17	515.03	353.5029259	498.654503
13	138.21	102.11	287.13	516.74	306.891685	390.6563244
14	138.37	138.11	347.59	553.22	330.3253908	298.0438604
15	138.4	272.32	426.98	687.52	413.2637113	188.0269911
					Sum of Squares:	3371.894621

Regression Coefficients		
k1	k2	k3
1587.09865	0.27493631	0.509878

Table C-25. Quarry 2, 50% RCA - 50% crushed rock test mixture, Test #1

Seq. No.	Chamber Confining Pressure (kPa)	Actual Applied Max. Axial Stress (kPa)	Resilient Modulus (MPa)	Bulk Stress (kPa)	Calculated Resilient Modulus (MPa)	Squared Difference Between the Real and Calculated Resilient Modulus (Mpa)
1	19.61	21.47	115.26	80.3	139.7692834	600.7049709
2	19.67	45.6	162.65	104.61	160.8762486	3.146194199
3	19.63	57.7	164.55	116.59	171.6734115	50.74299156
4	33.75	33.5	134.18	134.75	152.9990708	354.1574268
5	33.76	68.14	191.08	169.42	183.677344	54.79931526
6	33.42	102.61	236.8	202.87	215.5129118	453.1401254
7	68.28	68.56	194.62	273.4	188.3708709	39.05161458
8	68.38	140.41	277.31	345.55	256.4165612	436.5357862
9	68.54	206.28	323.3	411.9	323.4149498	0.013213464
10	103.23	70.76	190.82	380.45	193.3789378	6.548162705
11	103.28	103.55	232.08	413.39	223.9760421	65.67413341
12	103.52	206.18	346.02	516.74	326.9006735	365.5486464
13	138.23	101.07	206.64	515.76	224.0850242	304.3288698
14	138.27	138.48	261.78	553.29	260.4851109	1.676737746
15	138.37	276.98	384.13	692.09	406.7489804	511.6182743
					Sum of Squares:	3247.686463

Regression Coefficients		
k1	k2	k3
1230.68498	0.04865242	1.315007

Table C-26. Quarry 2, 50% RCA - 50% crushed rock test mixture, Test #2

Seq. No.	Chamber Confining Pressure (kPa)	Actual Applied Max. Axial Stress (kPa)	Resilient Modulus (MPa)	Bulk Stress (kPa)	Calculated Resilient Modulus (MPa)	Squared Difference Between the Real and Calculated Resilient Modulus (MPa)
1	19.61	22.55	141.23	81.38	163.585463	499.7667267
2	19.67	48.35	171.55	107.36	184.344411	163.696954
3	19.63	58.9	168.51	117.79	192.6529037	582.8797973
4	33.75	31.8	145.51	133.05	178.557397	1092.130448
5	33.76	66.25	201.51	167.53	204.9725652	11.98935808
6	33.42	102.55	281.44	202.81	232.4072369	2404.211861
7	68.28	69.35	198.61	274.19	218.5813164	398.8534791
8	68.38	141.22	307.51	346.36	272.2867895	1240.674555
9	68.54	207.33	361.15	412.95	321.4219265	1578.319821
10	103.23	71.22	289.91	380.91	228.01221	3831.33641
11	103.28	104.51	258.55	414.35	252.9866947	30.9503658
12	103.52	208.91	361.54	519.47	330.8014341	944.8594336
13	138.23	103.25	207.66	517.94	258.4725787	2581.918156
14	138.27	139.61	281.54	554.42	285.8162302	18.2861448
15	138.37	277.84	328.51	692.95	388.8127129	3636.417179
					Sum of Squares:	19016.29069

Regression Coefficients		
k1	k2	k3
1518.11146	0.11135562	0.859474

Table C-27. Quarry 2, 50% RCA - 50% crushed rock test mixture, Test #3

Seq. No.	Chamber Confining Pressure (kPa)	Actual Applied Max. Axial Stress (kPa)	Resilient Modulus (MPa)	Bulk Stress (kPa)	Calculated Resilient Modulus (MPa)	Squared Difference Between the Real and Calculated Resilient Modulus (MPa)
1	19.61	21.81	127.61	80.64	148.7272499	445.9382418
2	19.67	46.51	165.87	105.52	169.4667878	12.93688246
3	19.63	62.33	165.31	121.22	182.7828584	305.3007823
4	33.75	38.11	139.03	139.36	167.177211	792.265487
5	33.76	69.51	194.62	170.79	193.2203825	1.958929159
6	33.42	105.41	256.48	205.67	223.4705352	1089.624768
7	68.28	71.22	194.93	276.06	202.1197865	51.69303035
8	68.38	139.51	289.26	344.65	260.2742922	840.1712545
9	68.54	206.58	338.32	412.2	319.4022052	357.8829617
10	103.23	72.44	238.01	382.13	208.4222149	875.4370265
11	103.28	104.65	242.89	414.49	235.7510746	50.96425536
12	103.52	203.81	349.70	514.37	322.768899	725.2841992
13	138.23	103.61	205.31	518.3	239.1498338	1145.134355
14	138.27	139.88	268.84	554.69	270.6922591	3.430863913
15	138.37	275.47	352.20	690.58	393.1014008	1672.92459
					Sum of Squares:	8370.947627

Regression Coefficients		
k1	k2	k3
1344.02962	0.08006301	1.098748

Table C-28. Quarry 2, 70% RCA - 30% RAP test mixture, Test #1

Seq. No.	Chamber Confining Pressure (kPa)	Actual Applied Max. Axial Stress (kPa)	Resilient Modulus (MPa)	Bulk Stress (kPa)	Calculated Resilient Modulus (MPa)	Squared Difference Between the Real and Calculated Resilient Modulus (MPa)
1	19.7	12.56	153.53	71.66	108.9845798	1984.294458
2	19.64	39.8	113.1	98.72	132.0864672	360.485935
3	20.03	61.9	151.24	121.99	150.5190171	0.519816374
4	33.58	36.15	135.98	136.89	152.0562057	258.4443903
5	33.75	63.87	162.91	165.12	172.9848583	101.5027705
6	33.71	101.95	197.01	203.08	200.5042946	12.21009503
7	68.41	67.05	211.64	272.28	217.6485541	36.10272275
8	68.65	138.65	277.38	344.6	266.4772424	118.8701241
9	68.53	211.74	319.76	417.33	314.6700336	25.90775812
10	103.72	70.11	249.79	381.27	254.3812926	21.07996729
11	103.65	104.03	269.4	414.98	277.2388797	61.4480343
12	103.8	209.39	345.53	520.79	346.7928072	1.594682091
13	138.55	105.42	311.59	521.07	307.6840319	15.25658675
14	138.57	140.08	344.16	555.79	330.9251526	175.1611869
15	138.39	282.02	416.88	697.19	422.9536604	36.88935048
					Sum of Squares:	3209.767878

Regression Coefficients		
k1	k2	k3
1226.58527	0.44953747	0.42664

Table C-29. Quarry 2, 70% RCA - 30% RAP test mixture, Test #2

(This test was excluded as an outlier.)

Seq. No.	Chamber Confining Pressure (kPa)	Actual Applied Max. Axial Stress (kPa)	Resilient Modulus (MPa)	Bulk Stress (kPa)	Calculated Resilient Modulus (MPa)	Squared Difference Between the Real and Calculated Resilient Modulus (MPa)
1	20.19	17.9	90.74	78.47	102.2418097	132.2916271
2	20.27	38.12	94.47	98.93	113.6577681	368.1704461
3	20.33	57	111.66	117.99	124.5552366	166.2871281
4	34.2	36.65	102.61	139.25	112.6615165	101.0329849
5	34.14	68.68	133.63	171.1	131.264049	5.597723942
6	34.4	106.22	175.64	209.42	153.8199838	476.1131058
7	69.03	72.19	144.34	279.28	133.0953096	126.443062
8	69.05	131.4	189.87	338.55	169.1317292	430.075876
9	69.08	207.29	233	414.53	217.8712356	228.8795134
10	104.04	68.83	127.73	380.95	130.9430038	10.32339328
11	103.99	110.78	170.34	422.75	156.1964036	200.0413203
12	103.85	214.43	249.93	525.98	222.3990653	757.9523636
13	138.75	99.62	135.16	515.87	149.25263	198.6022208
14	138.88	133.94	162.76	550.58	170.3996173	58.36375287
15	138.72	266.39	216.87	682.55	257.2159493	1627.795621
					Sum of Squares:	4887.97014

Regression Coefficients		
k1	k2	k3
909.5686	-0.0039063	1.282266

Table C-30. Quarry 2, 70% RCA - 30% RAP test mixture, Test #3

Seq. No.	Chamber Confining Pressure (kPa)	Actual Applied Max. Axial Stress (kPa)	Resilient Modulus (MPa)	Bulk Stress (kPa)	Calculated Resilient Modulus (MPa)	Squared Difference Between the Real and Calculated Resilient Modulus (MPa)
1	19.66	21.81	154.41	80.79	106.0788955	2335.895663
2	19.67	46.51	101.54	105.52	121.9361018	415.9601764
3	20.31	62.33	122.41	123.26	132.2481343	96.7888872
4	33.66	38.11	138.54	139.09	138.6551591	0.013261616
5	33.68	69.51	142.54	170.55	154.952243	154.0637766
6	33.72	105.41	185.61	206.57	172.1857874	180.209484
7	68.51	71.22	181.65	276.75	195.5073049	192.0248982
8	68.66	139.51	209.41	345.49	222.8525849	180.70309
9	68.55	206.58	268.41	412.23	247.4156044	440.7646484
10	103.74	72.44	221.54	383.66	228.718235	51.52705788
11	103.81	104.65	188.91	416.08	240.7086212	2683.097155
12	103.84	203.81	288.17	515.33	275.116252	170.4003358
13	138.58	103.61	304.41	519.35	267.5657931	1357.495584
14	138.66	139.88	298.51	555.86	279.872564	347.3540216
15	138.42	275.47	304.51	690.73	322.3643722	318.778606
					Sum of Squares:	8925.076646

Regression Coefficients		
k1	k2	k3
1153.74905	0.47881862	0.115373

APPENDIX D:
FOAM GLASS LIGHTWEIGHT AGGREGATE DATA TABLES

Table D-1. Grain size analysis for material LWA-A

	LWA-A-1			LWA-A-2			LWA-A-3			LWA-A Overall			
Total dry weight (g)	10032.1		g	10045.6		g	10009.7		g	30087.4		g	
SIEVE SIZE (mm)	**Frac. Wt. (g)**	**Cum. Wt. (g)**	**% Passing**	**Frac. Wt. (g)**	**Cum. Wt. (g)**	**% Passing**	**Frac. Wt. (g)**	**Cum. Wt. (g)**	**% Passing**	**Frac. Wt. (g)**	**Cum. Wt. (g)**	**% Passing**	**Frac. %**
106.0	0.0	0.0	100.0%	0.0	0.0	100.0%	0.0	0.0	100.0%	0.0	0.0	100.0%	0.0%
75.0	0.0	0.0	100.0%	0.0	0.0	100.0%	0.0	0.0	100.0%	0.0	0.0	100.0%	0.0%
63.0	0.0	0.0	100.0%	46.5	46.5	99.5%	0.0	0.0	100.0%	46.5	46.5	99.8%	0.2%
53.0	113.1	113.1	98.9%	255.6	302.1	97.0%	358.6	358.6	96.4%	727.3	773.8	97.4%	2.4%
37.5	3305.3	3418.4	65.9%	3920.4	4222.5	58.0%	4143.6	4502.2	55.0%	11369.3	12143.1	59.6%	37.8%
26.5	4422.8	7841.2	21.8%	4294.9	8517.4	15.2%	4180.0	8682.2	13.3%	12897.7	25040.8	16.8%	42.9%
19.0	1342.8	9184.0	8.5%	1118.9	9636.3	4.1%	771.6	9453.8	5.6%	3233.3	28274.1	6.0%	10.7%
16.0	165.8	9349.8	6.8%	99.4	9735.7	3.1%	91.3	9545.1	4.6%	356.5	28630.6	4.8%	1.2%
13.2	75.1	9424.9	6.1%	39.9	9775.6	2.7%	48.4	9593.5	4.2%	163.4	28794.0	4.3%	0.5%
9.5	88.5	9513.4	5.2%	20.6	9796.2	2.5%	31.5	9625.0	3.8%	140.6	28934.6	3.8%	0.5%
4.75	27.1	9540.5	4.9%	5.9	9802.1	2.4%	18.5	9643.5	3.7%	51.5	28986.1	3.7%	0.2%
pan	416.7	9957.2	N/A	223.1	10025.2	N/A	312.0	9955.5	N/A	951.8	29937.9	N/A	3.7%

Table D-2. Grain size analysis for material LWA-B

	LWA-B-1			LWA-B-2			LWA-B-3			LWA-B Overall			
Total dry weight (g)	10545.0		g	10101.6		g	10128.3		g	30774.9		g	
SIEVE SIZE (mm)	**Frac. Wt. (g)**	**Cum. Wt. (g)**	**% Passing**	**Frac. Wt. (g)**	**Cum. Wt. (g)**	**% Passing**	**Frac. Wt. (g)**	**Cum. Wt. (g)**	**% Passing**	**Frac. Wt. (g)**	**Cum. Wt. (g)**	**% Passing**	**Frac. %**
106.0	0.0	0.0	100.0%	0.0	0.0	100.0%	0.0	0.0	100.0%	0.0	0.0	100.0%	0.0%
75.0	0.0	0.0	100.0%	0.0	0.0	100.0%	0.0	0.0	100.0%	0.0	0.0	100.0%	0.0%
63.0	43.7	43.7	99.6%	100.3	100.3	99.0%	99.6	99.6	99.0%	243.6	243.6	99.2%	0.8%
53.0	336.0	379.7	96.4%	228.2	328.5	96.7%	364.1	463.7	95.4%	928.3	1171.9	96.2%	3.0%
37.5	2930.5	3310.2	68.6%	3029.1	3357.6	66.8%	3148.0	3611.7	64.3%	9107.6	10279.5	66.6%	29.6%
26.5	4873.3	8183.5	22.4%	4672.0	8029.6	20.5%	4415.7	8027.4	20.7%	13961.0	24240.5	21.2%	45.4%
19.0	1819.9	10003.4	5.1%	1615.2	9644.8	4.5%	1621.1	9648.5	4.7%	5056.2	29296.7	4.8%	16.4%
16.0	114.4	10117.8	4.1%	137.1	9781.9	3.2%	160.6	9809.1	3.2%	412.1	29708.8	3.5%	1.3%
13.2	35.2	10153.0	3.7%	45.4	9827.3	2.7%	46.9	9856.0	2.7%	127.5	29836.3	3.0%	0.4%
9.5	24.2	10177.2	3.5%	41.5	9868.8	2.3%	42.2	9898.2	2.3%	107.9	29944.2	2.7%	0.4%
4.75	8.5	10185.7	3.4%	14.0	9882.8	2.2%	17.4	9915.6	2.1%	39.9	29984.1	2.6%	0.1%
pan	258.7	10444.4	N/A	212.7	10095.5	N/A	203.3	10118.9	N/A	674.7	30658.8	N/A	2.6%

Table D-3. Crushed particle content calculations for material LWA-A

Sample	LWA-A Sample #1						
Size Fraction	Mass Tested (g)	Percent of Total Sample	Relative Percent for Test	Crushed Particle Mass (g)	Uncrushed Particle Mass (g)	Percent Crushed Per Fraction	Weighted Per Fraction
26.5-19.0mm	500.1	10.7	81.68	496.9	3.2	99.36	8115.67
19.0-13.2mm	*not tested*	1.7	12.98	*not tested*	*not tested*	99.36	1289.41
13.2-9.5mm	*not tested*	0.5	3.82	*not tested*	*not tested*	99.36	379.24
9.5-6.7mm	*not tested*	0.1	0.76	*not tested*	*not tested*	99.36	75.85
6.7-4.75mm	*not tested*	0.1	0.76	*not tested*	*not tested*	99.36	75.85
	Total =	13.1				**Weighted Avg.**	**99.4%**

Sample	LWA-A Sample #2						
Size Fraction	Mass Tested (g)	Percent of Total Sample	Relative Percent for Test	Crushed Particle Mass (g)	Uncrushed Particle Mass (g)	Percent Crushed Per Fraction	Weighted Per Fraction
26.5-19.0mm	508.5	10.7	81.68	505.1	3.4	99.33	8113.33
19.0-13.2mm	*not tested*	1.7	12.98	*not tested*	*not tested*	99.33	1289.03
13.2-9.5mm	*not tested*	0.5	3.82	*not tested*	*not tested*	99.33	379.13
9.5-6.7mm	*not tested*	0.1	0.76	*not tested*	*not tested*	99.33	75.83
6.7-4.75mm	*not tested*	0.1	0.76	*not tested*	*not tested*	99.33	75.83
	Total =	13.1				**Weighted Avg.**	**99.3%**

Sample	LWA-A Sample #3						
Size Fraction	Mass Tested (g)	Percent of Total Sample	Relative Percent for Test	Crushed Particle Mass (g)	Uncrushed Particle Mass (g)	Percent Crushed Per Fraction	Weighted Per Fraction
26.5-19.0mm	511.0	10.7	81.68	509.6	1.4	99.73	8145.56
19.0-13.2mm	*not tested*	1.7	12.98	*not tested*	*not tested*	99.73	1294.15
13.2-9.5mm	*not tested*	0.5	3.82	*not tested*	*not tested*	99.73	380.63
9.5-6.7mm	*not tested*	0.1	0.76	*not tested*	*not tested*	99.73	76.13
6.7-4.75mm	*not tested*	0.1	0.76	*not tested*	*not tested*	99.73	76.13
	Total =	13.1				**Weighted Avg.**	**99.7%**

Sample	LWA-A Overall						
Size Fraction	Mass Tested (g)	Percent of Total Sample	Relative Percent for Test	Crushed Particle Mass (g)	Uncrushed Particle Mass (g)	Percent Crushed Per Fraction	Weighted Per Fraction
26.5-19.0mm	1519.6	10.7	81.68	1511.6	8.0	99.47	8124.94
19.0-13.2mm	*not tested*	1.7	12.98	*not tested*	*not tested*	99.47	1290.88

13.2-9.5mm	*not tested*	0.5	3.82	*not tested*	*not tested*	99.47	379.67
9.5-6.7mm	*not tested*	0.1	0.76	*not tested*	*not tested*	99.47	75.93
6.7-4.75mm	*not tested*	0.1	0.76	*not tested*	*not tested*	99.47	75.93
	Total =	13.1				**Weighted Avg.**	**99.5%**

Table D-4. Crushed particle content calculations for material LWA-B

Sample	LWA-B Sample #1						
Size Fraction	Mass Tested (g)	Percent of Total Sample	Relative Percent for Test	Crushed Particle Mass (g)	Uncrushed Particle Mass (g)	Percent Crushed Per Fraction	Weighted Per Fraction
26.5-19.0mm	700.9	16.4	88.17	700.9	0.0	100.00	8817.20
19.0-13.2mm	*not tested*	1.7	9.14	*not tested*	*not tested*	100.00	913.98
13.2-9.5mm	*not tested*	0.4	2.15	*not tested*	*not tested*	100.00	215.05
9.5-6.7mm	*not tested*	0.05	0.27	*not tested*	*not tested*	100.00	26.88
6.7-4.75mm	*not tested*	0.05	0.27	*not tested*	*not tested*	100.00	26.88
	Total =	18.6				**Weighted Avg.**	**100.0%**

Sample	LWA-B Sample #2						
Size Fraction	Mass Tested (g)	Percent of Total Sample	Relative Percent for Test	Crushed Particle Mass (g)	Uncrushed Particle Mass (g)	Percent Crushed Per Fraction	Weighted Per Fraction
26.5-19.0mm	709.9	16.4	88.17	709.9	0.0	100.00	8817.20
19.0-13.2mm	*not tested*	1.7	9.14	*not tested*	*not tested*	100.00	913.98
13.2-9.5mm	*not tested*	0.4	2.15	*not tested*	*not tested*	100.00	215.05
9.5-6.7mm	*not tested*	0.05	0.27	*not tested*	*not tested*	100.00	26.88
6.7-4.75mm	*not tested*	0.05	0.27	*not tested*	*not tested*	100.00	26.88
	Total =	18.6				**Weighted Avg.**	**100.0%**

Sample	LWA-B Sample #3						
Size Fraction	Mass Tested (g)	Percent of Total Sample	Relative Percent for Test	Crushed Particle Mass (g)	Uncrushed Particle Mass (g)	Percent Crushed Per Fraction	Weighted Per Fraction
26.5-19.0mm	704.2	16.4	88.17	704.2	0.0	100.00	8817.20
19.0-13.2mm	*not tested*	1.7	9.14	*not tested*	*not tested*	100.00	913.98
13.2-9.5mm	*not tested*	0.4	2.15	*not tested*	*not tested*	100.00	215.05
9.5-6.7mm	*not tested*	0.05	0.27	*not tested*	*not tested*	100.00	26.88
6.7-4.75mm	*not tested*	0.05	0.27	*not tested*	*not tested*	100.00	26.88
	Total =	18.6				**Weighted Avg.**	**100.0%**

Sample	LWA-B Overall						
Size Fraction	Mass Tested (g)	Percent of Total Sample	Relative Percent for Test	Crushed Particle Mass (g)	Uncrushed Particle Mass (g)	Percent Crushed Per Fraction	Weighted Per Fraction
26.5-19.0mm	2115.0	16.4	88.17	2115.0	0.0	100.00	8817.20
19.0-13.2mm	*not tested*	1.7	9.14	*not tested*	*not tested*	100.00	913.98

13.2-9.5mm	*not tested*	0.4	2.15	*not tested*	*not tested*	100.00	215.05
9.5-6.7mm	*not tested*	0.05	0.27	*not tested*	*not tested*	100.00	26.88
6.7-4.75mm	*not tested*	0.05	0.27	*not tested*	*not tested*	100.00	26.88
	Total =	18.6				**Weighted Avg.**	**100.0%**

Table D-5. Flat and elongated particle content calculations for material LWA-A

Sample	LWA-A Sample #1						
Size Fraction	Mass Tested (g)	Percent of Total Sample	Relative Percent for Test	Flat & Elongated Particle Mass (g)	Cubical Particle Mass (g)	Percent Flat and Elongated Per Fraction	Weighted Per Fraction
37.5-26.5mm	1500.0	42.9	76.61	0.0	1500.0	0.0000	0.0000
26.5-19.0mm	1000.1	10.7	19.11	8.2	991.9	0.8199	15.6663
19.0-13.2mm	*not tested*	1.7	3.04	*not tested*	*not tested*	0.8199	2.4890
13.2-9.5mm	*not tested*	0.5	0.89	*not tested*	*not tested*	0.8199	0.7321
9.5-6.7mm	*not tested*	0.1	0.18	*not tested*	*not tested*	0.8199	0.1464
6.7-4.75mm	*not tested*	0.1	0.18	*not tested*	*not tested*	0.8199	0.1464
	Total =	56.0				**Weighted Avg.**	**0.2%**

Sample	LWA-A Sample #2						
Size Fraction	Mass Tested (g)	Percent of Total Sample	Relative Percent for Test	Flat & Elongated Particle Mass (g)	Cubical Particle Mass (g)	Percent Flat and Elongated Per Fraction	Weighted Per Fraction
37.5-26.5mm	1500.2	42.9	76.61	0.0	1500.2	0.0000	0.0000
26.5-19.0mm	1001.4	10.7	19.11	7.1	994.3	0.7090	13.5471
19.0-13.2mm	*not tested*	1.7	3.04	*not tested*	*not tested*	0.7090	2.1523
13.2-9.5mm	*not tested*	0.5	0.89	*not tested*	*not tested*	0.7090	0.6330
9.5-6.7mm	*not tested*	0.1	0.18	*not tested*	*not tested*	0.7090	0.1266
6.7-4.75mm	*not tested*	0.1	0.18	*not tested*	*not tested*	0.7090	0.1266
	Total =	56.0				**Weighted Avg.**	**0.2%**

Sample	LWA-A Sample #3						
Size Fraction	Mass Tested (g)	Percent of Total Sample	Relative Percent for Test	Flat & Elongated Particle Mass (g)	Cubical Particle Mass (g)	Percent Flat and Elongated Per Fraction	Weighted Per Fraction
37.5-26.5mm	1499.9	42.9	76.61	0.0	1499.9	0.0000	0.0000
26.5-19.0mm	1002.1	10.7	19.11	8.5	993.6	0.8482	16.2070
19.0-13.2mm	*not tested*	1.7	3.04	*not tested*	*not tested*	0.8482	2.5749
13.2-9.5mm	*not tested*	0.5	0.89	*not tested*	*not tested*	0.8482	0.7573
9.5-6.7mm	*not tested*	0.1	0.18	*not tested*	*not tested*	0.8482	0.1515
6.7-4.75mm	*not tested*	0.1	0.18	*not tested*	*not tested*	0.8482	0.1515
	Total =	56.0				**Weighted Avg.**	**0.2%**

Sample	LWA-A Overall						
Size Fraction	**Mass Tested (g)**	**Percent of Total Sample**	**Relative Percent for Test**	**Flat & Elongated Particle Mass (g)**	**Cubical Particle Mass (g)**	**Percent Flat and Elongated Per Fraction**	**Weighted Per Fraction**
37.5-26.5mm	4500.1	42.9	76.61	0.0	4500.1	0.0000	0.0000
26.5-19.0mm	3003.6	10.7	19.11	23.8	2979.8	0.7924	15.1402
19.0-13.2mm	*not tested*	1.7	3.04	*not tested*	*not tested*	0.7924	2.4054
13.2-9.5mm	*not tested*	0.5	0.89	*not tested*	*not tested*	0.7924	0.7075
9.5-6.7mm	*not tested*	0.1	0.18	*not tested*	*not tested*	0.7924	0.1415
6.7-4.75mm	*not tested*	0.1	0.18	*not tested*	*not tested*	0.7924	0.1415
	Total =	56.0				**Weighted Avg.**	**0.2%**

Table D-6. Flat and elongated particle content calculations for material LWA-B

Sample	**LWA-B Sample #1**						
Size Fraction	**Mass Tested (g)**	**Percent of Total Sample**	**Relative Percent for Test**	**Flat & Elongated Particle Mass (g)**	**Cubical Particle Mass (g)**	**Percent Flat and Elongated Per Fraction**	**Weighted Per Fraction**
37.5-26.5mm	1499.7	45.4	81.07	0.0	1499.7	0.0000	0.0000
26.5-19.0mm	1000.2	16.4	29.29	1.2	999.0	0.1200	3.5136
19.0-13.2mm	*not tested*	1.7	3.04	*not tested*	*not tested*	0.1200	0.3642
13.2-9.5mm	*not tested*	0.4	0.71	*not tested*	*not tested*	0.1200	0.0857
9.5-6.7mm	*not tested*	0.1	0.09	*not tested*	*not tested*	0.1200	0.0107
6.7-4.75mm	*not tested*	0.1	0.09	*not tested*	*not tested*	0.1200	0.0107
	Total =	64.0				**Weighted Avg.**	**0.0%**

Sample	**LWA-B Sample #2**						
Size Fraction	**Mass Tested (g)**	**Percent of Total Sample**	**Relative Percent for Test**	**Flat & Elongated Particle Mass (g)**	**Cubical Particle Mass (g)**	**Percent Flat and Elongated Per Fraction**	**Weighted Per Fraction**
37.5-26.5mm	1501.8	45.4	81.07	0.0	1501.8	0.0000	0.0000
26.5-19.0mm	1001.1	16.4	29.29	3.5	997.6	0.3496	10.2387
19.0-13.2mm	*not tested*	1.7	3.04	*not tested*	*not tested*	0.3496	1.0613
13.2-9.5mm	*not tested*	0.4	0.71	*not tested*	*not tested*	0.3496	0.2497
9.5-6.7mm	*not tested*	0.1	0.09	*not tested*	*not tested*	0.3496	0.0312
6.7-4.75mm	*not tested*	0.1	0.09	*not tested*	*not tested*	0.3496	0.0312
	Total =	64.0				**Weighted Avg.**	**0.1%**

Sample	**LWA-B Sample #3**						
Size Fraction	**Mass Tested (g)**	**Percent of Total Sample**	**Relative Percent for Test**	**Flat & Elongated Particle Mass (g)**	**Cubical Particle Mass (g)**	**Percent Flat and Elongated Per Fraction**	**Weighted Per Fraction**
37.5-26.5mm	1500.7	45.4	81.07	0.0	1500.7	0.0000	0.0000
26.5-19.0mm	1001.6	16.4	29.29	2.7	998.9	0.2696	7.8945
19.0-13.2mm	*not tested*	1.7	3.04	*not tested*	*not tested*	0.2696	0.8183
13.2-9.5mm	*not tested*	0.4	0.71	*not tested*	*not tested*	0.2696	0.1925
9.5-6.7mm	*not tested*	0.1	0.09	*not tested*	*not tested*	0.2696	0.0241
6.7-4.75mm	*not tested*	0.1	0.09	*not tested*	*not tested*	0.2696	0.0241
	Total =	64.0				**Weighted Avg.**	**0.1%**

Sample	LWA-B Overall						
Size Fraction	**Mass Tested (g)**	**Percent of Total Sample**	**Relative Percent for Test**	**Flat & Elongated Particle Mass (g)**	**Cubical Particle Mass (g)**	**Percent Flat and Elongated Per Fraction**	**Weighted Per Fraction**
37.5-26.5mm	4502.2	45.4	81.07	0.0	4502.2	0.0000	0.0000
26.5-19.0mm	3002.9	16.4	29.29	7.4	2995.5	0.2464	7.2168
19.0-13.2mm	*not tested*	1.7	3.04	*not tested*	*not tested*	0.2464	0.7481
13.2-9.5mm	*not tested*	0.4	0.71	*not tested*	*not tested*	0.2464	0.1760
9.5-6.7mm	*not tested*	0.1	0.09	*not tested*	*not tested*	0.2464	0.0220
6.7-4.75mm	*not tested*	0.1	0.09	*not tested*	*not tested*	0.2464	0.0220
	Total =	64.0				**Weighted Avg.**	**0.1%**

Table D-7. Aggregate sample preparation for Micro-Deval testing (based on MTO LS-618)

Grading	Grading A	
Passing	**Retained**	**Mass (g)**
19.0mm	16.0mm	50
16.0mm	13.2mm	50
13.2mm	9.5mm	100
	TOTAL	**200**

Table D-8. Micro-Deval abrasion resistance testing results for material LWA-A

Material	**LWA-A**		
Sample	**Sample #1**	**Sample #2**	**Sample #3**
Initial Mass (g)	201.1	200.6	201.3
Final Mass (g)	191.8	193.2	182.7
Percent Loss	4.6%	3.7%	9.2%
Average	5.9%		
Std. Dev.	3.0%		

Table D-9. Micro-Deval abrasion resistance testing results for material LWA-B

Material	**LWA-B**		
Sample	**Sample #1**	**Sample #2**	**Sample #3**
Initial Mass (g)	200.5	200.5	201.1
Final Mass (g)	196.9	194.1	192.3
Percent Loss	1.8%	3.2%	4.4%
Average	3.1%		
Std. Dev.	1.3%		

Table D-10. Freezing and thawing resistance testing analysis for material LWA-A

Sample	LWA-A Sample #1						
Size Fraction	Initial Mass (g)	Final Mass (g)	Mass Lost (g)	Percent Loss Per Fraction	Percent of Total Sample	Relative Percent for Test	Weighted Per Fraction
37.5-26.5mm	236.2	235.1	1.1	0.4657	42.9	76.61	35.6765
26.5-19.0mm	215.1	213.5	1.6	0.7438	10.7	19.11	14.2127
19.0-13.2mm	*not tested*	*not tested*	*not tested*	0.7438	1.7	3.04	2.2581
13.2-9.5mm	*not tested*	*not tested*	*not tested*	0.7438	0.5	0.89	0.6641
9.5-4.75mm	*not tested*	*not tested*	*not tested*	0.7438	0.2	0.36	0.2657
						Weighted Avg. =	0.5%

Sample	LWA-A Sample #3						
Size Fraction	Initial Mass (g)	Final Mass (g)	Mass Lost (g)	Percent Loss Per Fraction	Percent of Total Sample	Relative Percent for Test	Weighted Per Fraction
37.5-26.5mm	240.8	240.1	0.7	0.2907	42.9	76.61	22.2695
26.5-19.0mm	221.1	221.0	0.1	0.0452	10.7	19.11	0.8642
19.0-13.2mm	*not tested*	*not tested*	*not tested*	0.0452	1.7	3.04	0.1373
13.2-9.5mm	*not tested*	*not tested*	*not tested*	0.0452	0.5	0.89	0.0404
9.5-4.75mm	*not tested*	*not tested*	*not tested*	0.0452	0.2	0.36	0.0162
						Weighted Avg. =	0.2%

Sample	LWA-A Sample #3						
Size Fraction	Initial Mass (g)	Final Mass (g)	Mass Lost (g)	Percent Loss Per Fraction	Percent of Total Sample	Relative Percent for Test	Weighted Per Fraction
37.5-26.5mm	232.7	232.6	0.1	0.0430	42.9	76.61	3.2921
26.5-19.0mm	218.0	217.8	0.2	0.0917	10.7	19.11	1.7529
19.0-13.2mm	*not tested*	*not tested*	*not tested*	0.0917	1.7	3.04	0.2785
13.2-9.5mm	*not tested*	*not tested*	*not tested*	0.0917	0.5	0.89	0.0819
9.5-4.75mm	*not tested*	*not tested*	*not tested*	0.0917	0.2	0.36	0.0328
						Weighted Avg. =	0.1%

Sample	LWA-A Overall						
Size Fraction	Initial Mass (g)	Final Mass (g)	Mass Lost (g)	Percent Loss Per Fraction	Percent of Total Sample	Relative Percent for Test	Weighted Per Fraction
37.5-26.5mm	709.7	707.8	1.9	0.2677	42.9	76.61	20.5092
26.5-19.0mm	654.2	652.3	1.9	0.2904	10.7	19.11	5.5493

19.0-13.2mm	*not tested*	*not tested*	*not tested*	0.2904	1.7	3.04	0.8817
13.2-9.5mm	*not tested*	*not tested*	*not tested*	0.2904	0.5	0.89	0.2593
9.5-4.75mm	*not tested*	*not tested*	*not tested*	0.2904	0.2	0.36	0.1037
						Weighted Avg. =	**0.3%**

Table D-11. Freezing and thawing resistance testing analysis for material LWA-B

Sample	LWA-B Sample #1						
Size Fraction	Initial Mass (g)	Final Mass (g)	Mass Lost (g)	Percent Loss Per Fraction	Percent of Total Sample	Relative Percent for Test	Weighted Per Fraction
37.5-26.5mm	311.9	311.9	0.0	0.0000	45.4	70.94	0.0000
26.5-19.0mm	300.8	300.7	0.1	0.0332	16.4	25.63	0.8519
19.0-13.2mm	*not tested*	*not tested*	*not tested*	0.0332	1.7	2.66	0.0883
13.2-9.5mm	*not tested*	*not tested*	*not tested*	0.0332	0.4	0.63	0.0208
9.5-4.75mm	*not tested*	*not tested*	*not tested*	0.0332	0.1	0.16	0.0052
						Weighted Avg. =	**0.01%**

Sample	LWA-B Sample #3						
Size Fraction	Initial Mass (g)	Final Mass (g)	Mass Lost (g)	Percent Loss Per Fraction	Percent of Total Sample	Relative Percent for Test	Weighted Per Fraction
37.5-26.5mm	309.5	309.4	0.1	0.0323	45.4	70.94	2.2920
26.5-19.0mm	299.8	299.0	0.8	0.2668	16.4	25.63	6.8379
19.0-13.2mm	*not tested*	*not tested*	*not tested*	0.2668	1.7	2.66	0.7088
13.2-9.5mm	*not tested*	*not tested*	*not tested*	0.2668	0.4	0.63	0.1668
9.5-4.75mm	*not tested*	*not tested*	*not tested*	0.2668	0.1	0.16	0.0417
						Weighted Avg. =	**0.1%**

Sample	LWA-B Sample #3						
Size Fraction	Initial Mass (g)	Final Mass (g)	Mass Lost (g)	Percent Loss Per Fraction	Percent of Total Sample	Relative Percent for Test	Weighted Per Fraction
37.5-26.5mm	310.6	304.6	6.0	1.9317	45.4	70.94	137.0332
26.5-19.0mm	302.7	302.7	0.0	0.0000	16.4	25.63	0.0000
19.0-13.2mm	*not tested*	*not tested*	*not tested*	0.0000	1.7	2.66	0.0000
13.2-9.5mm	*not tested*	*not tested*	*not tested*	0.0000	0.4	0.63	0.0000
9.5-4.75mm	*not tested*	*not tested*	*not tested*	0.0000	0.1	0.16	0.0000
						Weighted Avg. =	**1.4%**

Sample	LWA-B Overall						
Size Fraction	Initial Mass (g)	Final Mass (g)	Mass Lost (g)	Percent Loss Per Fraction	Percent of Total Sample	Relative Percent for Test	Weighted Per Fraction
37.5-26.5mm	932.0	925.9	6.1	0.6545	45.4	70.94	46.4291
26.5-19.0mm	903.3	902.4	0.9	0.0996	16.4	25.63	2.5531

19.0-13.2mm	*not tested*	*not tested*	*not tested*	0.0996	1.7	2.66	0.2647
13.2-9.5mm	*not tested*	*not tested*	*not tested*	0.0996	0.4	0.63	0.0623
9.5-4.75mm	*not tested*	*not tested*	*not tested*	0.0996	0.1	0.16	0.0156
						Weighted Avg. =	**0.5%**

Table D-12. Resilient modulus measurements for material LWA-A

Testing Sequence	Average		Specimen #1			Specimen #2			Specimen #3		
	θ (kPa)	M_R (MPa)	θ (kPa)	M_R (MPa)	Pct. Diff. Rel. to M_R Avg.	θ (kPa)	M_R (MPa)	Pct. Diff. Rel. to M_R Avg.	θ (kPa)	M_R (MPa)	Pct. Diff. Rel. to M_R Avg.
1	82.33	65.41	82.31	66.83	2.2%	82.39	62.46	-4.5%	82.28	66.94	2.3%
2	103.12	72.27	103.06	74.05	2.5%	103.12	69.49	-3.9%	103.17	73.28	1.4%
3	123.87	79.61	123.62	81.76	2.7%	123.98	75.81	-4.8%	124.01	81.24	2.1%
4	137.88	85.36	137.91	86.27	1.1%	137.86	80.59	-5.6%	137.87	89.22	4.5%
5	172.20	94.98	172.12	98.33	3.5%	172.31	92.05	-3.1%	172.17	94.57	-0.4%
6	206.96	100.29	207.05	103.82	3.5%	206.86	94.82	-5.4%	206.95	102.22	1.9%
7	275.70	122.70	275.79	125.42	2.2%	275.68	116.16	-5.3%	275.62	126.53	3.1%
8	344.96	132.37	344.99	136.08	2.8%	345.04	125.50	-5.2%	344.85	135.54	2.4%
9	414.08	134.23	413.98	136.64	1.8%	414.23	128.59	-4.2%	414.03	137.44	2.4%
10	379.50	137.91	379.48	140.11	1.6%	379.43	131.36	-4.8%	379.59	142.28	3.2%
11	414.05	148.26	413.99	152.82	3.1%	414.15	139.88	-5.7%	414.01	152.09	2.6%
12	517.84	159.15	517.92	159.86	0.4%	517.92	153.86	-3.3%	517.68	163.73	2.9%
13	517.91	167.43	517.85	170.24	1.7%	518.04	159.52	-4.7%	517.84	172.54	3.1%
14	552.33	172.79	552.64	173.55	0.4%	552.07	165.26	-4.4%	552.27	179.55	3.9%
15	690.67	184.75	690.71	187.44	1.5%	690.62	176.54	-4.4%	690.68	190.26	3.0%

Table D-13. Resilient modulus measurements for material LWA-B

Testing Sequence	Average		Specimen #1			Specimen #2			Specimen #3		
	θ (kPa)	M_R (MPa)	θ (kPa)	M_R (MPa)	Pct. Diff. Rel. to M_R Avg.	θ (kPa)	M_R (MPa)	Pct. Diff. Rel. to M_R Avg.	θ (kPa)	M_R (MPa)	Pct. Diff. Rel. to M_R Avg.
1	82.22	66.14	82.24	63.80	-3.5%	82.15	66.98	1.3%	82.28	67.65	2.3%
2	103.08	73.84	103.02	74.20	0.5%	103.11	71.96	-2.5%	103.12	75.36	2.1%
3	123.89	83.39	123.92	83.25	-0.2%	124.05	80.57	-3.4%	123.70	86.36	3.6%
4	137.75	90.75	137.64	88.94	-2.0%	137.68	88.65	-2.3%	137.93	94.66	4.3%
5	172.25	102.64	172.11	102.20	-0.4%	172.18	100.50	-2.1%	172.46	105.21	2.5%
6	206.97	108.47	206.83	109.22	0.7%	207.10	105.25	-3.0%	206.98	110.94	2.3%
7	275.67	132.96	275.70	133.81	0.6%	275.52	129.83	-2.4%	275.79	135.23	1.7%
8	344.99	142.28	345.03	142.94	0.5%	345.04	139.14	-2.2%	344.91	144.77	1.8%
9	413.99	147.19	413.89	149.61	1.6%	414.12	142.29	-3.3%	413.96	149.67	1.7%
10	379.37	148.75	379.37	151.74	2.0%	379.43	142.55	-4.2%	379.30	151.95	2.2%
11	414.06	160.16	414.07	160.90	0.5%	414.00	158.54	-1.0%	414.10	161.03	0.5%
12	517.81	173.84	517.57	177.29	2.0%	517.89	168.97	-2.8%	517.97	175.25	0.8%
13	518.01	179.91	517.84	183.32	1.9%	518.17	175.94	-2.2%	518.00	180.48	0.3%
14	552.40	188.02	552.45	192.26	2.3%	552.62	184.05	-2.1%	552.12	187.77	-0.1%
15	690.92	203.36	691.06	207.43	2.0%	690.75	199.93	-1.7%	690.95	202.72	-0.3%

Table D-14. Relative density testing results for materials LWA-A and LWA-B

Material	Sample	Dry Weight of Container (g)	Dry Weight of Sample (g)	Total Weight (g)	Net Weight of Water (g)	Water Temp. (°C)	Water Density (g/cm^3)	Volume of Water (cm^3)	Volume of Sample (cm^3)	Density of Sample (g/cm^3)	
Water Only	N/A	8348.1	0.0	15475.6	7127.5	23.2	0.997490	7145.44	-	-	
Water Only	N/A	8348.1	0.0	15482.8	7134.7	22.4	0.997678	7151.31	-	-	
Water Only	N/A	8348.1	0.0	15474.5	7126.4	21.4	0.997904	7141.37	-	-	
Water Only	N/A	8348.1	0.0	15468.8	7120.7	20.6	0.998078	7134.41	-	-	
Water Only	Overall						**Average**	**7143.13**	**cm^3**		**<u>Percent Anomaly</u>**
Metal Block	Measured	-	3820.5	-	-	-	-	-	499.32	7.651	N/A
Metal Block	N/A	8348.1	3820.5	18799.8	6631.2	22.1	0.997747	6646.17	496.96	7.688	+0.47%
Metal Block	N/A	8348.1	3820.5	18799.5	6630.9	21.9	0.997792	6645.57	497.56	7.679	+0.35%
Metal Block	N/A	8348.1	3820.5	18799.9	6631.3	21.3	0.997926	6645.08	498.05	7.671	+0.25%
Metal Block	Overall								**Average**	**7.679**	+0.36%
LWA-A	1	8348.1	500.4	14298.7	5450.2	22.0	0.997770	5462.38	1680.75	0.298	+0.34%
LWA-A	2	8348.1	500.2	14315.5	5467.2	22.2	0.997724	5479.67	1663.46	0.301	+1.34%
LWA-A	3	8348.1	509.5	14274.2	5416.6	22.0	0.997770	5428.71	1714.42	0.297	+0.16%
LWA-A	4	8348.1	502.2	14257.6	5407.3	21.8	0.997815	5419.14	1723.99	0.291	-1.83%
LWA-A	Overall		2012.3	g					**Wtd. Avg.**	**0.297**	N/A
LWA-A	Overall								**Corrected**	**0.296**	-
LWA-B	1	8348.1	501.6	14617.7	5768.0	22.0	0.997770	5780.89	1362.24	0.368	-2.54%
LWA-B	2	8348.1	504.9	14630.0	5777.0	22.0	0.997770	5789.91	1353.22	0.373	-1.24%
LWA-B	3	8348.1	509.4	14665.0	5807.5	21.6	0.997860	5819.95	1323.18	0.385	+1.90%
LWA-B	4	8348.1	507.0	14668.0	5812.9	21.7	0.997837	5825.50	1317.63	0.385	+1.84%
LWA-B	Overall		2022.9	g					**Wtd. Avg.**	**0.378**	N/A
LWA-B	Overall								**Corrected**	**0.376**	-

Table D-15. Life Cycle Cost Analysis calculations – foam glass LWA vs. EPS geofoam

(All values below are in $ CAD.)

	Design Artificial Subgrade	**LWA**	**EPS**	**LWA**	**EPS**	**LWA**	**EPS**
	Design Lifetime ESALs	1×10^6	1×10^6	10×10^6	10×10^6	60×10^6	60×10^6
	Depth Hot Mix Asphalt (mm)	127.0	317.5	190.5	482.6	304.8	711.2
	Depth Granular Base (mm)	152.4	152.4	152.4	152.4	152.4	152.4
	Depth Granular Subbase (mm)	152.4	152.4	228.6	215.9	393.7	368.3
	Depth Lightweight Fill (mm)	5568.2	5377.7	5428.5	5149.1	5149.1	4768.1
	Road Length (m)	1000	1000	1000	1000	1000	1000
	Road Width (m)	15	15	15	15	15	15
	Volume Hot Mix Asphalt (m^3)	1905.0	4762.5	2857.5	7239.0	4572.0	10668.0
	Volume Granular Base (m^3)	2286.0	2286.0	2286.0	2286.0	2286.0	2286.0
	Volume Granular Subbase (m^3)	2286.0	2286.0	3429.0	3238.5	5905.5	5524.5
	Volume Lightweight Fill (m^3)	83523.0	80665.5	81427.5	77236.5	77236.5	71521.5
	Cost Hot Mix Asphalt	$492,443	$1,231,106	$738,664	$1,871,282	$1,181,862	$2,757,678
	Cost Granular Base	$96,698	$96,698	$96,698	$96,698	$96,698	$96,698
	Cost Granular Subbase	$80,582	$80,582	$120,872	$114,157	$208,169	$194,739
	Cost Lightweight Fill	$6,387,053	$8,927,109	$6,226,809	$8,547,627	$5,906,321	$7,915,158
	TOTAL COST - CONSTRUCTION	**$7,056,775**	**$10,335,494**	**$7,183,043**	**$10,629,764**	**$7,393,049**	**$10,964,273**
	Lifetime Horizon (years)	30	30	30	30	50	50
Year	**Rehabilitation Activities**	*All amounts below are in Net Present Worth (NPW)*					
3	**Rout and Crack Sealing (352 m/km)**	$1,520	$1,520	$1,520	$1,520	$1,520	$1,520
6	**Rout and Crack Sealing (352 m/km)**	$1,313	$1,313	$1,313	$1,313	$1,313	$1,313
9	**Rout and Crack Sealing (352 m/km)**	$1,135	$1,135	$1,135	$1,135	$1,135	$1,135
9	**Mill and Patch 5% of HMA to 50 mm**	$7,101	$7,101	$7,101	$7,101	$7,101	$7,101
12	**Rout and Crack Sealing (704 m/km)**	$1,960	$1,960	$1,960	$1,960	$1,960	$1,960

15	**Mill and Patch 20% of HMA to 50 mm**	$21,195	$21,195	$21,195	$21,195	$21,195	$21,195
18	**Rout and Crack Sealing (704 m/km)**	$1,463	$1,463	$1,463	$1,463	$1,463	$1,463
20	**Tack Coat**	$2,827	$2,827	$2,827	$2,827	$2,827	$2,827
20	**Mill 50 mm of HMA Throughout**	$9,964	$9,964	$9,964	$9,964	$9,964	$9,964
20	**Pave 50 mm of HMA Throughout**	$73,069	$73,069	$73,069	$73,069	$73,069	$73,069
21	**Rout and Crack Sealing (352 m/km)**	$632	$632	$632	$632	$632	$632
24	**Rout and Crack Sealing (352 m/km)**	$546	$546	$546	$546	$546	$546
28	**Rout and Crack Sealing (352 m/km)**	$449	$449	$449	$449	$449	$449
28	**Mill and Patch 20% of HMA to 50 mm**	$11,240	$11,240	$11,240	$11,240	$11,240	$11,240
30	**Major Rehabilitation of Pavement**	$207,785	$402,001	$291,169	$585,859	$448,095	$856,208
33	**Rout and Crack Sealing (352 m/km)**	-	-	-	-	$352	$352
36	**Rout and Crack Sealing (352 m/km)**	-	-	-	-	$304	$304
39	**Rout and Crack Sealing (352 m/km)**	-	-	-	-	$263	$263
39	**Mill and Patch 5% of HMA to 50 mm**	-	-	-	-	$1,643	$1,643
42	**Rout and Crack Sealing (704 m/km)**	-	-	-	-	$454	$454
45	**Mill and Patch 20% of HMA to 50 mm**	-	-	-	-	$4,904	$4,904
48	**Rout and Crack Sealing (704 m/km)**	-	-	-	-	$338	$338
50	**Tack Coat**	-	-	-	-	$654	$654
50	**Mill 50 mm of HMA Throughout**	-	-	-	-	$2,305	$2,305
50	**Pave 50 mm of HMA Throughout**	-	-	-	-	$16,907	$16,907
	TOTAL COST - REHABILITATION	**$342,198**	**$536,414**	**$425,582**	**$720,272**	**$610,632**	**$1,018,744**
	OVERALL TOTAL COST (NPW)	**$7,398,973**	**$10,871,909**	**$7,608,624**	**$11,350,036**	**$8,003,681**	**$11,983,017**